MYOCARDIAL EXCITATION-CONTRACTION COUPLING: ADAPTATION TO ENDURANCE EXERCISE AND SPECIES DIFFERENCES

by

Marion J. Thomas

B.Sc. (Kines), Simon Fraser University, 1984.

THESIS SUBMITTED IN PARTIAL FULFILLMENT OF THE REQUIREMENTS FOR THE DEGREE OF DOCTOR OF PHILOSOPHY

in the School

of

Kinesiology

SIMON FRASER UNIVERSITY

October 1996

APPROVAL

NAME: Marion J. Thomas

DEGREE: Doctor of Philosophy

TITLE OF THESIS: Myocardial Excitation-Contraction Coupling: Adaptation to Endurance Exercise and Species Differences

EXAMINING COMMITTEE:

Chair: Dr. J. Dickinson

Dr. G. Tibbits
Senior Supervisor
Professor, School of Kinesiology

Dr. W. Parkhouse
Professor, School of Kinesiology

Dr. K. Delaney
Biological Sciences, SFU

Dr. A. Farrell
Internal Examiner
Biological Sciences, SFU

Dr. R. Moore
External Examiner
Chair, Department of Kinesiology
University of Colorado at Boulder

Date Approved: 16 October 1996

PARTIAL COPYRIGHT LICENSE

I hereby grant to Simon Fraser University the right to lend my thesis, project or extended essay (the title of which is shown below) to users of the Simon Fraser University Library, and to make partial or single copies only for such users or in response to a request from the library of any other university, or other educational institution, on its own behalf or for one of its users. I further agree that permission for multiple copying of this work for scholarly purposes may be granted by me or the Dean of Graduate Studies. It is understood that copying or publication of this work for financial gain shall not be allowed without my written permission.

Title of Thesis/Project/Extended Essay

MYOCARDIAL EXCITATION - CONTRACTION COUPLING: ADAPTATION TO ENDURANCE EXERCISE AND SPECIES DIFFERENCES.

Author:
(signature)

(name)

Oct 30/96.
(date)

ABSTRACT

This thesis investigates the adaptive and evolutionary mechanisms of excitation-contraction (E-C) coupling of the heart. The first series of experiments comprise the first paper in which rodents participated in one of several different treadmill-training protocols. In each study, sarcolemmal (SL) Ca^{2+} channels or dihydropyridine receptors (DHPR) were enumerated in purified cardiac SL vesicles and/or ventricular homogenates from treadmill-trained (T) and sedentary-control (C) rats. Sarcoplasmic reticulum (SR) Ca^{2+} release channel or ryanodine receptor (RyR) densities were also assessed in three of the regimens. No differences were found in either DHPR or RyR density after training at the lower workrates in which functional adaptations have been previously demonstrated. At the higher training intensities DHPR and RyR expression increased, possibly the result of hypertrophic stimuli. The second paper assessed training-induced alterations in cytosolic free Ca^{2+} in single cardiomyocytes at one of the lower workrates. Simultaneous measurements of contractile properties and indo-1 (a Ca^{2+} indicator) emission fluorescence (R=405/480 nm) were recorded from electrically stimulated myocytes. Cardiomyocytes from T rats demonstrated enhanced contractile function in the presence of a reduced R_{peak}. Maximal SR releaseable Ca^{2+} as determined by R_{peak} during rapid cooling contractures was also significantly reduced in T myocytes. At the same workrate, the unaltered expression of DHPR and RyR and the lack of any increase in R_{peak} either during stimulated twitches or RCCs strongly suggest that a greater Ca^{2+} sensitivity of the contractile element contributes to the observed increase in contractility. The third paper assessed the effects of training on the Ca^{2+} binding protein, calmodulin (CaM). Calmidazolium, a CaM antagonist, inhibited DHPR binding significantly more (8-14%) in SL vesicles from T hearts, $p<0.05$. Denaturing gel electrophoresis and densitometry revealed a SL protein band from T samples,

with a M_r of ~16 and parallel to our CaM standard, that was 170% of C ($p<0.001$). A CaM ELISA failed to reveal any significant differences in the amount of CaM in any fraction collected during the SL isolation. The fourth paper assessed DHPR and RyR densities in ventricular homogenates from several evolutionary distinct species, the rat, trout, dogfish and hagfish. DHPR densities were the greatest in rat (29 sites/μm^3 cell volume), lower in trout (18 sites/μm^3), dogfish (13 sites/μm^3) and barely detectable in hagfish (2 sites/μm^3). RyR densities were highest in rat (65 sites/μm^3), lower in trout (21 sites/μm^3), dogfish (3 sites/μm^3) and the lowest in hagfish (<1 site/μm^3). RyR density correlated with the amount and complexity of SR. These data are consistent with a greater reliance on SL Ca^{2+} influx in lower vertebrates and suggest that SL Ca^{2+} channels may be modulated differently in the lower species.

DEDICATION

To my parents, George, Dylan, Tasha and Noemie.

ACKNOWLEDGEMENTS

I would like to thank the members of my supervisory commitee, Drs. Wade Parkhouse, Kerry Delaney and Glen Tibbits (senior supervisor) for the time and attention they devoted to my thesis. I am grateful for the generous assitance given to me by Dr. Stelvio Bandiera (UBC) who donated his lab and supervised the development of the Calmodulin ELISA. Thank you to Brian Hamman, Michelle Weymann and Dr. Gary Diffee for contributing the PN binding data. A special thanks to Haruyo Kashihara for her expert technical assistance provided during my time in CMRL. An appreciatory note to all those in the School of Kinesiology for helping out in many different capacities. Thanks to Dick Jol and Loekie Van Der Wal of the Animal Care Facility at SFU for their dedication and expertise in supervising the care and handling of the animals.

My sincere appreciation goes to my parents and family for their words of wisdom and encouragement. Finally, a special thanks to a very special person, George Prokopetz Alexander, whose relentless positivity gave me the will and motivation (*raison d'etre*) to continue until the end. I am forever grateful!

TABLE OF CONTENTS

LIST OF TABLES

LIST OF FIGURES

CHAPTER 2

CHAPTER 4

CHAPTER 5

CHAPTER 1

REVIEW OF THE LITERATURE

1 INTRODUCTION

Cardiac output must be carefully regulated in order to maintain appropriate blood flow to exercising muscle, brain and other tissues. Cardiac output is the product of heart rate and stroke volume. Stroke volume, in turn, is controlled primarily by the modulation of two parameters, preload or end-diastolic volume (EDV) and myocardial contractility. Myocardial contractility may be regulated by extrinsic factors such as β-adrenergic stimulation or intrinsically by mechanisms of excitation-contraction (E-C) coupling.

The enormous potential for plasticity in E-C coupling components is revealed by the ability of a wide variety of species to regulate myocardial contractility under myriad environmental demands. Even within a given species, this plasticity is evident in adaptations in E-C coupling components brought about by exercise training. The focus of this review is on mechanisms of E-C coupling that serve to regulate myocardial contractility in order to identify those components that have the potential for adaptation.

2 MAMMALIAN EXCITATION-CONTRACTION COUPLING

2.1. INTRODUCTION

Contraction of mammalian cardiac muscle begins with depolarization of the sarcolemma following pacemaker excitation. Voltage-sensitive Ca^{2+} channels open allowing Ca^{2+} ions to traverse the sarcolemmal (SL) membrane down a ~10,000-fold concentration gradient into the cytosol. In all mammalian cardiac preparations examined thus far, this influx of Ca^{2+} serves as a trigger for a larger release of Ca^{2+} from the sarcoplasmic reticulum (SR), a process defined as calcium-induced calcium release (CICR) (191). The resulting rise in cytosolic free Ca^{2+} leads to the binding of Ca^{2+} to the myofilament protein, Troponin C (TnC) which initiates cross bridge formation, and subsequent tension development. Relaxation occurs when cytosolic free Ca^{2+} is returned to resting levels by the removal to both the extracellular space and SR in magnitudes that are proportional to their respective contributions (13).

2.2. CONTRACTILE ACTIVATION

2.2.1. Contractile Proteins

2.2.1.1 *Ultrastruture of the contractile element*

The ultrastructure of cardiac muscle has been thoroughly reviewed (170). Electron microscopy of heart muscle reveals the distinct banding pattern of the myofibrils observed in all striated muscle. The light and dark patterning is produced by alternating thin actin filaments forming the light or I (isotropic) band and thick myosin filaments

which form the dark or A (anisotropic) band. The A band also contains M lines located at the middle of the myosin filament which are believed to play a role in maintaining myosin alignment. In contrast to the A-band, which remains a constant width during contraction, the I-band shortens consistent with myofilament overlap and the sliding filament theory of muscle contraction. In the middle of each I-band anchoring the thin filaments is the Z line. At rest, the distance between two Z lines varies from 2.0 to 2.5 μm and makes up the functional unit called the sarcomere. High resolution electron microscopy has revealed the presence of periodic cross-bridges from the myosin to the actin filaments. In cross section each myosin filament is surrounded by six actin filaments in a hexagonal array. The distance between each myosin filament in cross section is between 20 and 30 nm. The myofilaments occupy approximately one-half of the cell volume in the mammalian ventricular myocardium (29, 134).

2.2.1.2 *Actomyosin ATPase*

The thick filament is composed predominantly of myosin molecules. Each mammalian cardiac myosin molecule comprises two heavy chain (HC) subunits (α,β) and four regulatory light chains. The two HC subunits are combined to form one of V1 (α,α), V2 (α,β) or V3 (β,β) isoforms. The V1 isoform is distinguishable by having a high intrinsic ATPase activity, rapid rate of contraction and fast electrophoretic mobility in nondissociating gels, V2 has intermediate properties and V3 has the lowest ATPase activity, rate of contraction and gel mobility. The rat heart contains a high percentage of V1 (70-80%) as expected from the high heart rate. In general, larger mammalian species have 80-100% of the V3 isoform (5). The capacity to respond to changing cardiovascular

demands may be determined, in part, by the ability to "up" or "down" regulate myosin ATPase activity.

The thin filament is made up of a backbone of two helical strands of globular actin molecules. Each double stranded tropomyosin molecule lies in the groove between the actin strands and spans ~7 actin monomers. A troponin complex attaches to tropomyosin at regular intervals of 7 actins. The troponin complex is made up of three subunits; troponin C (TnC) is the Ca^{2+} binding protein, troponin T (TnT) binds tropomyosin, and troponin I (TnI) inhibits actin from binding to the myosin heads. TnC in fast skeletal muscle contains four similar amino acid sequences representing two low affinity (regulatory) Ca^{2+}-specific sites (I and II) and two high affinity Ca^{2+}-Mg^{2+} sites (III and IV). Cardiac TnC has the distinctive feature that site I has two amino acid substitutions, the result of which eliminates the ability to selectively bind Ca^{2+}. With the exception of TnC, for which there is no evidence of isoforms within a given tissue, most of the other thin filament proteins exist as populations of isoforms. TnT and TnI genes express different isoforms during development through alternate splicing. As many as five TnT isoforms produced by alternative gene splicing have been identified in mammalian hearts (4). The cardiac TnI isoform contains a serine residue that is not found in skeletal muscle TnI. Phosphorylation of TnI reduces the Ca^{2+} affinity of TnC through cooperative interactions in the troponin complex. The functional role for the different isoforms of TnI and TnT are not completely understood although it is known they can affect myosin ATPase activities (115, 166). The potential for differential isoform expression offers an important response by the heart to long-term changes in cardiovascular demands such as

those which occur during ontogeny, exercise training and changing metabolic and environmental demands (e.g. starvation, hormonal conditions, temperature) (166).

2.2.2 Ca^{2+} requirements

2.2.2.1 *Cytosolic Ca^{2+} buffering*

The importance of cytosolic Ca^{2+} buffering is illustrated by the fact that the measured free Ca^{2+} transient represents <3 % of the total Ca^{2+} transient in heart muscle (49, 76, 146). The majority of the Ca^{2+} entering across the SL and released from the SR is bound to various cytosolic Ca^{2+} binding sites with the relative amount depending upon the number of binding sites, the amount of each buffer and their respective association constants (K_a). Ca^{2+} binding moieties such as TnC, calmodulin, ATP, creatine phosphate, external mitochondrial and SR surfaces, and the inner SL surface are all known to bind Ca^{2+} during contraction (49, 76). Several studies have attempted to determine this buffering capacity quantitatively using: 1) isolated canine cardiac myofilaments (168), 2) calculations based on known ligand concentrations and binding constants (49), 3) rabbit ventricular homogenates (146), and 4) permeabilized rabbit cardiomyocytes (76). Although the amount of Ca^{2+} bound to the various intracellular buffers at diastolic free Ca^{2+} levels (~0.1 μM) is unknown, at 1 μM the bound Ca^{2+} is estimated to vary between 16 and 72 μmoles per kg wet weight from these studies. Finally, in order to generate half maximal tension, free Ca^{2+} must reach a pCa of 5.2 to

5.7 (2 to 6 μM). The addition of ~40-60 μmol/kg wet wt is required taking into consideration the known cytosolic buffering (49, 168).

2.2.2.2 *Ca^{2+} sensitivity*

The myofilaments in cardiac muscle are activated by Ca^{2+} in a graded manner such that the relationship between free Ca^{2+} (expressed as pCa=-log [Ca^{2+}]) and force is highly cooperative. Initial experiments were performed on papillary muscle that had been mechanically or chemically skinned (48, 66). In these experiments relatively small differences in Ca^{2+} sensitivity were observed in a number of mammalian species. The pCa values for half-maximal force production ($pCa_{½}$) were typically between 5.2 and 5.7. When similar experiments were performed on intact muscle using aequorin, much steeper force-pCa curves were observed with a pCa½ between 6.1 and 6.3 (60, 196). Reasons for this discrepancy are not yet known but may involve the loss of constituents during skinning which normally enhance Ca^{2+} sensitivity, or inaccuracies in pCa determination.

While many factors are known to influence the force-pCa relationship, temperature, sarcomere length and pH are particularly relevant when considering different species or adaptive responses such as chronic exercise. Lower temperatures and shorter sarcomere lengths decrease both Ca^{2+} sensitivity and maximum force generated by the myofilaments (66, 87). Similarly, acidosis also decreases both the Ca^{2+} sensitivity and maximum force. (26, 51). While the mechanisms are not clearly understood, thin filament proteins may be involved. It has been shown that both ATPase activity and TnC Ca^{2+} binding in the prenatal heart are unaffected by acidosis (167). No differences are seen between adult and prenatal hearts in myosin heavy chain profiles with nondissociating gels. However,

differences were noted in the thin filament regulatory proteins, TnI and TnT, when the Tn complex was subject to urea gel-electrophoresis (PAGE). These results suggest that the difference in pH sensitivity is due to alterations in either TnI or TnT rather than TnC.

2.3. Regulation Of Ca^{2+} Delivery To Myofibrils

2.3.1 Action potential

The cardiac action potential (AP) in mammals reflects a multitude of ionic currents across the SL which change over the course of a single beat. With the advent of the patch clamp technique to record ionic currents in isolated cardiomyocytes, knowledge about the role of these currents in mammalian E-C coupling has increased tremendously. While the shape and duration of the cardiac AP varies from species to species, for a given species, these parameters will vary depending upon heart rate, temperature, location within the heart (eg. conducting fibers, atria, ventricle, endo- epicardium) as well as other factors and often reflected by altered E-C coupling (55).

The AP plateau phase is associated with an inward Ca^{2+} current (I_{ca}) and has been found in all cardiac cells studied to date. It has been known since the work of Ringer (1883) that extracellular Ca^{2+} is necessary for cardiac muscle contraction. Variations in extracellular Ca^{2+} concentration ($[Ca^{2+}]_o$) leads to changes in the magnitude of contractile force. As with varying $[Ca^{2+}]_o$, varying the frequency of APs also leads to changes in contractile force magnitude. In addition, isolated cardiac I_{ca} are facilitated by an increase in stimulation frequency, being larger and more slowly inactivating (116). I_{ca} obtained from whole cell patch recordings were increased by ~25% in guinea pig ventricular

myocytes when stimulation frequency was increased from 0.2 to 1 Hz (121). Simultaneous measurements of Ca^{2+} currents and intracellular Ca^{2+} has now yielded quantitative models of myocardial E-C coupling in mammals (191).

2.3.2 SL Ca^{2+} influx

2.3.2.1 *Estimates of SL Ca^{2+} influx*

SL Ca^{2+} influx occurs rapidly through the transient opening of voltage-sensitive SL Ca^{2+} channels. Each channel contributes ~3 million Ca^{2+} ions per second with the peak unitary Ca^{2+} current reached in ~2-3 msec at positive membrane potentials (72). Estimates of SL Ca^{2+} influx, based upon a variety of techniques, range from 10-20 μmol per kg wet weight in ~40 msec and are insufficient to support contraction in the adult mammalian ventricle (11, 49, 70, 97). In mammals, this relatively small influx of Ca^{2+} triggers the release of a much greater amount of Ca^{2+} through functionally coupled SR Ca^{2+} release channels (158).

2.3.2.2 *L-type Ca^{2+} channel*

a. Structure. Voltage-sensitive, L-type Ca^{2+} channels in the sarcolemma represent an oligomeric complex consisting of a channel-forming α_1 subunit, and the disulfide-linked α_2-δ, β and possibly γ subunits (41, 116). Each α_1 subunit comprises four repeats of six putative transmembrane helices or segments (S1-S6), and represents a functional channel which binds a class of Ca^{2+} channel antagonists, the dihydropyridines (DHP) (101, 120). Recently, the use of subscripts was agreed upon to identify the genes from

which the α_1 subunit originates. These are S for the skeletal muscle isoform, A-B and D-E for the various brain isoforms, and C representing the cardiac isoform (24). In cardiac muscle, only the α_{1C} and β_2 subunits have been fully cloned and sequenced (120, 140). Receptor sites for several classes of drugs have been located on the α_{1C} subunit and several phosphorylation sites identified (74). The S4 segment is highly conserved among voltage-sensitive ion channels and is believed to represent the voltage-sensor. The α_{1C} gene product has a molecular weight of 243 kDa based upon sequencing full length cDNA (101, 120). Recent experiments using chimeric Ca^{2+} channels expressed in HEK 293 cells have provided evidence for a Ca^{2+} inactivation site located near the proximal fourth of the α_{1C} carboxyl terminus (42). Evidence that the additional subunits may be involved in channel modulation comes from expression studies. When mRNA for the α_{2S} was coinjected with mRNA derived from the α_{1C} cDNA in *Xenopus* oocytes, both I_{ca} and activation kinetics were enhanced (120). The β subunit has also been shown to enhance Ca^{2+} channel activation and inactivation kinetics and drug sensitivity when coexpressed with α_{1C} in oocytes and COS cells (140, 188).

b. Modulation. Cardiac Ca^{2+} channels are modulated by numerous factors including: pharmacological agents (eg. dihydropyridines, calmodulin antagonists), voltage, temperature, extra- and intracellular cations, and intracellular enzyme cascades (eg. cAMP, cGMP, phosphinositide, fatty acids) (116). Myocardial DHPRs are also modulated by β-adrenergic agonists which indirectly act via cAMP-dependent phosphorylation (150) or directly through the G_s α-subunit, to increase probability of

channel opening (64, 112). In addition, Ca^{2+}-calmodulin dependent protein kinase and protein kinase C have been shown to modulate I_{ca} in chick cell reaggregates (25) and phosphorylate DHPRs (73, 128). Recently, the I_{ca} activation rate has been correlated with α_{1S} subunit density in cultured myotubes from mice (2). The reasons for this relationship are unknown and currently under investigation.

c. Localization and density. In cardiac muscle, DHPRs are localized at or near dyadic couplings between the SR membrane and surface SL or T-tubules (32). In contrast, skeletal muscle DHPRs are found predominantly in the T-tubules. Another distinctive feature regarding the spatial relationship between cardiac DHPR and RyRs is an apparent lack of the organized array seen in skeletal muscle even though they are within 20 nm of each other (173). In skeletal muscle DHPR tetramers are physically coupled to the cytoplasmic domains of alternating RyR tetramers (27, 58). While considerably higher DHPR densities are found in skeletal muscle, estimates of mammalian cardiac DHPR densities range between 7-30 receptors per μm^3 cell volume depending upon species, the experimental approach and associated assumptions (17, 101).

2.3.2.3 *Na^+/Ca^{2+} exchange*

Ca^{2+} entry via the SL Na^+/Ca^{2+} exchanger can contribute to direct activation of the myofilaments (21). Large contractions have been elicited either by lowering the extracellular Na^+ concentration ($[Na^+]_o$) or raising the intracellular Na^+ concentration ($[Na^+]_i$). In rabbit ventricular muscle, contractions activated by action potentials were blocked in the presence of nifedipine, a DHP Ca^{2+} channel antagonist (15). However,

when $[Na^+]_i$ was raised to 15-20 mM, large contractions were elicited upon depolarization (0.5 Hz) in the presence of nifedipine (15). The SL Na^+/Ca^{2+} exchanger is electrogenic transporting 3 Na^+ ions for every Ca^{2+} ion. Ca^{2+} influx or efflux via the Na^+/Ca^{2+} exchanger depends upon the Na^+ and Ca^{2+} concentration gradients and the membrane potential. The electrochemical driving forces (DF) for Na^+ and Ca^{2+} may be expressed as:

$$DF_{Na} = 3(E_{Na} - E_m) \text{ and } DF_{Ca} = 2\,(E_{Ca} - E_m)$$

where, E_{Na} and E_{Ca} are the equilibrium potentials for Na^+ and Ca^{2+} ions $\{E_{ion} = (RT/zF)\ \ln([ion]_o/[ion]_i)\}$ and E_m is the membrane potential. Thus the potential at which DF_{Na} and DF_{Ca} are equal reflects the equilibrium potential for Na^+/Ca^{2+} exchange ($E_{Na/Ca}$) and the potential at which the Na^+/Ca^{2+} exchange current reverses modes. The $E_{Na/Ca}$ is therefore expressed as

$$E_{Na/Ca} = 3E_{Na} - 2E_{Ca}$$

The driving force for Na^+/Ca^{2+} exchange ($DF_{Na/Ca}$) depends upon both the $E_{Na/Ca}$ and E_m,

$$DF_{Na/Ca} = E_{Na/Ca} - E_m$$

During an AP, changes in the E_m causes a rise in $[Ca^{2+}]_i$ and thus E_{Ca} and therefore $E_{Na/Ca}$ change. Ca^{2+} influx or reverse mode is favoured when $E_{Na/Ca}$ is more positive to

E_m. Using appropriate values for the above parameters, one would predict that this reverse mode could be favoured at some point during the plateau phase of the AP. The amplitude of the Na^+/Ca^{2+} exchange current is not only subject to the driving forces but also to kinetic limitations. For example, the DF for Ca^{2+} extrusion may be large during diastole but the net extrusion of Ca^{2+} is limited by the low $[Ca^{2+}]_i$ relative to the Na^+/Ca^{2+} exchanger's K_m for Ca^{2+}. Based on data from intact muscles and thermodynamic considerations, it seems probable that under normal conditions the Na^+/Ca^{2+} exchanger serves mainly as a means of Ca^{2+} extrusion. However, the importance of Na^+/Ca^{2+} exchange in contributing to Ca^{2+} influx under physiologically relevant conditions remains the focus of debate (95, 159).

2.3.3 SR Ca^{2+} release

2.3.3.1 *Estimates of SR Ca^{2+} release*

In the mammalian heart, Ca^{2+} released from the SR is a major source of Ca^{2+} for contraction. The numerous studies in support of Ca^{2+}-induced, Ca^{2+}-release (CICR) were initially based upon data from skinned fibers (49) and supported more recently by observations from isolated myocytes with intact SL (20, 126). Rapid cooling of either multicellular or isolated cell preparations simultaneously enhances the release of Ca^{2+} from the SR and inhibits Ca^{2+} uptake mechanisms thereby inducing a rapid cooling contracture (RCC) (30). The magnitude of the contracture is believed to be a valid index of relative SR releasable Ca^{2+} (30).

Estimates of the amount of Ca^{2+} released from the SR during a RCC, based upon indo-1 measurements of free Ca^{2+}, taking into account estimates of cytosolic Ca^{2+} buffering, suggest release of 150-300 μmoles per kg wet weight, which is more than sufficient to support contraction (14). Recently, a model was developed to estimate the net flux of Ca^{2+} out of the SR during a simulated twitch (164). The maximum flux was estimated to be ~40-160 μmoles per kg wet weight in ~40 msec, clearly, a rate consistent with contractile activation.

2.3.3.2 *SR Ca^{2+} release channels*

a. Structure. The purification of the ryanodine receptor (RyR) from junctional SR and associated Ca^{2+} channel activity lead to the identification of the RyR as the SR Ca^{2+} release channel (79, 91). Three separate genes have now been identified encoding the isoforms RyR1 (skeletal), RyR2 (heart), and RyR3 (brain and smooth muscle). RyRs are homotetramers of ~560 kDa with each subunit having a large cytoplasmic domain spanning the ~15 nm gap between the SR and DHPRs located in the T-tubules or SL (127, 133). In the heart, the RyR has been localized to two discrete areas in the SR membrane, the junctional and corbular SR (85). In chicken myocardium, RyRs in the junctional SR form peripheral couplings and are in close proximity to DHPRs, those located in the corbular SR are not associated with DHPRs (173). The evidence that corbular SR contains RyRs and calsequestrin (Ca^{2+} binding SR protein), in addition to storing Ca^{2+}, suggests participation in E-C coupling (50, 85). Evidence for the functional coupling between peripheral RyRs and DHPRs is provided by recent experiments using rat cardiomyocytes which demonstrate that Ca^{2+} entering through SL Ca^{2+} channels was

substantially more effective in gating SR Ca^{2+} release compared to Ca^{2+} entering via the Na^{+}/Ca^{2+} exchanger (158). In addition, the SL Ca^{2+} channels were inactivated by Ca^{2+} released from the SR even in the presence of intracellular EGTA which suggests that the SR released Ca^{2+} has preferrential access to the DHPR.

b. Modulation. In both skeletal and cardiac muscle, SR Ca^{2+} release channels/RyRs are modulated directly and indirectly by a large variety of effectors including Ca^{2+}, Mg^{2+}, ryanodine, caffeine, adenine nucleotides, fatty acids, calmodulin, pH and temperature (38, 96, 116, 117). The major difference between skeletal and cardiac RyRs relates to their sensitivity and gating by Ca^{2+}. Micromolar concentrations of Ca^{2+} stimulate the release of Ca^{2+} from cardiac SR vesicles. The bell-shaped Ca^{2+} dependence of release is maximal around 5-20 μM (38, 118). While Mg^{2+} is a potent inhibitor of Ca^{2+} release in SR vesicles isolated from skeletal muscle, physiological (mM) concentrations have little effect on the binding of Ca^{2+} to cardiac RyR receptors (118). Nanomolar concentrations of ryanodine open the SR Ca^{2+} release channel to a subconductance state while higher concentrations (>10 μM) completely block the channel. Adenine nucleotides shift the half-maximal Ca^{2+} concentration for CICR from 2 to 0.8 μM (119). The cardiac isoform (RyR2) has a unique phosphorylation site for Ca^{2+}-CaM dependent protein kinase which is not found on either RyR1 or RyR3 (193). The cardiac RyR also has a unique property of opening in response to rapid cooling to temperatures below 5°C. This characteristic has provided a useful tool in the assessment of SR releaseable Ca^{2+}.

Analysis of [^{3}H]-ryanodine binding has provided substantial information about the function of the release channel. [^{3}H]-ryanodine binding shows Ca^{2+} dependence with a threshold of ~1μM, with optimal binding around 10 μM to 1 mM. Both high- and low-affinity binding sites exist on the homotetramer. The ratio of high- to low-affinity binding sites was reported to be 1:3 (143). Equilibrium binding experiments in cardiac SR have described dissociation constants of K_1=1-4 nM, K_2= 30-50 nM, K_3=500-800 nM, and K_4=2-4 μM for binding of up to four ryanodine molecules per tetramer (143). Hill coefficients of <1 for the low-affinity sites suggest that sequential binding of one to three ryanodine molecules to initially identical sites on the open channel proceeds through allosterically coupled negative cooperativity (33, 143).

c. Localization and density. Estimates for the number of mammalian cardiac RyRs are considerably greater than DHPR densities and vary from 27 to ~100 receptors per μm^3 cell volume depending upon species and preparation (17). The stoichiometric relationship between the DHPR and RyR also has important implications in E-C coupling. In skeletal muscle, it appears that a RyR/DHPR ratio of 0.5 is highly conserved phylogenetically (3, 27, 57). This type of arrangement is consistent with the current E-C coupling model in skeletal muscle in which the DHPR has a physical link with the RyR (27). In contrast, the RYR/DHPR ratio in the mammalian myocardium is considerably higher (2 to 10), more variable and species specific (17). These architectural and functional differences help to explain the observed differences in E-C coupling between these two tissues.

2.3.4 Ca^{2+} regulation by mitochondria

Mitochondrial involvement in E-C coupling has been ruled out, at least in the mammalian myocardium, based upon several pharmacological and kinetic arguments (7, 8, 13, 49). Although mitochondria have a considerable storage capacity for Ca^{2+} (~140 mmol/kg wet wgt) (31) they are not considered to be of prime importance in the regulation of Ca^{2+} levels on a beat-by-beat basis. Reasons for this include: 1) that pCa has to be sustained at levels greater than ~1μM in order to accumulate Ca^{2+} (123), 2) the rate of Ca^{2+} uptake is 2 orders of magnitude too slow (8), 3) no mechanism for rapid Ca^{2+} release has been identified and 4) blocking Ca^{2+} release does not affect contraction (8).

2.4 Myocardial Relaxation

2.4.1 Estimates of Ca^{2+} removal

In order for relaxation to occur, ~40-60 μmoles of Ca^{2+} per kg wet weight must be removed during a single cardiac cycle, the time interval of which is dependent upon heart rate. In the mammalian heart, this Ca^{2+} removal occurs predominantly by the SR Ca^{2+}-ATPase and to a lesser extent the SL Na^{+}/Ca^{2+} exchanger. The maximum SR Ca^{2+} uptake rate in permeabilized rat myocytes has been determined to be 56 μmoles per kg wet weight per second at 23°C (76). Extrapolation to 37°C yields ~168 μmoles per kg wet weight per second. Based upon SL vesicular measurements, the SL Na/Ca exchanger is capable of removing Ca^{2+} at a rate of ~100 μmoles per kg wet weight per second although the affinity for Ca^{2+} is considerably lower compared to that of the SR Ca^{2+}

ATPase (148). Thus it appears that the SR Ca^{2+} ATPase and the Na^{+}/Ca^{2+} exchanger are together more than sufficient to promote relaxation in the time required. Recent experiments on ventricular myocytes and other preparations have demonstrated that the relative role of each mechanism is highly species and condition dependent with the Na^{+}/Ca^{2+} exchanger being the major contributor to Ca_i-transient decay in rabbit while the SR Ca^{2+} ATPase predominates in the rat heart (10, 13, 16). In rat ventricular myocytes loaded with indo-1, the relative contributions to relaxation were estimated to be ~87% for SR Ca^{2+} ATPase, 8.7% for Na^{+}/Ca^{2+} exchange, 2.6% for SL Ca^{2+} ATPase, and 1.7% for mitochondria (129).

2.4.1.1 *SL Ca^{2+} ATPase*

The SL Ca^{2+} ATPase, while having a high affinity for Ca^{2+} (K_m = 63 nM), does not appear to be involved in significant calcium removal on a beat-to-beat basis in the myocardium of mammalian species studied due to a low maximum transport rate of ~2.4 nmol Ca^{2+} per kg wet weight per second under optimal conditions (43). When both the SR Ca^{2+} ATPase and Na^{+}/Ca^{2+} exchanger are inhibited, relaxation essentially does not occur (13).

2.4.1.2 *SR Ca^{2+} ATPase*

Both the SR Ca^{2+} ATPase and its regulatory protein, phospholamban, are major constituents in the membrane of the longitudinal SR and nonjunctional regions of the terminal cisternae (54). The Ca^{2+} ATPase has a K_m for Ca^{2+} of 1-5 μM, an affinity which can be increased 3-5 fold by phospholamban phosphorylation (161, 174). Two Ca^{2+} ions

are transported for each ATP utilized at a maximal rate of 10-15 ions/pump/sec. Unlike fast-twitch muscle, the cardiac SR Ca^{2+} ATPase is associated with and under direct regulation by a ~22 kDa protein, phospholamban (80, 88, 94).

a. Structure. Of the three known Ca^{2+} ATPase (SERCA) genes, SERCA2 encodes the slow-twitch/cardiac isoform through alternative splicing (107). The rabbit cardiac SR Ca^{2+} ATPase has been extensively characterized including cloning and sequencing of full length cDNA (108, 197).

b. Modulation. Phospholamban is a homopentamer comprising ~6 kDa monomers associated through noncovalent interactions. When phosphlamban is phosphorylated by one of several mechanisms including a Ca^{2+} and calmodulin-dependent protein kinase, maximal Ca^{2+} ATPase activity and Ca^{2+} binding affinity are both increased (80, 160, 174). Phospholamban, due to its direct association with the SR Ca^{2+} ATPase, is an important regulator of myocardial contractility. *In vitro* experiments demonstrate that when phospholamban is phosphorylated by cAMP- or Ca^{2+} and calmodulin-dependent protein kinase, Ca^{2+} ATPase activity and SR Ca^{2+} uptake is markedly increased (80, 88, 160). Phospholamban knockout in transgenic mice substantially increases intraventricular pressure development and maximal rates of pressure development under conditions of constant heart rate and cardiac power (106).

c. Localization and density. Estimates of Ca^{2+} ATPase density reveal ~3,700 per μm^3 cell volume based upon a phosphoenzyme formation of 5.9 µmol/kg wet wt (100) and a cylindrical myocyte model with a mass of 22 ng and volume of $21x10^{-9}cm^3$.

2.3.1.3 *Na^+/Ca^{2+} exchange*

Much of what is known about the SL Na^+/Ca^{2+} exchanger comes from studies using purified SL vesicles. The SL Na^+/Ca^{2+} exchanger normally functions in Ca^{2+} extrusion mode (145, 147). A high capacity for Ca^{2+} extrusion is demonstrated by maximum transport rates of ~100 μmol per kg wet wt per sec in purified SL vesicles (148) and isolated ventricular myocytes (122). The K_m for Na^+ is ~30 mM while the K_m for Ca^{2+} is estimated to be ~1-40 μM with the lower values having been determined in giant SL patches (148). There are apparently significant variations in exchanger activity among isolated myocytes from different species reflecting, perhaps, differences in relative roles of SL Ca^{2+} influx and SR Ca^{2+} release (157). Whether these are due to differences in exchanger densities, modulation or distribution remains to be determined.

a. Structure. The plasma membrane Na^+/Ca^{2+} exchanger is single polypeptide of ~108 kDa encoded by a single gene with 11 putative transmembrane domains and one large cytoplasmic hydrophobic domain (89, 98, 131). To date, four types of Na^+/Ca^{2+} exchangers have been cloned and are discussed using the current nomenclature (130). In addition to the cardiac isoform (NCX1), several tissue-specific alternatively spliced isoforms have been identified (89, 98). NCX1 from the hearts of a number of species including canine, bovine, guinea pig and rat have been cloned and functionally expressed (1, 104, 131, 184). The SL Na^+/Ca^{2+} exchanger from these species is >90% homologous based upon sequence comparison. An exception to this high degree of homology is the second exchanger (CalX) cloned from *Drosophila*, which shares only 52% sequence

homology to NCX1 (185). The third isoform (NCX2) was cloned from a rat brain cDNA library and shares 62% homology with NCX1 (102). Transcripts of NCX2 have only been observed in brain and skeletal muscle. The fourth exchanger, NCKX1, found in rod outer segments, is not a true Na^+/Ca^{2+} exchanger as it exchanges K^+ in addition to Na^+ and Ca^{2+} but shares two regions of sequence similarity to NCX1 and overall topological similarity.

b. Modulation. A multitude of factors have been cited as modifiers of NCX1 activity including Ca^{2+}, pH, temperature and phospholipids (12, 148). A Ca^{2+} binding regulatory site distinct from the Ca^{2+} transport site has been identified on the cytoplasmic loop by site-directed mutagenesis (111). When Ca^{2+} binds to this regulatory site, the exchanger is activated (69). In addition to indirect regulation by ATP, several phosphorylation sites, and a putative calmodulin binding site have been identified on the large cytoplasmic domain between transmembrane repeats 6 and 7 of the exchanger (103, 131).

c. Localization and density. Charge movements obtained in giant membrane patches from guinea-pig SL indicate about 400 exchangers per μm^2 (71). Immunofluorescence and immunoelectron microscopy experiments in guinea pig cardiomyocytes have localized the exchanger to predominantly the T-tubular system with patchy labelling of the peripheral sarcolemma (56).

3 EXERCISE-INDUCED ADAPTATIONS OF CARDIAC FUNCTION

3.1 INTRODUCTION

Changes in Ca^{2+} handling have been suggested to be a component of the adaptatve response by the heart to chronic exercise training. This review will address the potential of Ca^{2+} handling in mediating exercise-induced alterations in myocardial contractility.

The physiological effects of endurance exercise training are well documented in both human and animal models, however, controversy surrounds the nature of the underlying adaptive mechanisms. Reasons for this lie in the myriad methodologies, training paradigms and different animal models used to determine the adaptive mechanisms (53). Taking this into consideration, a review of the cardiovascular adaptations to endurance exercise will be presented.

Cardiovascular responses to endurance training include increases in maximal values of oxygen uptake, stroke volume and cardiac output with little or no change in maximal heart rate (28, 44). In humans, ~80% of the potential increase in maximum oxygen delivery resulting from endurance training is due to augmented stroke volume (SV) with the remaining 20% due to improved oxygen extraction (28). There is consistent agreement that chronic exercise training of sufficient intensity results in a decreased heart rate, and therefore a greater SV for a given submaximal cardiac output (28, 44). The mechanisms contributing to greater submaximal and maximal SV remain controversial. Since SV can be affected by both extramyocardial and myocardial factors, the effect of endurance training on these parameters will be examined.

3.2 Extramyocardial Adaptations

3.2.1 Heart Rate

In mammals, the normal heart rate increase to acute exercise is mediated by a combination of vagal withdrawal and β-adrenergic stimulation. Chronic endurance training produces a well documented bradycardia both at rest and at any given submaximal cardiac output (28). It has been suggested that training causes an increase in parasympathetic activity at rest but the mechanisms contributing to the reduced HR during submaximal exercise remain equivocal (156). Complete vagal blockade in humans produces a heart rate of about 130 beats per minute above which increased β-adrenergic stimulation is required. However, no significant changes in plasma or myocardial tissue levels of epinephrine or norepinephrine are observed at rest in the trained individual (39, 141). Consistent with bradycardia, lower plasma catecholamine concentrations at any absolute submaximal work load have been cited while no differences are observed at the same relative work intensity (28, 156).

Nonneural mechanisms may also contribute to the observed training induced bradycardia. Several studies have demonstrated a decrease in the intrinsic rate of the atrial pacemaker and sinoatrial node (163, 165).

3.2.2 Coronary Vasculature

An important effect of physical training on cardiac function is an increase in the size of the coronary vascular bed with changes involving neogenesis of capillaries in addition

to changes in the larger vessels (93). Consistent with greater coronary vascularity is an increased coronary blood flow observed in chronically instrumented, trained dogs (172).

3.2.3 Preload

By definition, the greater SV observed with training must involve an increased preload or end-diastolic volume (EDV), decreased end-systolic volume (ESV) or both. Increased preload or EDV remains a small but significant adaptation to exercise training (28, 44). Echochardiography, a non-invasive technique, has provided some evidence for an increase in ventricular preload in healthy male subjects trained by jogging (194). Animal studies using isolated working heart preparations have demonstrated enhanced SV but often fail to show whether their results are due to greater EDV or some other intrinsic mechanism (138). Using radionuclide angiography, more direct evidence of EDV augmentation during submaximal and maximal swimming in trained individuals was observed (149). Factors which may contribute to enhanced EDV are improved venous return and greater total blood volume.

A slower heart rate for a given workload would allow a longer filling time and may prove to be an important adaptation to training by leading to greater venous return and EDV (18). However, maximum heart rates do not change while maximum cardiac outputs can increase by as much as 20%. Greater total blood volume may also contribute to enhanced EDV with training. Small but statistically significant changes in total blood volume occur with training, usually without major changes in hemoglobin concentration or hematocrit (149, 152, 156). Several studies have been cited which have involved the reinfusion of blood into sedentary and trained subjects (28). Greater SV and cardiac

outputs were found in the trained but not untrained subjects in response to acute blood volume increases.

3.2.4 Afterload

In addition to greater EDV, a reduction in ESV further adds to SV enhancement. Smaller ESV may occur as a result of increased contractility, and/or a reduced resistance to flow. The increase in SV seen in trained subjects has not been associated with a fall in mean arterial blood pressure even though a fall in total peripheral resistance (TPR) has been documented (37). During maximal exercise at similar arterial pressures a marked reduction in TPR enables the trained athlete to generate cardiac outputs twice that of sedentary persons. A striking feature of the training response is a marked increase in the size of the skeletal muscle capillary bed with the major site of decreased resistance occuring at the arteriolar level. It appears that training causes an important increase in the maximal vascular conductance of working muscle in response to local rather than systemic mechanisms (28). While training-induced adaptations do occur at the level of working muscle, afterload is not reduced and therefore does not contribute to the reduction in ESV.

3.3 Myocardial Adaptations

3.3.1 Cardiac Hypertrophy

While cardiac hypertrophy is often an expected adaptation to chronic exercise training, experimental evidence does not unequivocally support this conclusion. Cross-sectional studies using echocardiographic analysis indicate that differences in cardiac dimensions between endurance-trained athletes and non-athletes are small with average increases of

0.3 mm in wall thickness and only 2.1 mm in end-diastolic diameter (142). Many animal studies have reported small but significant changes in heart size (59, 68, 154). These studies are often confounded by a number of factors such as gender, mode of training (eg. swimming vs running), or the indices used to determine the extent of hypertrophy (eg. heart weight, heart weight/body weight ratio) (142). A significant number of studies, in which treadmill-trained female rodents are used, demonstrate enhanced cardiac function in the absence of significant cardiac hypertrophy (6, 177, 180). When total work is calculated based upon body mass, treadmill speed and percent grade, and the total number of exercise sessions, no differences were noted between the % increase in the hypertrophic index and either the total work (kg•m) performed or the relative power output (W/kg) (142). Thus, while cardiac hypertrophy occurs and is related to intensity and duration of exercise, it is not obligatory for improved cardiac performance.

3.3.2 Myocardial Contractility

Another potential intrinsic adaptation to exercise training is an increase in myocardial contractility. A change in contractility by definition involves length-independent mechanisms. Many experimental parameters have been used as indices with which to measure changes in contractility. However, indices such as V_{max} (maximum rate of cross-bridge turnover), dP/dt (or dT/dt) (rate of change in pressure or tension development), rate of fiber shortening, dFlow/dt (rate of change in aortic blood flow) and peak LVP (left ventricular pressure) all have a confounding length dependence. The use of papillary muscle, ventricular strips and more recently isolated single cardiomyocytes has permitted greater control over fiber length.

Isolated muscle strips from trained rats generated greater active tension compared to sedentary animals (40). In another study using a working heart preparation, trained hearts had greater ejection fractions, greater fiber shortening and increased dP/dt for a given filling pressure, all in the absence of hypertrophy (18). Investigators, using isolated cardiac tissue from trained hearts, have observed increases in contractility (68, 124, 138, 155, 177, 180), while others have found no change or even a decrease (132, 192).

Two distinct approaches have been taken to investigate the possible mechanisms which may contribute to enhanced myocardial contractility and thus greater stroke volumes with endurance exercise training. One approach has focused on alterations in the contractile element and the other on changes to the various components of E-C coupling which ultimately alter the amount of Ca^{2+} delivered to the myofilaments.

3.3.2.1 *Contractile element*

Some investigators have attributed the enhanced cardiac function, at least in part, to an increase in actomyosin ATPase activity (22, 23). While such alterations have been confirmed using rats subjected to swimming regimens (22, 23), rats that have been treadmill-trained do not appear to undergo alterations in cardiac myosin isoform composition or ATPase activity (52, 109, 135, 180). Treadmill-training of pigs also failed to induce changes in either myosin or myofibrillar ATPase activities (92). Myosin light chain-2 phoshorylation (LC-P) has been proposed to augment myocardial force production. In another study, the extent of LC-P remained unaltered in trained hearts at rest and under conditions of equivalent workload and heart rate as assessed by gel densitometry (52). Extensive *in vitro* experiments have not provided any evidence to suggest that the contractile element undergoes any adaptations resulting from chronic

treadmill training. However, recent experiments using single myocytes have revealed some indication that the contractile element may indeed be altered after training. In this study, enhanced contractile activation was demonstrated in cardiomycytes isolated from treadmill trained rats (125). The reasons for this apparent discrepency are unclear but may involve either different experimental conditions, loss of regulatory factors in the *in vitro* preparations or changes to the contractile element independent of the contractile proteins.

3.3.2.2 *E-C Coupling Alterations*

Alterations in E-C coupling leading to enhanced myocardial contractility will either increase the delivery of Ca^{2+} to the contractile element or enhance the contractile element sensitivity to a given level of Ca^{2+}. In addition to possible adaptations in Ca^{2+} buffering, three organelles could potentially contribute to an increase in Ca^{2+} delivery: 1) the mitochondria, 2) the sarcoplasmic reticulum, and 3) the sarcolemma.

a. Mitochondria. As previously mentioned mitochondria have been clearly implicated to be more important for long term Ca^{2+} regulation rather than for beat-to-beat regulation of contractility (8, 13). *In vitro* studies on the effects of exercise training on myocardial mitochondria function in several species show no improvement in function (139, 171).

b. Sarcoplasmic reticulum. There is limited evidence regarding the nature of SR adaptations with training. Several studies cite evidence which suggest that training increases Ca^{2+} uptake by the SR which may explain the increased rate of cardiac relaxation sometimes observed in trained rats (99, 109, 137, 176). Other studies have failed to demonstrate any differences with chronic training (171, 175). Interpretation of

these data is made difficult due to variations in the mode of training (eg. swimming vs running), animal gender and species. Virtually nothing is known about the effect of training on SR Ca^{2+} release.

c. Sarcolemma. It has been proposed that exercise-induced adaptation of SL function may result in a greater delivery of Ca^{2+} to the contractile element (177). Electrophysiological analysis reaveals a prolonged plateau phase of the action potential in ventricular endocardium from the treadmill-trained rats. In the same study, papillary muscles also generated greater peak isometric twitch tensions (177). Increased SL Ca^{2+} influx may directly activate the myofilaments or trigger an even greater release of Ca^{2+} from the SR. *In vitro* studies have shown an increase in the DHPR density (190), and Na^{+}/Ca^{2+} exchange affinity for Ca^{2+} (178) with training. Marked changes in the lipid composition of cardiac SL vesicles were also observed in another study (182). Specific SL content of total phospholipid and phosphatidylserine (PS) increased by 23 and 50%, respectively. This may be an important adaptation to exercise since PS is an anionic phospholipid known to bind Ca^{2+} and stimulate the Na^{+}/Ca^{2+} exchanger (144). However, the consequences of such changes remain to be determined. In contrast to these data, a recent study found that cardiomyocytes from trained rats shortened to a greater extent in the presence of an apparent reduction in peak cytosolic Ca^{2+} (125). Clearly, exercise adaptations in the mechanisms of E-C coupling are proving to be complex.

d. Ca^{2+} buffering by Calmodulin. As mentioned the major known intracellular Ca^{2+} buffers include the Ca^{2+} binding sites on the external SR, the Ca^{2+} high affinity site on the internal SL, the Ca^{2+}-specific site on TnC, and calmodulin (CaM), all of which

have binding affinities (K_D) in the low (1-100) μM range. Virtually nothing is known regarding the nature (if any) of exercise adaptations in these components. There is, however, some indirect evidence implicating CaM in exercise adaptations.

CaM, a small ubiquitous Ca^{2+} binding protein, posseses four Ca^{2+} binding sites with affinities in the micromolar range. Upon Ca^{2+} binding, CaM produces stable conformers capable of interacting with and activating a number of cytosolic and membrane enzymes including cyclic nucleotide phosphodiesterase, SL Ca^{2+} ATPase, myosin light chain kinase, SR-phospholamban protein kinase, SR Ca^{2+} release channel, and phosphorylase kinase (35, 119, 186, 187). In addition, exogenously added CaM has been shown to modulate Ca^{2+}-dependent Na^{+} channels (151) as well as spontaneous Ca^{2+}-dependent APs in cultured ventricular cell reaggregates isolated from chick embryos (25).

Dihydropyridine (DHP) binding is known to be strongly voltage- and Ca^{2+}-dependent (90, 105). CaM antagonists, a group of agents known to bind to and inhibit CaM and CaM-dependent processes, were found to inhibit radiolabelled DHP binding in rabbit ventricular microsomes at doses similar to CaM inhibition (81). At 1 μM, calmidazolium inhibited [^{3}H]nitrendipine binding by 83%, while the same concentration of trifluoperazine inhibited binding by 28%. In another study, exogenously added CaM (50 nM) increased specific [^{3}H]PN200-110 binding by 200% (189). These data suggest that CaM may play a role in modulating Ca^{2+} channel activity.

To date there has only been one report of total CaM determined in hearts of treadmill-trained and sedentary-control rats (136). While no significant changes were noted, an

indirect method of phosphodiesterase activation was used and the amounts cited were several orders of magnitude lower than typically reported for heart. Because CaM is known to be distributed between both SL and cytosolic compartments, measuring total CaM may not reveal differences in membrane-bound CaM levels after training. Because CaM has been implicated in SL Ca^{2+} channels and that SL Ca^{2+} channel density increases with training in both homogenate and purified SL (190), the potential exists for exercise-induced changes in the levels of SL-bound CaM in the heart.

3.4 Working Hypotheses

The experiments described in this dissertation use three separate approaches (papers I, II, and III) to further investigate the nature of exercise adaptations in the E-C coupling components. The working hypotheses is that myocardial contractility is enhanced with treadmill-training and this is due, at least in part, to greater Ca^{2+} delivery to the myofilaments.

The first approach (paper I) assesses the effects of treadmill-training under four different workrates on DHPR and RyR densities in ventricular homogenates using the same female rat model. The second approach (paper II) assesses possible training-induced alterations in cytosolic Ca^{2+} transients in isolated cardiomyocytes. The third approach addresses whether or not total or SL CaM levels are enhanced as the result of endurance training.

4 E-C COUPLING IN LOWER VERTEBRATES

4.1 INTRODUCTION

Environmental factors such as varying pH, oxygen availability and seasonal temperature changes place unique demands on the hearts of lower vertebrates. In order to meet these demands different strategies have evolved in E-C coupling mechanisms in order to maintain contractility in the different species. For example, trout (*Oncorhynchus mykiss*) are able to maintain high cardiac outputs at both warm (15-20°C) and cold (4-9°C) temperatures despite the negative inotropic effects of cold temperatures. This compensation may be the result of hyperplasia, hypertrophy, alterations in myofilament Ca^{2+} sensitivity or quantitative changes in Ca^{2+} delivery. Those factors involving E-C coupling mechanisms will be reviewed.

4.2 MYOCARDIAL ANATOMY

The most striking comparative feature is that fish, unlike mammals, have a single ventricle receiving venous blood which is subsequently pumped to the gills for oxygenation. In many of these species, including the more primitive hagfish, the myocardium lacks any form of coronary circulation and consists entirely of spongy trabeculae which are nourished by the venous circulation. In the more active species such as the teleosts and the elasmobranchs which are known to tolerate hypoxia, the spongy layer is surrounded by an outer compact layer of varying thickness which supplies oxygenated blood via a coronary circulation. While any differences in E-C coupling

between spongy and compact layers within a given species have yet to be determined, important differences have been noted among the lower vertebrates and under different temperatures in the trout heart (75, 77). Another noteable feature is the smaller myocyte diameters of 2-6 μm compared to ~20-25 μm observed in mammals.

4.3 Contractile Activation

4.3.1 Contractile proteins

4.3.1.1 *Ultrastructure of the contractile element*

The sarcomere structure in the myocardial cells of cyclostomes, elasmobranchs and teleosts is comparable to that observed in the hearts of mammals (153). A, I and Z bands are readily seen under the electron microscope. M lines have not been as well documented, nor has the composition of the N lines which are located on either side of the Z band. In general, less is known about the protein composition of the various bands and their functional roles. As in mammalian striated muscle, six actin-containing thin filament surround each myosin filament which are spaced 20-30 nm apart (153). In some species the myofibrils are located in the periphery of the cell, in other species they are evenly distributed. Morphometric analysis has indicated that the proportion of the cell occupied by myofibrils varies somewhat between species and also between atria (37% of cell volume) and ventricle (47% of cell volume) (195). In the tuna, *Thunnus alalunga,* no significant differences exist between the spongy and compact layers, where the myofibrils occupy 55% and 52% of cell volume, respectively.

4.3.1.2 *Actomyosin ATPase*

Non-dissociating gel electrophoresis has revealed the presence of a single but distinct native myosin isoform in both atria and ventricular tissue of several teleosts (86). However, two isoforms are apparent in the ventricles of goldfish (*Carassius auratus* L.) and arctic char (*Salvelinus alpinus*) (86, 110). The existence of multiple myosin isoforms has been demonstrated using histochemical and immunological techniques even though these isoforms could not be resolved electrophoretically. An example of this is the electrophoretic detection of one myosin isoform in carp ventricle with a myosin ATPase activity ~60% higher on average in the compact compared to that of the spongiosa myocardium (9). These results suggest the presence of multiple myosin isoforms, some of which may not be electrophoretically resolveable. Not only are multiple isoforms present in heart, differential isoform expression is demonstrated by temperature compensation, studied thus far only in fish skeletal muscle (84).

Temperature compensation by poikilotherm fish enables better swimming performance than would otherwise be predicted by seasonal variations in temperature. The majority of studies have focused on the compensatory mechanisms in skeletal muscle. Myofibrillar ATPase activity from goldfish skeletal muscle is ~3 times higher in fish acclimated to 1°C than to 26°C and marked differences in thermal stability were also observed (83). Both electrophoresis (SDS-PAGE) and peptide mapping have failed to reveal any differences in carp fast and slow skeletal myosin heavy chain (MHC) profiles due to temperature compensation (84). In contrast, northern blot analysis has provided evidence of differential MHC isoform expression in warm vs cold-adapted carp skeletal muscle (61). Temperature compensation in some fish species leads to changes in ventricular

mass, heart rate, and mechanical efficiency (63). Myofibrillar changes in response to cold have yet to be examined in the fish heart.

Little is known about the presence or absence of thin filament protein isoforms in the hearts of lower vertebrates. The stimuli for differential isoform expression known to occur in mammals are also present in the enviroment of fishes (eg. starvation, exercise, temperature adaptation). More sensitive techniques and further investigation may reveal a greater diversity than is currently known. The plasticity offered by differential isoform expression would enable fishes to maintain myocardial contractility under those environmental conditions known to depress function.

4.3.1.3 *Ca^{2+} requirements*

As indicated previously, the amount of Ca^{2+} required to generate contractile force depends upon the cytosolic Ca^{2+} buffering capacity and the affinity of TnC for Ca^{2+}. At present, little is known about either the extent of cytosolic Ca^{2+} buffering, or the affinity of TnC for Ca^{2+} in lower vertebrates. Compared to mammals and based on myocyte dimensions, the relative contribution of internal SL Ca^{2+} binding sites would be more while the external SR Ca^{2+} binding sites would be less. Myofibrillar volume is appoximately the same as that in mammals, thus the concentration of TnC would be expected to be similar. Assuming a similar Ca^{2+} requirement and substantially less SR involvement, greater SL influx would be predicted. However, the amount of Ca^{2+} required to generate tension in the hearts of lower vertebrates awaits quantitative knowledge of cytosolic Ca^{2+} buffering. In addition, the temperature and pH dependence

of the buffer K_a values may be of physiological consequence in the maintenance of contractility when exposed to different environments.

In cardiac muscle of homeotherms, the Ca^{2+} sensitivity of the contractile element is profoundly temperature sensitive with reductions in both maximal force and myofibrillar Ca^{2+} sensitivity as temperature is lowered below physiological (66). This potentially cardioplegic influence of lower temperatures must be overcome in poikilotherms either by greater Ca^{2+} delivery or increased Ca^{2+} sensitivity of the contractile apparatus. In the frog, tension generated by skinned cardiac myofibrils are less temperature sensitive compared to rat and more sensitive to Ca^{2+} at any given temperature over the range of 1 to 22°C (67). It appears that a thermal adaptation in Ca^{2+} sensitivity helps to maintain myocardial contractility at lower temperatures experienced by at least some of the lower vertebrate species.

Both pH and temperature can alter the Ca^{2+} sensitivity of myofibrillar ATPase activity. In poikilotherms, a 10°C temperature drop is associated with an increase in pH of ~0.16 to 0.19 units. This α-stat regulation (eg. the stabilization of α-imidazole groups by changing pH_i with varying temperature) could potentially compensate for the desensitizing effects of temperature on myofilament Ca^{2+} sensitivity (169). However, recent experiments have suggested that this α-stat regulation is insufficient to compensation for the temperature effects on myofibrillar Ca^{2+} sensitivity in trout heart (36). Reasons given for this were that the temperature sensitivity of trout myofibrillar ATPase and tension is much greater than the rat preparations and the α-stat pH change

did not offset the temperature effect. It was suggested this was due to an inherent difference involving either TnC or TnI (36). Adaptations in myocardial E-C coupling mechanisms due to chronic exposure to lower temperatures remain largely unknown.

4.4 Regulation Of Ca^{2+} Delivery

4.4.1 Action Potential

In mammals, the action potential duration (APD) varies among species being comparatively short in the rat ventricle, ~100 msec at 23°C, with little or no plateau phase to a longer APD of ~375 msec at 23°C observed in the rabbit (162). Much larger species-dependent variations in APD occur among the lower vertebrates which are also subject to lower physiological temperatures. The longest APDs recorded have been observed in amphibian (~ 723 msec) and agnathan (~1000 msec) ventricles at room temperature (78, 82). Interpretations based upon APD are complicated by the different temperatures under which measurements were taken. It is well known that lower temperatures prolong APD. These recordings, while suggestive, do not necessarily reflect the magnitude of SL Ca^{2+} influx.

The nature of the relationship between the AP and contractile characteristics provides some indirect evidence that the SR is not an important source of Ca^{2+} in some species. Similar to frog, the flounder has a long AP plateau phase and is not sensitive to ryanodine, an agent that affects the ability of the SR to release Ca^{2+} (47). Both frog and elasmobranch venticles lack the post-extrasystolic potentiation attributable to SR Ca^{2+} release. In addition, twitch force is highly sensitive to APD in these species (113).

4.4.2 SL Ca^{2+} influx

Unlike mammalian myocardium, there is some evidence to suggest that SL Ca^{2+} influx is sufficient to support contraction in the poikilotherm heart. The myocardium of lower vertebrates comprises myocytes of smaller diameters which lack T-tubules. The smaller myocyte diameters may serve to reduce diffusional distances and the need for T-tubules. If the I_{ca} densities were comparable, the same SL Ca^{2+} influx into a smaller myocyte volume with similar buffering characteristics could provide a greater rise in cytosolic free Ca^{2+}.

In order for the poikiolotherm to maintain contractility at their physiologically lower temperatures, fundamental differences would be expected in either SL Ca^{2+} channel density or temperature dependence. In mammals, the SL Ca^{2+} channel is highly temperature sensitive with a Q_{10} of ~3.0 (34). Recently, the SL Ca^{2+} channel from trout heart was purified and partially characterized. While the α_{1C} appears to be of similar molecular weight, structural differences were apparent in the regulatory α_2 subunit (Tuana, B.S. *et al*, in preparation). In addition, DHPR density as measured by radiolabelled ligand binding to purified SL vesicles from trout heart was greater than that measured in purified rat SL (179). However, it is unknown whether the differences in DHPR density are real or reflect species differences in SL purification. The I_{ca} density has yet to be determined in this species, but measurements from frog ventricular myocytes suggest the Ca^{2+} current density is close to mammalian values (116). Ca^{2+} channel density alterations also provides a means by which SL Ca^{2+} influx could

potentially be altered in order to maintain contractility at the lower temperatures. In support of this, DHPR density in ventricular homogenates from cold-adapted trout increased by ~17% compared to warm-adapted trout (65).

4.4.3 SR Ca^{2+} release

A role for SR Ca^{2+} release in a number of poikilotherm hearts, including several teleosts, is generally dismissed because electron microscopy reveals a relative sparseness and lack of organizational complexity of SR. The SR which typically accounts for ~7% of myocyte volume in rat only accounts for ~0.5% in fish and amphibians (153). Experiments measuring contractile force in ventricular strips do not show substantial reductions in force in the presence of ryanodine or caffeine under physiological stimulation frequencies and temperatures (45, 77). However, a role for SR Ca^{2+} release in E-C coupling cannot be ruled out in all lower vertebrates, particularly the more active teleosts and endotherms where a more rapid cycling of Ca^{2+} may be required to maintain brief active states consistent with high heart rates. Potentiation of twitch force has been demonstrated in ventricular strips from trout at 15°C and to a greater extent at 25°C, which can be abolished by ryanodine (75). However, in trout ventricle which has a shorter AP and less pronounced plateau phase compared to either amphibia or flounder, changes in APD are still correlated to changes in twitch force under some conditions (77).

4.4.4 Mitochondrial Ca^{2+} regulation

The contribution by mitochondria to regulation of Ca^{2+} delivery has yet to be assessed in the hearts of lower vertebrates. Due to the slower rate of tension development in many

poikilotherm hearts (181), a role for mitochondrial Ca^{2+} uptake and release can not be automatically precluded as it has in the faster beating mammalian heart.

4.5 Myocardial Relaxation

Currently, it is not known to what extent, if any, the SL Ca^{2+} ATPase and mitochondria participate in relaxation. This part of the review will therefore focus on what is known about the role of SR and SL in the relaxation process.

4.5.1 SR Ca^{2+} uptake

While the SR is sparsely developed in the hearts of poikilotherms studied thus far, there is some evidence that the SR Ca^{2+} ATPase may participate in myocardial relaxation is some species such as the trout. $^{45}Ca^{2+}$ uptake by the SR in both thin sections and crude homogenate preparations from trout at 10°C and 15°C, respectively, were similar to that observed in rat heart at 37°C (46, 114). These *in vitro* data suggest that the SR is capable of functioning at rates comparable to mammals at physiological temperatures.

4.5.2 SL Ca^{2+} efflux

Several lines of evidence suggest that Na^+/Ca^{2+} exchange may play a prominant role in mechanical relaxation of the teleost heart. Elevation of extracellular Na^+ was found to reduce the positive inotropy due to an increase in stimulation frequency from 0.2 to 1.0 Hz in ventricular strips from trout (45, 77). An increase in twitch force was observed in paced ventricular strips of flounder (*Platichthys flesus* L.) upon lowering extracellular Na^+ while at the same time $^{45}Ca^{2+}$ efflux decreased (62). The exchanger from both

amphibia (19) and trout (183) is less temperature sensitive compared with mammals. The trout exchanger exhibits a Q_{10} of ~1.2 compared to >2.0 for the canine exchanger. At 7°C, initial rates of Na^+-dependent Ca^{2+} uptake in the trout were 4 to 7-fold higher in reconstituted and native vesicles, respectively, compared to the canine exchanger (183). This suggests the differences between trout and canine Na^+/Ca^{2+} exchange activity are intrinsic to the protein and independent of the lipid environment. However, there is substantial homology between mammalian and lower vertebrate Na^+/Ca^{2+} exchanger. A cDNA probe from the canine cardiac Na^+/Ca^{2+} exchanger hybridizes to trout mRNA and western blots of mammalian, amphibian and trout SL display identical banding patterns using rabbit polyclonal antibodies (183).

Thus far it appears that the Na^+/Ca^{2+} exchange is the primary means of Ca^{2+} extrusion in the hearts of lower vertebrates. However, the relative roles of the SR Ca^{2+} ATPase, SL Ca^{2+} ATPase and Na^+/Ca^{2+} exchange in contributing to mechanical relaxation remain to be examined in fish heart.

4.6 Working Hypotheses

Compared to mammals, lower vertebrates generally have a paucity of SR, lower heart rates, smaller myocyte diameters, and at least in the trout a pronounced AP plateau phase and more active Na^+/Ca^{2+} exchange. Based on this information it has been proposed that SL influx of Ca^{2+} plays a more prominant role as a source of contractile Ca^{2+} in lower vertebrates. Secondly, among the lower vertebrates DHPR and RyR densities are

proposed to correlate with the cardiovascular demands (eg. heart rate and cardiac output) of each species. To test these hypotheses DHPR and RyR binding densities were determined in crude homogenates of phylogenetically distinct species (rat, trout, dogfish and hagfish).

5 SUMMARY OF HYPOTHESES

5.1 General Hypothesis

The main premise of this thesis is that myocardial E-C coupling varies with phylogeny and perturbations such as exercise, temperature compensation, pharmacological intervention and ontogeny.

5.1.1 Exercise Adaptations

The first premise of this thesis is that endurance exercise-training leads to enhanced myocardial contractility. This increase in contractility is due, at least in part, to greater Ca^{2+} delivery to the myofilaments.

5.1.1.1 *Specific Hypothesis.* Endurance treadmill-training increases the amount of Ca^{2+} delivered to the contractile element, at least in part, by increasing DHPR and/or RyR densities.

5.1.1.2 *Specific Hypothesis.* The peak intracellular free Ca^{2+} concentration is increased with each beat as a consequence of training and is due, at least in part, to an adaptation in the ability of the SR to sequester, store and release more Ca^{2+}.

5.1.1.3 *Specific Hypothesis.* The relative amount of calmodulin is increased as a consequence of exercise training.

5.1.2 Phylogenetic Differences (Mammals vs Lower Vertebrates)

The second premise of this thesis is that the hearts of lower vertebrates compared to mammals rely to a greater extent on extracellular Ca^{2+} to support contraction. One of several ways to increase SL Ca^{2+} influx is to increase the density of SL Ca^{2+} channels.

5.1.2.1 *Specific Hypothesis.* The density of dihyropyridine receptors (DHPR), in receptor number per unit cell volume, will be the same or greater in ventricular homogenates from lower vertebrates compared to mammals.

5.1.2.2 *Specific Hypothesis.* The density of ryanodine receptors, in receptor number per unit cell volume, will be less in ventricular homogenates from lower vertebrates compared to mammals.

5.1.3 Phylogenetic Differences (Lower Vertebrates)

The third premise of this thesis is that among the lower vertebrates, E-C coupling will vary according to the cardiovascular demands of each species.

5.1.3.1 *Specific Hypothesis.* The trout, capable of the higher heart rates and cardiac outputs compared to the dogfish and hagfish, will express DHPR and RyR densities greater than those in the dogfish which will express greater DHPR and RyR densities compared to the hagfish.

6 REFERENCES

1. Aceto, J. F., M. Condrescu, C. Kroupis, H. Nelson, N. Nelson, D. Nicoll, K. D. Philipson, and J. P. Reeves. Cloning and expression of the bovine cardiac sodium-calcium exchanger. Arch. Biochem. Biophys. 298: 553-560, 1992.

2. Adams, B. A., T. Tanabe, and K. G. Beam. Ca^{2+} current activation rate correlates with alpha1 subunit density. Biophys. J. 71: 156-162, 1996.

3. Anderson, K., R. Grunwald, A. El-Hashem, R. Sealock, and G. Meissner. High affinity ryanodine and PN200-110 binding to rabbit skeletal muscle triads. Biophys. J. 57: 171a, 1990.

4. Anderson, P. A. W., G. E. Moore, and R. N. Nassar. Developmental changes in the expression of rabbit left ventricular troponin T. Circ. Res. 63: 742-747, 1988.

5. Baldwin, K. M. Effects of chronic exercise on biochemical and functional properties of the heart. Med. Sci. Spts. Exerc. 17: 522-528, 1985.

6. Baldwin, K. M., W. W. Winder , and J. O. Holloszy. Adaptation of actomyosin ATPase in different types of muscle to endurance exercise. Am. J. Physiol. 229: 422-426, 1975.

7. Balke, C. W., T. M. Egan, and G. W. Wier. Processes that remove calcium from the cytoplasm during excitation-contraction coupling in intact rat heart cells. J. Physiol. 474: 447-462, 1994.

8. Basani, R. A., J. W. M. Basani, and D. M. Bers. Mitochondrial and sarcolemmal Ca^{2+} reduce $[Ca]_i$ during caffeine contractures in rabbit cardiac myocytes. J. Physiol. 453: 591-608, 1992.

9. Bass, A., B. Ostadal, V. Pelouch, and V. Vitek. Differences in weight parameters, myosin-ATPase activity and the enzyme pattern of energy supplying metabolism between the compact and the spongious cardiac musculature of carp (Cyprinus carpio) and turtle (testudo horsfieldi). Pflugers. Arch. 343: 65-77, 1973.

10. Bassani, J. W., R. A. Bassani, and D. M. Bers. Relaxation in rabbit and rat cardiac cells: species-dependent differences in cellular mechanisms. J. Physiol. 476: 279-293, 1994.

11. Bers, D. M. Early transient depletion of extracellular calcium during individual muscle contraction. Am. J. Physiol. 244: H462-H468, 1983.

12. Bers, D. M. Excitation-contraction coupling and cardiac contractile force. Dordrecht: Kluwer Academic Publishers, 1991.

13. Bers, D. M., and J. H. B. Bridge. Relaxation of rabbit ventricular muscle by Na-Ca exchange and sarcoplasmic reticulum calcium pump. Circ. Res. 65: 334-342, 1989.

14. Bers, D. M., J. H. B. Bridge, and K. W. Spitzer. Intracellular Ca^{2+} transients during rapid cooling contractures in guinea-pig ventricular myocytes. J. Physiol. 417: 537-553, 1989.

15. Bers, D. M., D. M. Christensen, and T. X. Nguyen. Can Ca entry via Na-Ca exchange directly activate cardiac muscle contraction? J. Mol. Cell. Cardiol. 20: 405-414, 1988.

16. Bers, D. M., and G. A. Langer. Uncoupling cation effects on cardiac contractility and sarcolemmal calcium binding. Am. J. Physiol. 237: H332-H341, 1979.

17. Bers, D. M., and V. A. Stiffel. Ratio of ryanodine to dihydropyridine receptors in cardiac and skeletal muscle and implications for E-C coupling. Am. J. Physiol. 264: C1587-C1593, 1993.

18. Bersohn, M. M., and J. Scheuer. Effects of physical training on end-diastolic volume and myocardial performance of isolated rat hearts. Circ. Res. 140: 510-516, 1977.

19. Bersohn, M. M., R. Vemuri, D. S. Schuil, and K. D. Philipson. Effect of temperature on Na^{+}-Ca^{2+} exchange in sarcolemma from mammalian and amphibian hearts. Biochimica et Biophysica Acta 1062: 19-23, 1991.

20. Beuckelmann, D. J., and W. G. Wier. Mechanism of release of calcium from sarcoplasmic reticulum of guinea-pig cardiac cells. J. Physiol. 405: 233-255, 1988.

21. Beuckelmann, D. J., and W. G. Wier. Sodium-calcium exchange in guinea-pig cardiac cells: Exchange current and changes in intracellular Ca^{2+}. J. Physiol. 414: 499-520, 1989.

22. Bhan, A. K., and J. Scheuer. Effects of physical training on cardiac actomyosin adenosine triphosphatase activity. Am. J. Physiol. 223: 1486-1490, 1972.

23. Bhan, A. K., and J. Scheuer. Effects of physical training on cardiac myosin ATPase activity. Am. J. Physiol. 228: 1178-1182, 1975.

24. Birnbaumer, L., K. P. Campbell, W. A. Catterall, M. M. Harpold, F. Hofmann, W. A. Horne, Y. Mori, A. Schwartz, T. Snutch, T. Tanabe, and R. W. Tsien. The naming of voltage-gated calcium channels. Neuron 13: 505-506, 1994.

25. Bkaily, G., and N. Sperelakis. Calmodulin is required for full activation of the calcium slow channels in heart cells. J. Cyclic Nucleo. Prot. Phos. Res. 11: 25-34, 1986.

26. Blanchard, E. M., and R. J. Solaro. Inhibition of the activation and troponin calcium binding of dog cardiac myofibrils by acidic pH. Circ. Res. 55: 382-391, 1984.

27. Block, B. A., T. Imagawa, K. P. Campbell, and C. Franzini-Armstrong. Structural evidence for direct interaction between the molecular components of the transverse-tubule/sarcoplasmic reticulum junction in skeletal muscle. J. Cell. Biol. 107: 2587-2600, 1988.

28. Blomqvist, C. G., and B. Saltin. Cardiovascular adaptations to physical training. Ann. Rev. Physiol. 45: 169-189, 1983.

29. Bossen, E. H., J. R. Sommer, and R. A. Waugh. Comparative stereology of mouse atria. Tissue Cell 13: 71-77, 1981.

30. Bridge, J. H. B. Relationsips between sarcoplasmic reticulum and sarcolemmal calcium transport revealed by rapidly cooling rabbit ventricular muscle. J. Gen. Physiol. 88: 437-473, 1986.

31. Carafoli, E. Mitochondria, Ca^{2+} transport and the regulation of heart contraction and metabolism. J. Mol. Cell. Cardiol. 7: 83-89, 1975.

32. Carl, S. L., K. Felix, A. H. Caswell, N. R. Brandt, and W. J. J. Ball. Immunolocalization of sarcolemmal dihydropyridine receptor and sarcoplasmic reticular triadin and ryanodine receptor in rabbit ventricle and atrium. J. Cell Biol. 129: 673-682, 1995.

33. Carroll, S., J. G. Skarmeta, X. Yu, K. D. Collins, and G. Inesi. Interdependence of ryanodine binding, oligomeric receptor interactions, and Ca^{2+} release regulation in junctional sarcoplasmic reticulum. Archs. Biochem. Biophys. 290: 239-247, 1991.

34. Cavalie, A., T. F. McDonald, D. Pelzer, and W. Trautwein. Temperature-induced transitory and steady-state changes in the calcium current of guinea pig ventricular myocytes. Pflugers Arch. 405: 294-296, 1985.

35. Cheung, W. Y. Calmodulin plays a pivotal role in cellular regulation. Science 207: 19-27, 1980.

36. Churcott, C. S., C. D. Moyes, B. H. Bressler, K. M. Baldwin, and G. F. Tibbits. Temperature and pH effects on Ca^{2+} sensitivity of cardiac myofibrils: a comparison of trout and mammals. Am. J. Physiol. 267: R62-R70, 1994.

37. Clausen, J. P. Effect of physical training on cardiovascular adjustments to exercise in man. Pysiol. Rev. 57: 779-815, 1977.

38. Coronado, R., J. Morrissette, M. Sukhareva, and D. M. Vaughan. Structure and function of ryanodine receptors. Am. J. Physiol. 266: C1485-C1504, 1994.

39. Cousineau, D., R. J. Ferguson, J. DeChamplain, P. Gauthier, P. Cote, and M. Bourassa. Catecholamines in coronary sinus during exercise in man before and after training. J. Appl. Physiol. 43: 801-806, 1977.

40. Crews, J., and E. E. Aldinger. Effect of chronic exercise on myocardial function. Am. Heart J. 74: 536-542, 1967.

41. De Jongh, K. S., C. Warner, and W. A. Catterall. Subunits of purified calcium channels. J. Biol. Chem. 265: 14738-14741, 1990.

42. De Leon, M., Y. Wang, L. Jones, E. Perez-Reyes, X. Wei, T. W. Soong, T. P. Snutch, and D. T. Yue. Essential Ca^{2+}-binding motif for Ca^{2+}-sensitive inactivation of L-type Ca^{2+} channesl. Science 270: 1502-1506, 1995.

43. Dixon, D. A., and D. H. Haynes. Kinetic characterization of the Ca^{2+}-pumping ATPase of cardiac sarcolemma in four states of activation. J. Biol. Chem. 264: 13612-13622, 1989.

44. Dowell, R. T. Cardiac adaptations to exercise. Exer. Spt. Sci. Rev. 11: 99-116, 1983.

45. Driedzic, W. R., and H. Gesser. Differences in force-frequency relationships and calcium dependency between elasmobranch and teleost hearts. J. Exp. Biol. 140: 227-241, 1988.

46. Dybro, L., and H. Gesser. Capacity of the sarcoplasmic reticulum (SR) and contractility in heart of 5 vertebrate species. Acta Physiol. Scand. 128: 52A, 1986.

47. El-Sayed, M. F., and H. Gesser. Sarcoplasmic reticulum, potassium, and cardiac force in rainbow trout and plaice. Am. J. Physiol. 257: R599-R604, 1989.

48. Fabiato, A. Calcium release in skinned cardiac cells: Variations with species, tissues, and development. Fed. Proc. 41: 238-2244, 1982.

49. Fabiato, A. Calcium-induced release of calcium from the cardiac sarcoplasmic reticulum. Am. J. Physiol. 245: C1-C14, 1983.

50. Fabiato, A. Time and calcium dependence of activation and inactivation of calcium-induced calcium release of calcium from the sarcoplasmic reticulum of a skinned canine cardiac Purkinje cell. J. Gen. Physiol. 85: 247-289, 1985.

51. Fabiato, A., and F. Fabiato. Effects of pH on the myofilaments and the saracoplasmic reticulum of skinned cells from cardiac and skeletal muscles. J. Physiol. 276: 233-255, 1978.

52. Fitzsimons, D. P., P. W. Bodell, R. E. Herrick, and K. M. Baldwin. Left ventricular functional capacity in the endurance-trained rodent. J. Appl. Physiol. 69: 305-312, 1990.

53. Flaim, S. F., W. J. Minteer, D. P. Clark, and R. Zelis. Cardiovascular response to acute aquatic and treadmill exercise in the untrained rat. J. Appl. Physiol. Respirat. Environ. Exercise Physiol. 46: 302-308, 1979.

54. Fleischer, S., and M. Inui. Biochemistry and biophysics of excitation-contraction coupling. Ann. Rev. Biophys. Chem. 18: 333-364, 1989.

55. Fozzard, H. A., and M. F. Arnsdorf. Cardiac electrophysiology. New York: Raven Press, Ltd., 1992.

56. Frank, J. S., G. Mottino, D. Reid, R. S. Molday, and K. D. Philipson. Distribution of the Na^{+}-Ca^{2+} exchange protein in mamalian cardiac myocytes: an immunofluorescence and immunocolloidal gold-labeling study. J. Cell Biol. 117: 337-345, 1992.

57. Franzini-Armstrong, C., and L. Castellani. The foot protein is ancient. Biophys. J. 55: 206A, 1989.

58. Franzini-Armstrong, C., and J. W. Kish. Alternate disposition of tetrads in peripheral couplings of skeletal muscle. J. Ms. Res. Cell Motil. 16: 319-324, 1995.

59. Fuller, E. O., and D. O. Nutter. Endurance training in the rat II: Performance of isolated and intact heart. J. Appl. Physiol. 51: 941-947, 1981.

60. Gao, W. D., P. H. Backx, M. Azan-Backx, and E. Marban. Myofilament Ca^{2+} sensitivity in intact versus skinned rat ventricular muscle. Circ. Res. 74: 408-415, 1994.

61. Gerlach, G. F., L. Turay, K. T. A. Malik, J. Lida, A. Scutt, and G. Goldspink. Mechanisms of temperature acclimation in carp: a molecular biology approach. Am. J. Physiol. 259: R237-R244, 1990.

62. Gesser, H., and A. Mangor-Jensen. Contractility and ^{45}Ca fluxes in heart muscle of flounder at a lowered extracellular NaCl concentration. J. Exp. Biol. 109: 201-207, 1984.

63. Graham, M. S., and A. P. Farrell. Myocardial oxygen consumption in trout acclimated to 5°C and 15°C. Physiol. Zool. 63: 536-554, 1990.

64. Hamilton, S. L., J. Codina, M. J. Hawkes, A. Yatani, T. Sawada, F. M. Strickland, S. C. Froehner, A. M. Spiegel, L. Toro, E. Stefani, L. Birnbaumer, and A. M. Brown. Evidence for direct interaction of G_S-a with the Ca^{2+} channel of skeletal muscle. J. Biol. Chem. 266: 19528-19535, 1991.

65. Hamman, B. N., and G. F. Tibbits. Cardiac dihydropyridine receptor (DHPR) density is increased in the cold-acclimated trout oncorhynchus mykiss. The Physiologist 57: A-94, 1994.

66. Harrison, S. M., and D. M. Bers. The influence of temperature on the calcium sensitivity of the myofilaments of skinned ventricular muscle from the rabbit. J. Gen. Physiol. 93: 411-427, 1989.

67. Harrison, S. M., and D. M. Bers. Temperature dependence of myofilament Ca sensitivity of rat, guinea pig, and frog ventricular muscle. Am. J. Physiol. 258: C274-C281, 1990.

68. Hepp, A., M. Hansis, R. Gulch, and R. Jacob. Left ventricular isovolumetric pressure-volume relations, "diastolic tone", and contractility in the rat heart after physical training. Basic Res. Cardiol. 69: 516-528, 1974.

69. Hilgemann, D. W. Nature 344: 242-245, 1990.

70. Hilgemann, D. W. Extracellular calcium transients at single excitations in rabbit atrium measured with tetramethylmurexide. J. Gen. Physiol. 87: 707-735, 1986.

71. Hilgemann, D. W., D. A. Nicoll, and K. D. Philipson. Charge movement during Na^+ translocation by native and cloned cardiac Na^+/Ca^{2+} exchanger. Nature 352: 715-718, 1991.

72. Hirano, Y., H. A. Fozzard, and C. T. January. Characteristics of L- and T-type Ca2+ currents in canine cardiac purkinje cells. Am. J. Physiol. 256: H1478-H1492, 1989.

73. Hosey, M. M., M. Borsotto, and M. Lazdunski. Phosphorylation and dephosphorylation of dihydropyridine-sensitive voltage-dependent Ca^{2+} channel

in skeletal muscle membranes by cAMP- and Ca^{2+}-dependent processes. Proc. Natl. Acad. Sci. USA. 83: 3733-3737, 1986.

74. Hosey, M. M., and M. Lazdunski. Calcium channels: Molecular pharmacology, structure and regulation. J. Membr. Biol. 104: 81-105, 1988.

75. Hove-Madsen, L. The influence of temperature on ryanodine sensitivity and the force-frequency relationship in the myocardium of rainbow trout. J. Exp. Biol. 167: 47-60, 1992.

76. Hove-Madsen, L., and D. M. Bers. Indo-1 binding to protein in permabilized ventricular myocytes alters its spectral and Ca binding properties. Biophys. J. 63: 89-97, 1992.

77. Hove-Madsen, L., and H. Gesser. Force-frequency relation in the myocardium of rainbow trout. J. Comp. Physiol. B. 159: 61-69, 1989.

78. Hume, J. R., and W. Giles. Active and passive electrical properties of single bullfrog atrial cells. J. Gen. Physiol. 78: 19-42, 1982.

79. Inui, M., A. Saito, and S. Fleischer. Isolation of the ryanodine receptor from cardiac sarcoplasmic reticulum and identity with the feet structures. J. Biol. Chem. 262: 15637-15642, 1987.

80. James, P. M., M. Inui, M. Tada, M. Chiesi, and E. Carafoli. Nature and site of phospholamban regulation of the calcium pump of sarcoplasmic reticulum. Nature 342: 90-92, 1989.

81. Janis, R. A., J. G. Sarmiento, S. C. Maurer, G. T. Bolger, and D. J. Triggle. Characteristics of the binding of [^{3}H]NTP to rabbit ventricular membranes:

modification by other calcium channel antagonists and by the calcium channel agonist Bay K8644. J. Pharm. Exp. Ther. 231: 8-15, 1984.

82. Jensen, D. The aneural heart of the hagfish. Ann. N. Y. Acad. Sci. 127: 443-458, 1965.

83. Johnston, I. A., W. Davison, and G. Goldspink. Adaptations in Mg^{2+}-activated myofibrillar ATPase activity induced by temperature acclimation. FEBS Lett. 50: 293-295, 1975.

84. Johnston, I. A., J. D. Fleming, and T. Crockford. Thermal acclimation and muscle contractile properties in cyprinid fish. Am. J. Physiol. 259: R231-R236, 1990.

85. Jorgensen, A. O., A. C. Shen, W. Arnold, P. S. McPherson, and K. P. Campbell. The Ca^{2+}-release channel/ryanodine receptor is localized in junctional and corbular sarcoplasmic reticulum in cardiac muscle. J. Cell Biol. 120: 969-980, 1993.

86. Karasinski, J. Myosin isozymes of fish hearts. Comp. Biochem. Physiol. 91B: 359-363, 1988.

87. Kentish, J. C., H. E. D. J. ter Keurs, L. Ricciardi, J. J. J. Bucx, and M. I. M. Noble. Comparison between the sarcomere length-force relations of intact and skinned trabeculae from rat right ventricle. Circ. Res. 58: 755-768, 1986.

88. Kim, H. W., N. A. E. Steenaart, D. G. Ferguson, and E. G. Kranias. Functional reconstitution of the cardiac sarcoplasmic reticulum Ca^{2+} ATPase with phospholamban in phospholipid vesicles. J. Biol. Chem. 265: 1702-1709, 1990.

89. Kofuji, P., W. J. Lederer, and D. H. Schulze. Mutually exclusive and cassette exons underlie alternatively spliced isoforms of the Na/Ca exchanger. J. Biol. Chem. 269: 5145-5149, 1994.

90. Kokubun, S., B. Prod'hom, C. Becker, H. Porzig, and H. Reuter. Studies on Ca channels in intact cardiac cells: Voltage-dependent effects and cooperative interactions of dihydropyridine enantiomers. Mol. Pharmacol. 30: 571-584, 1986.

91. Lai, F. A., H. P. Erickson, Q. Liu, and G. Meissner. Purification and reconstitution of the calcium-release channel from skeletal muscle. Nature 331: 315-319, 1988.

92. Laughlin, M. H., C. C. Hale, L. Novela, D. Gute, N. Hamilton, and C. D. Ianuzzo. Biochemical characterization of exercise-trained porcine myocardium. J. Appl. Physiol. 71: 229-235, 1991.

93. Laughlin, M. H., and R. M. McAllister. Exercise training-induced coronary vascular adaptation. J. Appl. Physiol. 73: 2209-2225, 1992.

94. Le Peuch, C. J., and J. G. Demaille. Covalent regulation of the cardiac sarcoplasmic reticulum calcium pump. Cell Calcium 10: 397-400, 1989.

95. LeBlanc, N., and J. R. Hume. Sodium current-induced release of calcium from cardiac sarcoplasmic reticulum. Science 248: 372-375, 1990.

96. Lee, H. C., R. Aarhus, and R. M. Graeff. Sensitization of calcium-induced calcium release by cyclic ADP-ribose and calmodulin. J. Biol. Chem. 270: 9060-9066, 1995.

97. Lee, K. S., and L. W. Tsien. Reversal of current through calcium channels in dialysed single heart cells. Nature 297: 498-501, 1982.

98. Lee, S. L., A. S. Yu, and J. Lytton. Tissue-specific expression of Na^{+}-Ca^{2+} exchanger isoforms. J. Biol. Chem. 269: 14849-14852, 1994.

99. Levine, S. N., and G. T. Kinasewitz. Exercise conditioning increases rat myocardial calcium uptake. J. Appl. Physiol. 60: 1673-1679, 1986.

100. Levitsky, D. O., B. D. S., T. S. Levchenko, V. N. Smirnov, and E. I. Chazov. Calcium-binding rate and capacity of cardiac sarcoplasmic reticulum. J. Mol. Cell. Cardiol. 13: 785-796, 1981.

101. Lew, W. Y. W., L. V. Hryshko, and D. M. D.M. Bers. Dihydropyridine receptors are primarily functional L-type calcium channels in rabbit ventricular myocytes. Circulation Res. 69: 1139-1145, 1991.

102. Li, Z., S. Matsuoka, L. V. Hryshko, D. A. Nicoll, M. M. Bersohn, E. P. Burke, R. P. Lifton, and K. D. Philipson. J. Biol. Chem. 269: 17434-17439, 1994.

103. Li, Z., D. A. Nicoll, A. Collins, D. W. Hilgemann, A. G. Filoteo, J. T. Penniston, J. N. Weiss, J. M. Tomich, and K. D. Philipson. Identification of a peptide inhibitor of the cardiac sarcolemmal Na^{+}-Ca^{2+} exchanger. J. Biol. Chem. 266: 1014-1020, 1991.

104. Low, W., J. Kasir, and H. Rahamimoff. Cloning of the rat heart Na^{+}-Ca^{2+} exchanger and its functional expression in HeLa cells. FEBS lett. 316: 63-67, 1993.

105. Luchowski, E. M., F. Yousif, D. J. Triggle, S. C. Maurer, J. G. Sarmiento, and R. A. Janis. Effects of Metal Cations and Calmodulin Antagonists on [^{3}H]

Nitrendipine Binding in Smooth and Cardiac Muscle. Jn. Pharm. Exp. Ther. 230: 607-613, 1984.

106. Luo, W., I. L. Grupp, J. Harrer, S. Ponniah, G. Grupp, J. J. Duffy, T. Doetschman, and E. G. Kranias. Targeted ablation of the phospholamban gene is associated with markedly enhanced myocardial contractility and loss of beta-agonist stimulation. Circ. Res. 75: 401-409, 1994.

107. Lytton, J., and D. H. MacLennan. Sarcoplasmic reticulum. In: The heart and cardiovascular system (Second ed.), edited by H. A. Fozzard, E. Haber, R. B. Jennings and A. M. Katz. New York: Raven Press, 1992, p. 1203-1222.

108. MacLennan, D. H., C. J. Brandl, B. Korczak, and N. M. Green. Amino-acid equence of a Ca^{2+} + Mg^{2+}-dependent ATPase from rabbit muscle sarcoplasmic reticulum, deduced from its complementary DNA sequence. Nature 316: 696-700, 1985.

109. Malhotra, A., S. Penpargkul, T. Schaible, and J. Scheuer. Contractile proteins and sarcoplasmic reticulum in physiologic cardiac hypertrophy. Am. J. Physiol. 241: H263-H267, 1981.

110. Martinez, I., J. S. Christiansen, R. Ofstad, and R. L. Olsen. Comparison of myosin isoenzymes present in skeletal and cardiac muscles of the Arctic char Salvelinus alpinus (L.) - Sequential expression of different myosin heavy chains during development of the fast white skeletal muscle. Eur. J. Biochem. 195: 743-753, 1991.

111. Matsuoka, S., D. A. Nicoll, L. V. Hryshko, D. O. Leviatsky, J. N. Weiss, and K. D. Philipson. Regulation of the cardiac Na^{+}-Ca^{2+} exchanger by Ca^{2+}.

Mutational analysis of the Ca^{2+}-binding domain. J. Gen. Physiol. 105: 403-420, 1995.

112. Mattera, R., M. P. Graziano, A. Yatani, A. Ahou, R. Graf, J. Codina, L. Birnbaumer, A. G. Gilman, and A. M. Brown. Splice variants of the alpha-subunit of the G protein G_S activate both adenylyl cyclase and calcium channels. Science 243: 804-807, 1989.

113. Maylie, J., M. G. Nunzi, and M. Morad. Excitation-contraction coupling in ventricular muscle of dogfish (Squalus acanthias). Bull. Mt. Desert Island Biol. Lab. 19: 84-87, 1979.

114. McArdle, H. J., and I. A. Johnston. Ca^{2+}-uptake by tissue sections and biochemical characteristics of sarcoplasmic reticulum isolated from fish fast and slow muscles. Eur. J. Cell Biol. 25: 103-107, 1981.

115. McAuliffe, J. J., L. Gao, and R. J. Solaro. Changes in myofibrillar activation and troponin C Ca^{2+} binding associated with troponin T isoform switching in developing rabbit heart. Circ. Res. 66: 1204-1216, 1990.

116. McDonald, T. F., S. Pelzer, W. Trautwein, and D. J. Pelzer. Regulation and modulation of calcium channels in cardiac, skeletal, and smooth muscle cells. Physiol. Rev. 74: 365-507, 1994.

117. Meissner, G. Ryanodine receptor/Ca^{2+} release channels and their regulation by endogenous effectors. Ann. Rev. Physiol. 56: 485-508, 1994.

118. Meissner, G., E. Darling, and J. Eveleth. Kinetics of rapid Ca^{2+} release by sarcoplasmic reticulum: effects of Ca^{2+}, Mg^{2+}, and adenine nucleotides. Biochem. 25: 236-244, 1986.

119. Meissner, G., and J. S. Henderson. Rapid calcium release from cardiac sarcoplasmic reticulum vesicles is dependent on Ca^{2+} and is modulated my Mg^{2+}, adenine nucleotide, and calmodulin. J. Biol. Chem. 262: 3065-3073, 1987.

120. Mikami, A., K. Imoto, T. Tanabe, T. Niidome, Y. Mori, H. Takeshima, S. Narumiya, and S. Numa. Primary structure and functional expression of the cardiac dihydropyridine-sensitive calcium channel. Nature 340: 230-233, 1989.

121. Mitra, R., and M. Morad. Two types of calcium channels in guinea pig ventricular myocytes. Proc. Natl. Acad. Sci. USA 83: 5340-5344, 1986.

122. Miura, Y., and J. Kimura. Sodium-calcium exchange current. J. Gen. Physiol. 93: 1129-1145, 1989.

123. Miyata, H., H. S. Silverman, S. J. Sollott, E. G. Lakatta, M. D. Stern, and R. G. Hansford. Measurement of mitochondrial free Ca^{2+} concentration in living single rat cardiac myocytes. Am. J. Physiol. 261: H1123-H1134, 1991.

124. Mole, P. Increased contractile potential of papillary muscles from exercise-trained rat hearts. Am. J. Physiol. 234: H421-H425, 1978.

125. Moore, R. L., T. I. Musch, R. V. Yelamarty, R. C. Scaduto Jr., A. M. Semanchick, M. Elensky, and J. Y. Cheung. Chronic exercise alters contractility and morphology of isolated rat cardiac myocytes. Am. J. Physiol. 264: C1180-C1189, 1993.

126. Nabauer, M., G. Callewaert, L. Cleeman, and M. Morad. Regulation of calcium release is gated by calcium current, not gating charge, in cardiac myocytes. Science 244: 800-803, 1989.

127. Nakai, J., T. Imagawa, Y. Hakamata, M. Shigekawa, H. Takeshima, and S. Numa. Primary structure and functional expression from cDNA of cardiac muscle ryanodine receptor/calcium release channel. FEBS lett. 271: 169-177, 1990.

128. Nastainczyk, W., A. Rohrkasten, M. Sieber, C. Rudolph, C. Schachteie, D. Marme, and F. Hofmann. Phosphorylation of the purified receptor for calcium channel blockers by cAMP kinase and protein kinase C. Eur. J. Biochem. 169: 137-142, 1987.

129. Negretti, N., S. C. O'Neill, and D. A. Eisner. The relative contributions of different intracellular and sarcolemmal systems to relaxation in rat ventricular myocytes. Cardiovasc. Res. 27: 1826-1830, 1993.

130. Nicoll, D. A., L. V. Hryshko, S. Matsuoka, J. S. Frank, and K. D. Philipson. Mutation of amino acid residues in the putative transmembrane segments of the cardiac sarcolemmal Na^{+}-Ca^{2+} exchanger. J. Biol. Chem. 271: 13385-13391, 1996.

131. Nicoll, D. A., S. Longi, and K. D. Philipson. Molecular cloning and functional expression of the cardiac sarcolemmal Na^{+}-Ca^{2+} exchanger. Science 250: 562-565, 1990.

132. Nutter, D. O., and E. O. Fuller. The role of isolated cardiac muscle preparations in the study of training effects on the heart. Med. Sci. Spts. 9: 239-245, 1977.

133. Otsu, K., H. F. Willard, V. K. Khanna, F. Zorzato, N. M. Green, and D. H. MacLennan. Molecular cloning of cDNA encoding the Ca^{2+} release channel (ryanodine receptor) of rabbit cardiac muscle sarcoplasmic reticulum. J. Biol. Chem. 265: 13472-13483, 1990.

134. Page, E. Quantitative ultrastructural analysis in cardiac membrane physiology. Am. J. Physiol. 235: C147-C158, 1978.

135. Pagiani, E. D., and R. J. Solaro. Coordination of cardiac myofibrillar and sarcotubular activities in rats exercised by swimming. Am. J. Physiol. 247: H909-H915, 1984.

136. Palmer, W. K., and S. Doukas. Cyclic AMP phosphodiesterase activity in the hearts of trained rats. Can. J. Physiol. Pharmacol. 61: 1017-1024, 1983.

137. Penpargkul, S., A. Malhotra, T. Schaible, and J. Scheuer. Cardiac contractile proteins and sarcoplasmic reticulum in hearts of rats trained by running. J. Appl. Physiol. 48: 409-413, 1980.

138. Penpargkul, S., and J. Scheuer. The effects of physical training upon the mechanical and metabolic performance of rat heart. J. Clin. Invest. 49: 1859-1868, 1970.

139. Penpargkul, S., A. Schwartz, and J. Scheuer. Effect of physical conditioning on cardiac mitochondrial function. J. Appl. Physiol. 45: 978-986, 1978.

140. Perez-Reyes, E., A. Castellano, H. S. Kim, P. Bertrand, E. Baggstrom, A. E. Lacerda, X. Wei, and L. Birnbaumer. Cloning and expression of a cardiac/brain subunit of the L-type calcium channel. J. Biol. Chem. 267: 1792-1797, 1992.

141. Peronnet, F., J. Cleroux, H. Perrault, D. Cousineau, J. DeChamplain, and R. Nadeau. Plasma norepinephrine response to exercise before and after training in humans. J. Appl. Physiol.: Respirat. Environ. Exercise Physiol. 48: 409-413, 1981.

142. Perrault, H., and R. A. Turcotte. Exercise-induced cardiac hypertrophy: Fact or fallacy? Spts. Med. 17: 288-308, 1994.

143. Pessah, I. N., and I. Zimany. Characterization of multiple [^{3}H]ryanodine binding sites on the Ca^{2+} release channel of sarcoplasmic reticulum from skeletal and cardiac muscle: Evidence for a sequential mechanism in ryanodine action. Molec. Pharmac. 39: 679-689, 1991.

144. Philipson, K. D. The role of phospholipids in the Ca^{2+} binding of isolated cardiac sarcolemma. J. Mol. Cell. Cardiol. 12: 1159-1173, 1980.

145. Philipson, K. D. Sodium-calcium exchange in plasma membrane vesicles. Ann. Rev. Physiol. 47: 561-571, 1985.

146. Pierce, G. N., K. D. Philipson, and G. A. Langer. Passive calcium-buffering capacity of a rabbit ventricular homogenate preparation. Am. J. Physiol. 249: C248-C255, 1985.

147. Reeves, J. P., and C. C. Hale. The stoichiometry of the cardiac sodium-calcium exchange system. J. Biol. Chem. 259: 7733-7739, 1984.

148. Reeves, J. P., and K. D. Philipson. Sodium-calcium exchange activity in plasma membrane vesicles. In: Sodium-calcium exchange, edited by T. J. A. Allen, D. Noble and H. Reuter. Oxford, U.K.: Oxford University Press, 1989, p. 27-53.

149. Rerych, S. K., P. M. Scholz, D. C. Sabiston, and R. H. Jones. Effects of exercise training on left ventricular function in normal subjects: A longitudinal study by radionuclide angiography. Am. J. Cardiol. 45: 244-251, 1980.

150. Reuter, H., S. Kokubun, and B. Prod'hom. Properties and modulation of cardiac calcium channels. J. Exp. Biol. 124: 191-201, 1986.

151. Saimi, Y., and K. Y. Ling. Calmodulin activation of calcium-dependent sodium channels in excised membrane patches of Paramecium. Science 249: 1441-1444, 1990.

152. Saltin, B., G. Blomqvist, J. H. Mitchell, R. L. Johnson, K. Wildenthal, and C. B. Chapman. Response to submaximal and maximal exercise after bed rest and training. Circ. 38(Suppl. 7): 1-78, 1968.

153. Santer, R. M. Morphology and innervation of the fish heart. Adv. Anat. Embryol. Cell Biol. 89: 1-102, 1985.

154. Schaible, T. F., and J. Scheuer. Cardiac function in hypertrophied hearts from chronically exercised female rats. J. Appl. Physiol. 50: 1140-1145, 1981.

155. Schaible, T. F., and J. Scheuer. Effects of physical training by running or swimming on ventricular performance of rat hearts. J. Appl. Physiol. 46: 854-860, 1979.

156. Scheuer, J., and C. M. Tipton. Cardiovascular adaptations to physical training. Ann. Rev. Physiol. 39: 221-251, 1977.

157. Sham, J. S., S. N. Hatem, and M. Morad. Species differences in the activity of the Na^{+}-Ca^{2+} exchanger in mammalian cardiac myocytes. J. Physiol. 488: 623-631, 1995.

158. Sham, J. S. K., L. Cleemann, and M. Morad. Functional coupling of Ca^{2+} channels and ryanodine receptors in cardiac myocytes. Proc. Natl. Acad. Sci. USA 92: 121-125, 1995.

159. Sham, J. S. K., L. Cleemann, and M. Morad. Gating of the cardiac Ca release channel: The role of Na^{+} current and Na^{+}-Ca^{2+} exchange. Science 255: 850-853, 1992.

160. Sham, J. S. K., L. R. Jones, and M. Morad. Phospholamban modulates the beta-adrenergic-enhanced Ca^{2+} uptake in mammalian ventricular myocytes. Am. J. Physiol. 261: H1344-H1349, 1991.

161. Shamoo, A. E., I. S. Ambudkar, M. S. Jacobson, and J. Bidlack. Regulation of calcium transport in cardiac sarcoplasmic reticulum. Curr. Top. Memb. Transp. 25: 131-145, 1985.

162. Shattock, M. J., and D. M. Bers. Inotropic response to hypothermia and the temperature-dependence of ryanodine action in isolated rabbit and rat ventricular muscle: Implications for excitation-contraction coupling. Circ. Res. 61: 761-771, 1987.

163. Sigvardsson, K., E. Svanfeldt, and A. Kilbom. Role of the adrenergic nervous system development of training-induced bradycardia. Physiol. Acta Scand. 101: 481-488, 1977.

164. Sipido, K. R., and W. G. Wier. Flux of Ca^{2+} across the sarcoplasmic reticulum of guinea-pig cardiac cells during excitation-contraction coupling. J. Physiol. 435: 605-630, 1991.

165. Smith, D. C., and A. El-Hage. Effect of exercise training on the chronotropic response of isolated rat atria to atropine. Experientia 34: 1027-1028, 1978.

166. Solaro, R. J., S. C. El-Saleh, J. C. Kentish, A. Meyer, and A. Martin. Transitions in isoform population of thick and thin filament proteins and calcium activation of force and ATP hydrolysis by cardiac myofilaments. New York: Alan R. Liss, 1989.

167. Solaro, R. J., P. Kumar, E. M. Blanchard, and A. F. Martin. Differential effects of pH on calcium activation of myofilaments of adult and perinatal dog hearts. Evidence for developmental differences in thin filament regulation. Circ. Res. 58: 721-729, 1986.

168. Solaro, R. J., R. M. Wise, J. S. Shiner, and F. N. Briggs. Calcium requirements for cardiac myofibrillar activation. Circ. Res. 34: 525-530, 1974.

169. Somero, G. N. Protons, osmolytes, and fitness of internal milieu for protein function. Am. J. Physiol. 251: R197-R213, 1986.

170. Sommer, J. R., and R. B. Jennings. Ultrastructure of cardiac muscle. New York: Raven Press, 1992.

171. Sordahl, L. A., G. K. Asimakis, R. T. Dowell, and H. L. Stone. Functions of selected biochemical systems from the exercise-trained dog heart. J. Appl. Physiol. 42: 426-431, 1977.

172. Stone, H. L. Coronary flow, myocardial oxygen consumption and exercise training in dogs. J. Appl. Physiol. 49: 759-768, 1980.

173. Sun, X., F. Protasi, M. Takahashi, H. Takeshima, D. G. Ferguson, and C. Franzini-Armstrong. Molecular architecture of membranes involved in excitation-contraction coupling of cardiac muscle. J. Cell Biol. 129: 659-671, 1995.

174. Tada, M., M. Kadoma, M. Inui, and J. Fujii. Regulation of Ca^{2+}-pump from cardiac sarcoplasmic reticulum. Methods Enzymol. 157: 107-153, 1988.

175. Tate, C., M. Hamra, G. Shin, G. Taffet, P. McBride, and M. Entman. Canine cardiac sarcoplasmic reticulum is not altered with endurance exercise training. Med. Sci. Spts. Exer. 25: 1246-1257, 1993.

176. Tate, C. A., G. E. Taffet, E. K. Hudson, S. L. Blaylock, R. P. McBride, and L. H. Michael. Enhanced calcium uptake of cardiac sarcoplasmic reticulum in exercise-trained old rats. Am. J. Physiol. 258: H431-H435, 1990.

177. Tibbits, G. F., R. J. Barnard, K. M. Baldwin, N. Cugalj, and N. K. Roberts. Influence of exercise on excitation-contraction coupling in rat myocardium. Am. J. Physiol. 240: H472-H480, 1981.

178. Tibbits, G. F., H. Kashihara, and K. O'Reilly. Na^{+}-Ca^{2+} exchange in cardiac sarcolemma: modulation of Ca^{2+} affinity by exercise. Am. J. Physiol. 256: C638-C643, 1989.

179. Tibbits, G. F., H. Kashihara, M. J. Thomas, J. E. Keen, and A. P. Farrell. Ca^{2+} transport in myocardial sarcolemma from rainbow trout. Am. J. Physiol. 259: R453-R460, 1990.

180. Tibbits, G. F., B. J. Koziol, N. K. Roberts, K. M. Baldwin, and R. J. Barnard. Adaptation of the rat myocardium to endurance training. J. Appl. Physiol. 44: 85-89, 1978.

181. Tibbits, G. F., C. D. Moyes, and L. Hove-Madsen. Excitation-contraction coupling in the teleost heart. In: Fish Physiology, edited by W. S. Hoar, D. J. Randall and A. P. Farrell. San Diego, CA: Academic Press, 1992, p. 267-304.

182. Tibbits, G. F., T. Nagatomo, M. Sasaki, and R. J. Barnard. Cardiac sarcolemma: Compositional adaptation to exercise. Science 213: 1271-1273, 1981.

183. Tibbits, G. F., K. Philipson, and H. Kashihara. Characterization of myocardial Na^{+}-Ca^{2+} exchange in rainbow trout. Am. J. Physiol. 262: C411-C417, 1992.

184. Tsuruya, Y., M. M. Bersohn, Z. Li, D. A. Nicoll, and K. D. Philipson. Molecular cloning and functional expression of the guinea pig cardiac Na^{+}-Ca^{2+} exchanger. Biochim. biophys. Acta 1196: 97-99, 1994.

185. Valdivia, C., P. Kofuji, W. J. Lederer, and D. H. Schulze. Characterization of the Na/Ca exchanger cDNA in Drosophila. Biophys. J. 68: A410, 1995.

186. Vieth, W. R., K. Nho, and S. Kale. Dual role of calmodulin in excitable cells. Ann. Biomed. Eng. 21: 669-677, 1993.

187. Vorherr, T., P. James, J. Krebs, A. Enyedi, D. J. McCormick, J. T. Penniston, and E. Carafoli. Interaction of calmodulin with the calmodulin binding domain of the plasma membrane Ca^{2+} pump. Biochem. 29: 355-365, 1990.

188. Wakamori, M., G. Mikala, A. Schwartz, and A. Yatani. Single-channel analysis of a cloned human heart L-type Ca2+ channel alpha1 subunit and the effects of a cardiac beta subunit. Biochem. Biophys. Res. Comm. 196: 1170-1176, 1993.

189. Weyman, M. Ca^{2+}-dependence of PN200-110 binding to highly-purified sarcolemma of the rat heart. In: Calcium antagonist binding to myocardial

sarcolemma: Adaptation to exercise. Burnaby: Simon Fraser University, 1987, p. 117.

190. Weyman, M., and G. F. Tibbits. Cardiac Ca-antagonist binding alterations with exercise training. Med. Sci. Spts. Exer. 29: S82, 1987.

191. Wier, W. G. Cytoplasmic $[Ca^{2+}]_i$ in mammalian ventricle: Dynamic control by cellular processses. Ann. Rev. Physiol. 52: 2440-2447, 1990.

192. Williams, J. F., and R. D. Potter. Effect of exercise conditioning on the intrinsic contractile state of cat myocardium. Circ. Res. 39: 425-428, 1976.

193. Witcher, D., R. Kovacs, H. Schulman, D. Cefali, and L. Jones. Unique phosphorylation site on the cardiac ryanodine receptor regulates calcium channel activity. J. Biol. Chem. 266: 11144-11152, 1991.

194. Wolfe, L. A., and D. A. Cunningham. Effects of chronic exercise on cardiac output and its determinants. Can. J. Physiol. Pharmacol. 60: 1089-1097, 1982.

195. Yamauchi, A., and G. Burnstock. On the fine structure of the trout heart. J. Anat. Lond. 103: 207-208, 1968.

196. Yue, D. T., E. Marban, and W. G. Wier. Relationship between force and intracellular $[Ca^{2+}]$ in tetanized mammalian heart muscle. J. Gen. Physiol. 87: 223-242, 1986.

197. Zarain-Herzberg, A., D. H. MacLennan, and M. Periasamy. Characterizztion of rabbit cardiac sarco(endo)plasmic reticulum Ca^{2+}-ATPase gene. J. Biol. Chem. 265: 4670-4677, 1990.

CHAPTER 2

EFFECT OF EXERCISE TRAINING ON RYANODINE AND DIHYDROPYRIDINE RECEPTOR DENSITIES IN RAT HEART

ABSTRACT

Potential mechanisms underlying enhanced myocardial contractility resulting from endurance treadmill-training were assessed. In two studies using five separate training protocols, the effects of different exercise intensities on the densities of the sarcolemmal (SL) L-type Ca^{2+} channel (dihydropyridine receptor- DHPR) and the sarcoplasmic reticulum Ca^{2+} release channel (ryanodine receptor - RyR) were studied using female rats randomly divided into either sedentary-control (C) or treadmill-trained (T) groups. In the first study, T rats were trained progressively until after ~11 weeks they ran 1 hr/day, 5 days/wk at either 30 m/min, 8% grade (T1M) or 32 m/min, 8% grade (T1H). No differences were found in either T group with respect to heart weights (HW), body weights (BW) nor SL characterization. Specific [^{3}H]-DHP binding to DHPR (DHPR B_{max}) in ventricular homogenates (HG) was increased by ~16%, in T1M vs C1M ($p<0.05$). DHPR B_{max} values in T1H were increased in the HG by ~50 % and in SL by ~36 % compared to C1H ($p<0.05$). The binding affinities remained unchanged by exercise. In the second study, T rats were trained to run at either 27 m/min, 5% grade (T2L), 28 m/min, 8% grade (T2LM) or 30 m/min, 8% grade (T2M) for ~11 weeks. No differences were noted in HW and BW in any T compared to C group with the exception of HW (T2LM). HW from T2LM showed a small but significant 10% increase compared to C2LM, $p<0.05$. No significant differences were observed in either the DHPR B_{max} or the binding affinities in homogenates from rats trained at any of the three work rates. RyR B_{max} was no different in T2L or T2LM compared to their respective controls.

However, RyR B_{max} was significantly higher in T2M vs C2M: 785±82 (n=15) vs 635±53 (n=15) fmol/mg ± S.E.M., respectively, $p<0.05$. RyR binding affinities remained unchanged in all groups with K_D values of 7-17 nM. These results suggest that DHPR and RyR are not altered after training at the lower workrates in which functional adaptations have been previously observed.

INTRODUCTION

It has been proposed that enhanced myocardial contractility, in the absence of significant hypertrophy, contributes to the observed increase in stroke volume in response to chronic endurance training. Possible cellular mechanisms of adaptation which may contribute to enhanced myocardial contractility include alterations in the Ca^{2+} sensitivity of the contractile element and/or Ca^{2+} delivery to the myofilaments. While remaining somewhat equivocal, *in vitro* evidence (i.e., myofibrillar ATPase activity) suggests that treadmill training does not involve significant alterations to the contractile element (1) while data from isolated myocyte preparations suggest it does (21). We have proposed that a modification in Ca^{2+} delivery to the myofilaments contributes to the observed increases in contractility (30). Indirect evidence in support of this proposal comes from several lines of investigation. Enhanced myocardial contractility has been documented in treadmill trained rodents using *in vivo* (14), isolated working heart (6), and papillary muscle (30, 32) preparations, all in the absence of significant hypertrophy. Several of these studies also failed to demonstrate changes in Ca^{2+}-activated myofibrillar ATPase activity (14, 30, 32). However, recent experiments using isolated myocytes from trained hearts with enhanced contractile activation have failed to show any significant increase in peak Ca^{2+} transients using the fluorescent dyes, fura-2 (21) or indo-1 (29) although both have shown enhanced contractile activation. On a physiological level, these data suggest that neither the SL nor the SR are involved in exercise-mediated changes in contractility. It is unknown to what extent cell growth and thus a dilution effect may have contributed to the reduction in Ca^{2+} transients from T myocytes. In addition, because we have previously seen an increase in the density of DHPR in purified SL (13, 34) it is important to substantiate or refute these observations using a biochemical approach.

The experiments outlined in this paper examined the effect of treadmill training at different intensities on the densities of the sarcolemmal L-type Ca^{2+} channel (dihydropyridine receptor - DHPR) and sarcoplasmic reticulum Ca^{2+} release channel

(ryanodine receptor - RyR) in rat hearts. A narrow range of training intensities was chosen for two reasons. The first was that functional changes have been shown to occur within the range 25 to 32 m/min. Above this range hypertrophy becomes significant while less strenuous exercise fails to evoke a myocardial training response. Second, by determining the various timecourses of adaptive changes in the heart, information about the nature of the cardiac response to exercise will be achieved.

In the first study, in which only DHPR densities were examined, a significant increase in DHP binding capacity to purified SL vesicles in response to training was observed. Several questions were raised regarding the reliability and universality of this phenomenon due to problems associated with the use of purified membrane fractions to quantitate receptor densities (11, 17). Also, since most of the DHP receptors in the heart have a close structural and functional relationship with RyR (28), it is important that RyR densities should be examined as well. Changes in RyR density have been documented using widely different perturbations. For example, RyR density was decreased in the hearts of swim-trained normal and hypertensive rats (15), cardiomyopathic hamsters (17) and diabetic rats (35), all of which, are known to produce various manifestations of either physiological or pathological hypertrophy.

Thus the aims of the experiments described in this chapter were: 1) to reassess whether or not DHPR density is altered in response to treadmill training, 2) to determine if there is an intensity threshold for this response, and 3) to determine if there is a concomitant increase in the density of the SR Ca^{2+} release channel (RyR).

METHODS

Animal Care and Training. The first study comprises two separate training protocols which were conducted by Dr. G. Diffee (G.D.) and M. Weyman (M.W.). A total of 148 female Sprague-Dawley rats were randomly divided into treadmill-trained (T1) and sedentary control (C1) groups. Both groups were housed in a light and temperature controlled room and provided food and water *ad libitum.* Group T1 participated in a treadmill-training protocol in which the workload was progressively increased until after 10 weeks the animals were capable of running 5 days/wk, 1 hr/day up an 8% grade at one of two velocities: moderate (T1M) - 30 m/min or high (T1H) - 32 m/min.

The second study comprises three separate training regimens carried out by Marion Thomas (M.T.) and Brian Hamman (B.H.). For each study, 20-30 female Wistar or Sprague-Dawley rats were randomly divided into treadmill-trained (T2) and sedentary-control (C2) groups. Again, both groups were housed in a light and temperature controlled room and provided food and water *ad libitum.* Group T2 participated in a treadmill-training protocol in which the workload was progressively increased until after 10 weeks the animals were capable of running 5 days/wk, 1 hr/day at one of three work intensities: 1) low (T2L) - 27 m/min, 5% grade, 2) low-moderate (T2LM) - 28 m/min, 8% grade, or 3) moderate (T2M) -30 m/min up an 8% grade.

In all of the studies, training was continued for a further 2-3 weeks after the final intensity was achieved. All animals were sacrificed at the same time each day and at least 24 hr after the last exercise bout to eliminate any acute effects of exercise.

Ventricular Homogenate Preparation. Hearts were rapidly excised and placed into a beaker of ice-cold homogenization medium (HM) containing: 250 mM sucrose, 20 mM

MOPS, pH 7.4 @ 37°C. After rinsing and removal of atria and connective tissue, the ventricles were blotted, weighed, and further rinsed in ice-cold HM. After mincing in ~5 ml HM, the hearts were individually homogenized with a Tekmar Tissumizer (5 times 3 sec on setting 40). The ventricular homogenates were then filtered through two layers of stainless steel wire mesh and brought to 15-20 ml per gram wet weight. Protein content was determined following the method of Bradford (7) using bovine serum albumin as the standard.

Sarcolemma Isolation. Sarcolemma were isolated in the first study only. For these experiments, rat cardiac SL vesicles were prepared by differential ultracentrifugation and discontinuous sucrose gradient fractionation as described (33). The SL marker K^+-stimulated *p*-nitrophenylphosphatase (K^+*p*NPPase) was assayed (33) in the crude HG and all fractions derived from the sucrose gradient. The purification index (PI) was defined as the ratio of the specific activity of K^+*p*NPPase in the SL fraction (F2) to that in the crude HG. Recovery was defined as the percentage of the total K^+*p*NPPase activity (μmol/hr) in the SL fraction compared with the crude HG.

[^{3}H]-dihydropyridine binding. In the first study, either [^{3}H]-nitrendipine (1M) or [^{3}H](+)PN200-110 (1H) binding experiments were performed on both the crude homogenate and the purified SL fractions. Total binding was determined by varying the amount of [^{3}H]-dihydropyridine over the range of 0.10-0.80 nM. Non-specific binding was determined in separate tubes containing the same DHP concentration as that for specific binding plus more than a hundred-fold excess of cold nifedipine to displace the radioactive ligand. All experiments were done in the dark and in duplicate. For the crude

homogenate and sarcolemmal fractions, either 150-400 or 10-20 μg protein, respectively, were added per tube. The reaction media contained 25 mM MOPS, pH 7.4 @23°C, and 2.5 mM $CaCl_2$in a final volume of 5 ml. After incubation at room temperature for 90 min, the separation of free from bound ligand was achieved by rapid vacuum filtration of a 2.25 ml aliquot using Whatman GF/C glass-fiber filters. Each filter was then washed 3 times with 4.5 ml of ice-cold 25 mM MOPS buffer. The filters were dried overnight in liquid scintillation vials, after which 5 ml Beckman Ready Protein® liquid scintillant was added followed by 2 hours of orbital shaking at 200 rpm to solubilize the protein. Vials were counted (Beckman LS 7000) using standard liquid scintillation procedures.

In the second study (2L, 2LM, 2M), specific DHP binding was determined in a manner identical to that described above with the following exceptions: [^{3}H](+)PN200-110 concentration was varied over the range of 0.025-1.6 nM, each tube contained 150-160 μg protein from crude homogenate only, and the number of samples was increased from 4 to 10 and 15. The greater range of PN concentrations was to ensure maximal binding was reached. The use of crude homogenates avoids problems associated with membrane purification and differential loss of DHPRs. Sample size was increased to improve the resolving power of our data.

[^{3}H]-ryanodine binding. Ryanodine binding was determined in the second study (2L, 2LM, 2M) only. In these experiments RyR and DHPR densities were determined from the same hearts. The method to determine RyR densities was adapted from the procedure of Chu *et al.* (9). Briefly, specific binding was determined by the addition of 5 nM [^{3}H]-ryanodine plus varying amounts (0 to 495 nM) of unlabelled ryanodine (Calbiochem) to

12 tubes containing 150 mM KCl, 20 mM MOPS (pH 7.4 @ 23°C), and 100 μM $CaCl_2$. Non-specific binding was measured after adding 100-fold excess unlabelled ryanodine to separate tubes. After the addition of ~250 μg protein of ventricular homogenate, tubes were incubated at room temperature for 2 hours to allow the binding to reach a maximum. Duplicates were taken for each of the 12 data points. Separation of bound and free ligands was achieved by rapid filtration using Whatman GF/C filters and rinsing twice with 4 ml ice-cold buffer (containing: 150 mM KCl, 20 mM MOPS, 100 μM $CaCl_2$) and once with 4 ml ice-cold 10% ethanol. After drying filters overnight in scintillation vials, 5 ml Beckman Ready Protein® liquid scintillant was added followed by 2 hours of orbital shaking at 200 rpm to solubilize the protein. Vials were then counted using standard liquid scintillation procedures.

Citrate synthase assay. Citrate synthase activities were determined in the second study only following the method of Srere (27). B.H. performed the citrate synthase assay on the right medial gastrocnemius muscles from T/C2L and T/C2LM while M.T. performed the experiments on medial gastrocnemius and soleus muscles from T/C2M. All muscles were frozen and stored in liquid nitrogen until assayed. The day before the assay was to be performed the muscle samples were weighed, thawed and placed into 9 volumes of ice-cold homogenization buffer containing 20 mM MOPS (pH 7.2 @ 23°C), 5 mM EDTA, and 0.1% Triton X-100. The tissue was minced, homogenized, sonicated (3 times for 10 sec) and re-frozen at -20°C. The following day samples were thawed, sonicated and centrifuged (4°C) at ~13,000 rpm for 5 min. to remove any non-solubilized material. A small aliquot (5 μl) of this supernatant was then added to the reaction medium (1 ml final volume) containing in mM: 0.5 acetyl Co-A, 0.1 DTNB and 20 TRIS (pH 8.0 @

23°C). The absorbance at 412 nm, which represents background thiolase activity, was monitored. After approximately 2 min, 100 µl oxaloacetate (0.3 mM final concentration) was added. The difference between slopes prior to, and after the addition of oxaloacetate was used to determine citrate synthase activity.

Data and statistical analysis. All DHPR binding data were analyzed by iterative non-linear regression and Scatchard analysis using GRAFIT® (Erithacus Software Ltd, UK) to determine B_{max} and K_D values from T and C groups. RyR binding data were also subjected to non-linear regression analysis using GRAFIT®, however, a two-site ligand binding model was used to determine the high affinity B_{max} and K_D values from T and C samples. Between group (T vs C) comparisons were made using a paired Student's *t*-test with a significance level set at $p < 0.05$.

Materials. Radioisotopes were purchased from New England Nuclear (Dupont, St. Laurent, Quebec). All biochemicals were obtained from Sigma Chemical Co. with the noted exceptions.

RESULTS

Study 1

Training response. In the first study, the mean values for body weight, and heart weight were not significantly different in the trained compared to control group at either of the two work rates. Heart-to-body weight ratios were significantly increased by 6% in T1M but not T1H (Table 1). Crude homogenate and purified SL vesicles isolated from rats trained under both the 1M and 1H work rates did not demonstrate any apparent differences between groups with respect to total protein, marker enzyme activities, relative purification, and percent recovery (Table 2).

DHPR binding. The maximum density of DHPR (B_{max}) was significantly ($p< 0.05$) increased in response to both work rates. In T1M, the crude homogenate DHPR B_{max} values were significantly ($p <0.05$) increased by ~16% in comparison to C1M. At the higher intensity, T1H demonstrated B_{max} values that were increased by ~50% in the HG (Table 3) and by ~36% in purified SL (Figure 1) fraction relative to C1H. At both intensities, the binding affinity (K_D) in each preparation was not significantly affected by training. In this study, the DHP binding data are best represented by a single class of high affinity binding sites as evidenced by the linear Scatchard plot (figure 1-inset).

Study 2

Training response. In this study, mean body weights from T and C groups were no different nor was the protein content of the ventricular homogenate isolated from each group trained at any of the three work rates (Table 1). The absolute ventricular weights from T2L and T2M were not significantly different compared to their respective controls, C2L and C2M. A significant ~10% increase in the ventricular weight in group T2LM was observed. However, when ventricular weights were normalized for differences in body weight, no significant differences were observed in the heart-to-body weight (HW/BW) ratios from any group. When the heart weights were expressed as a function

of body weight and fit to least-squares linear regression, the regression coefficient was not different to the mean HW/BW ratio for each group.

Citrate synthase. Work done at the three different intensities was reflected in the gastrocnemius citrate synthase activities from each group which ranged from 9 to 20 µmol/g wet wgt/min (Figure 2). T2M, T2LM and T2L were significantly ($p < 0.05$) increased by 24, 18, and 13% respectively, compared to their controls C2M, C2LM and C2L. In T2M the citrate synthase activity of the soleus ranged between 22 and 30 µmol/g wet wgt/min and was significantly ($p < 0.001$) increased by 35% over its control C2M.

DHPR binding Non-linear regression and Scatchard analysis did not reveal any training induced adaptation in either the B_{max} (pmol $\cdot$mg protein^{-1}) or K_D (pM) values between T and C groups at any intensity as shown in Table 3 and Figures 3, 4, and 5. In this study as well as the first, the DHP binding data are best represented by a single class of high affinity binding sites.

RyR binding - Figures 6, 7 and 8 illustrate specific [^{3}H]-ryanodine binding to the high affinity site in the same homogenate preparations as that used for DHPR. Using a wide range of ryanodine concentrations (0 to 500 nM), both high and low affinity binding sites were apparent in all preparations. B_{max} (pmol $\cdot$mg protein^{-1}) and K_D (nM) values for the high affinity site were obtained from non-linear regression and Scatchard analysis. While there was a trend for greater RyR density with increasing exercise intensity (Table 4), there were no significant ($p < 0.05$) differences in the B_{max} values for the high affinity site in T2LM or T2L compared to controls, C2LM and C2L. However, there was a significant ($p < 0.05$) increase of 24% in the B_{max} of the high affinity site in T2M compared to C2M. The K_D values for the high affinity site ranged from 7 to 17 nM and were unaltered by any training regimen.

DISCUSSION

Training response. In the two separate studies, two of the workloads (T1M, T2M) were similar to those in previous studies which produced changes in myocardial contractile function (30, 32). In this paper, we also examined the response to work rates that were both higher (T1H) and lower (T2LM, T2L) that those studied previously. In the first study, unfortunately, skeletal muscle mitochondrial markers were not measured and as a consequence training-induced mitochondrial biogenesis can not be evaluated. In the second study, all work rates (T2L, T2LM, T2M) induced significant increases in mitochondrial marker activity from skeletal muscle in a dose dependent manner. The magnitudes are similar to what has been observed previously. Specifically, the increases in citrate synthase activity found in T2M compares favorably with the following studies that our lab has published using training paradigms of similar to slightly higher intensity: 1) 36% increase in gastrocnemius malate dehydrogenase (31) and 2) 38% increase in gastrocnemius cytochrome C oxidase (30, 32). In the latter studies, contractile function was determined by using isometric force generation from isolated papillary muscles and the treadmill training paradigm resulted in significantly improved contractility. Although it is extremely difficult to compare treadmill paradigms based on treadmill speed, grade and duration, the degree of skeletal muscle adaptation suggests that the stimulus in T2M was of similar intensity. The ability to compare regimens using different mitochondrial markers is based on the observation that all mitochondrial enzymes have been shown to covary in response to varying activity levels (16).

The lack of any differences in body weights between the two groups at all work rates is consistent with the original observation of the female rodent's response to

exercise by Oscai *et al.* (22) and many subsequent studies. The effect of exercise on heart weight was small and not significant in any group except T2LM. The reason why HW in group T2LM was significantly greater than C2LM is not clear but it does highlight the difficulty of trying to match work rates from study to study. The fact that the HW changes are small is consistent with other studies using regimens in this range of work rates. Similarily, HW/BW ratios were essentially unchanged after training, with only T1M showing a small but significant increase, $p < 0.05$. This increase in HW/BW is within the range of 0-8% typically observed using similar training intensities (24, 31, 32). The greater HW/BW ratio found in T1M may reflect a small increase in myocyte length as we (19) and others (21) have shown previously in response to regimens over this intensity range. Alternatively, some other adaptation involving proliferation of non-myocyte tissue (ie. fibroblasts), or water retention (8, 24) is possible. These observations from the rodent model seems to mimic that found in training studies using human subjects in which VO_{2max} and maximum cardiac output can be increased significantly without a concomitant increase in left ventricular wall thickness (24). Thus based on our previous experiments and the results of others, we believe that regimens T1M, T1H and T2M induce similar improvements in cardiac contractility. Less is known about the chronic cardiac adaptation to regimens T2L and T2LM.

DHPR binding. The DHPR binding site and that of other Ca^{2+} channel blockers (e.g. verapimil and benzodiazapines) are known to be on the α_1 subunit of the L-type Ca^{2+} channel. The α_1 subunit represents the voltage sensing and pore components of the channel (20). The other subunits presumably play regulatory roles (23, 25) that are not

completely understood. Despite earlier controversy, the DHPR is now generally recognized as a functional Ca^{2+} channel in cardiac muscle (18). Furthermore, T-type Ca^{2+} channels, which do not bind DHP, are present in atrial but not ventricular myocytes (3). Thus the quantification of ventricular Ca^{2+} channel density by DHP binding is justified based on the literature and has been used by several groups to monitor the adaptation of the ventricles to a variety of perturbations including cardiomyopathy (2).

In the first study, we found significant increases in DHP B_{max} values in the trained groups (T1M, T1H) in both the purified SL (Figure 1) and crude homogenate fractions compared to their respective controls (C1M, C1H) (Table 3) but no changes were noted in the binding affinity. Furthermore, the training-induced increase in DHP B_{max} was substantially greater in the high (T1H) work intensity compared to the moderate (T1M) work intensity in both SL and homogenate fractions. K_D values were unaffected by either of these exercise paradigms. From these data, it was tempting to speculate that exercise training of sufficient intensity to increase myocardial contractile function but not to induce substantive cardiac hypertrophy, stimulates L-type Ca^{2+} channel synthesis and insertion into the sarcolemma. This notion was pursued further in the second study with some changes being made in the experimental protocol. In the first study, DHP binding was determined in both crude homogenate and highly purified sarcolemmal vesicles. However, we found in the first study that the extrapolation of DHP binding from highly purified sarcolemmal fractions to the intact cell to be problematic. While the SL marker K^+-*p*NNPase was increased about 20-fold in the purified SL fraction compared to the crude homogenate (Table 2), the DHP B_{max} was increased less than 2 fold (data not

shown). Thus the DHPRs are not copurifying with the SL membranes *per se*. From control experiments that we performed (data not shown), it was observed that much of the DHPR is lost in heavier fractions. In particular, one might expect the DHPR and RyR to copurify if they are physically coupled. To avoid this problem only crude homogenates were used. The crude homogenate represents 100 per cent of the DHPR population because there is no loss due to purification while the signal to noise ratio in this unpurified preparation remains very good. The latter is reflected in the S.E.M. being typically ~6% of the mean and the specific binding at 0.1 nM DHP being > 70% of total binding.

The second modification implemented was that the range of DHP ligand concentrations used in the binding assays was increased from the 0.1 - 0.5 nM (5 fold range) used in the first study to 0.025 - 1.6 nM (64 fold range) in the second study. These assay conditions allow for a better characterization B_{max} and K_D values.

While T1M and T2M did not produce similar increases in DHPR using the same exercise regimen, both studies yielded binding constants that were similar in magnitude to those previously reported by others for the rodent heart (4, 17). However, K_D values from the first study were at the high end of published values (141 and 151 pM in C1H and T1H respectively) and more than twice that of the six K_D values (46-68 pM) determined in the second study. The reason for this difference is not known but may reflect the narrower range of ligand concentrations and the smaller sample size in the first study (T1M).

In contrast to the first study, the second study showed no exercise-induced differences in the B_{max} values over the three slightly different training paradigms used. However, it should be pointed out that T1M and T2M were nominally the same intensity although the experiments were carried out by different investigators. Thus T1M showed a significant increase in B_{max} while T2M did not. The results from these two studies may be a reflection of the noise within the assay itself. It also could be argued that the results reflect different DHPR binding assay conditions between T1M and T2M. For example, the smaller range of ligand concentrations used in T/C1M may result in a less reliable estimate of B_{max}. However, the specific binding at the three highest concentrations of free ligand in T1M were all significantly greater than the respective controls. Furthermore, the estimated K_D had a tendency to be higher in the trained than control groups indicating that higher ligand concentrations would be required for complete saturation. Thus for the ligand concentrations used, the degree of saturation may be lower for a given ligand concentration. We suggest that this work intensity may represent a threshold for enhanced expression of the L-type Ca^{2+} channel. In a previous study (12), work of similar intensity also resulted in no significant increase in DHPR B_{max}, although clearly the specific binding had a pronounced tendency to be higher in the trained group. Thus the work load of 30 m/min, 8% grade for 60 minutes may represent a threshold point for an increase in sarcolemmal DHPR density.

RyR binding. The determination of cardiac RyR densities in the second study was prompted by the fact that we had observed training-induced increases in DHPR density in the first study. Because of the intimate functional and morphological relationship

between the DHPR and RyR in the heart, it seems logical that these two proteins may covary in response to a stimulus. This is the first report of RyR binding density in response to treadmill training. As shown in Figures 6, 7 and 8, specific [^{3}H]-ryanodine binding at the lower ligand concentrations (5-100 nM) is fit by a single high affinity binding site. The high affinity B_{max} (Table 4) and K_D values from the control groups are similar to those reported in homogenized isolated myocytes (4). A low affinity binding site was apparent at higher (200-500 nM) ligand concentrations. These data are neither shown nor discussed because their relevance is not clear. Consistent with the DHPR data, exercise training in this study had no significant influence on either the B_{max} or K_D of the high affinity RyR at the two lowest training intensities, 2L and 2LM. However, at the highest intensity (2M), RyR densities were significantly increased. One point worth noting about this increase is that it appears to be reflected by lower absolute control values when a comparison is made with control values from the other workrates. The reason for this difference is not clear but it must be noted that: 1) the trained and control samples were processed one pair at a time with identical solutions and conditions and 2) the three different training regimens of the second study were performed sequentially.

RyR/DHPR ratio. In skeletal muscle, a RyR/DHPR ratio of 0.5 is highly conserved phylogenetically and reflects the model of Block *et al.* (5). The RyR/DHPR ratios were not altered as the result of training at any intensity and ranged from 3.07 to 4.05. These ratios while lower than previous reports are still consistent with the Ca^{2+}-induced, Ca^{2+}-release mechansim of E-C coupling in cardiac muscle. In a study by Bers and Stiffel (4), in which these determinations were made in both cardiomyocytes and crude

homogenates, it was demonstrated that both the RyR and DHPR densities are about 75% greater in the cardiomyocyte preparation in comparison to the crude homogenate. This greater value was almost completely due to the removal of nonmyocyte cells, which contain little or no DHPR and RyR, during the myocyte isolation procedure. Since both values were comparably effected, the RyR:DHPR ratios in the myocyte and homogenate preparations were within ~8% of each other in this study, underlying the relatively small effect of nonmyocyte cell contamination on this ratio. Therefore, our data from the crude homogenates is likely to be an accurate reflection of the RyR:DHPR ratio in the myocyte. Our ratios from rat heart homogenates are lower than previously reported from homogenized rat cardiomyocytes (4). This difference is due almost entirely to higher DHPR B_{max} values (175-253 fmol/mg protein) in homogenates in this study compared to the 114 fmol/mg protein observed in rat myocytes in the study by Bers and Stiffel (4). The higher DHPR densities may reflect a reduced receptor degradation and/or different assay conditions. The ligand binding assays are similar in both studies with the main differences being the inclusion of 2.5 mM Ca^{2+} in the reaction medium in the present study and the vesicular harvesting done on Whatman GF/C (1.2 μm pore) in the present study as opposed to GF/B (1.0 μm pore) filters. Thus the reason for the differences are not obvious.

Implications for function. While a comprehensive functional analysis was not performed in the current study, previous investigations of treadmill-training at or near the work rates used in the present investigations have produced enhanced contractility in isolated myocytes (19, 29). Thus the increases in myocardial contractility previously

documented do not appear to result from increased DHPR or RyR density. However, changes in contractility in response to a chronic perturbation can be implemented in many ways exclusive of Ca^{2+} channel densities. In light of the reduced Ca^{2+} transients in cardiomyocytes from trained rats (21), it is quite possible that the significant increases in DHPR and RyR densities observed in the present study merely reflect cell growth. In addition, changes in Ca^{2+} channel densities do not necessarily imply changes in myocyte contractility. The exquisite regulation of Ca^{2+} fluxes through these channels must also be considered. It is well documented that a close functional coupling between the DHPR and RyR exists in the myocardium. For example, it has long been known that the Ca^{2+} flux through the DHPR regulates the opening of the RyR through the process of calcium-induced calcium release. More recently, it has been demonstrated that Ca^{2+} fluxes through both the DHPR and the RyR can regulate the inactivation kinetics of the DHPR (26). This regulation probably occurs because of the binding of Ca^{2+} by the EF hand configuration on the DHPR (10).

In conclusion, the changes observed in RyR and DHPR density in response to training are complex. In general, over the range of training intensities used in this study the effects were negligible. For the treadmill training intensity (30 m/min, 8% grade, 1 hr/day) that we have shown previously to induce a pronounced enhancement of contractile function, the results do not support an increase in DHPR density. The results from 1M and 2M should have been equivalent but were not. In 1M a small (16%) but significant increase in DHPR was observed but this was not corroborated by the results of 2M. A previous study (12) at this intensity also demonstrated no significant effect on

DHPR B_{max}. Interestingly, although the DHPR density was not significantly higher in T2M, the RyR densities were significantly increased, although these data are suspect due to the lower control values. From these studies, it could be argued that the moderate intensity of work reflected in T1M and T2M regimens may be in the range of a threshold for increased DHPR and RyR expression. The observed increases in DHPR and RyR densities in T1H, T1M and T2M may be implicated in the maintenance of myocardial contractility with the concomitant onset of myocyte hypertrophy that we and others have observed around this intensity.

REFERENCES

1. Baldwin, K. M. Effects of chronic exercise on biochemical and functional properties of the heart. *Med. Sci. Spts. Exerc.* 17: 522-528, 1985.

2. Bazan, E. M., J. Sole, A. Schwartz, and C. L. Johnson. Dihydropyridine receptor binding sites in the cardiomyopathic hamster heart are unchanged from control. *J. Mol. Cell. Cardiol.* 23: 111-117, 1991.

3. Bean, B. P. Classes of calcium channels in vertebrate cells. *Ann. Rev. Physiol.* 51: 367-384, 1989.

4. Bers, D. M., and V. A. Stiffel. Ratio of ryanodine to dihydropyridine receptors in cardiac and skeletal muscle and implications for E-C coupling. *Am. J. Physiol.* 264: C1587-C1593, 1993.

5. Block, B. A., T. Imagawa, K. P. Campbell, and C. Franzini-Armstrong. Structural evidence for direct interaction between the molecular components of the transverse-tubule/sarcoplasmic reticulum junction in skeletal muscle. *J. Cell. Biol.* 107: 2587-2600, 1988.

6. Bowles, D. K., R. P. Farrar, and J. W. Starnes. Exercise training improves cardiac function after ischemia in the isolated, working rat heart. *Am. J. Physiol.* 263: H804-H809, 1992.

7. Bradford, M. A rapid and sensitive method for the quantitation of microgram quantities of protein utilizing the principle of protein-dye binding. *Anal. Biochem.* 72: 248-254, 1976.

8. Campbell, S. E., B. Korecky, and K. Rakusan. Remodelling of myocyte dimensions in hypertrophic and atrophic rat hearts. *Circ. Res.* 68: 984-96, 1991.

9. Chu, A., C. Sumbilla, D. Scales, A. Piazza, and G. Inesi. Trypsin digestion of junctional sarcoplasmic reticulum vesicles. *Biochem.* 27: 2827-2833, 1988.

10. De Leon, M., Y. Wang, L. Jones, E. Perez-Reyes, X. Wei, T. W. Soong, T. P. Snutch, and D. T. Yue. Essential Ca^{2+}-binding motif for Ca^{2+}-sensitive inactivation of L-type Ca^{2+} channesl. *Science* 270: 1502-1506, 1995.

11. DePover, A., I. L. Grupp, G. Grupp, and A. Schwartz. Diltiazem potentiates the negative inotropic action of nimodipine in heart. *Biochem. biophys. Res. Commun.* **114**: 922-929, 1983.

12. Diffee, G. M. Effect of endurance exercise training on calcium channels in the rat myocardial sarcolemma. . Seattle, WA. USA: University of Washington, 1984.

13. Diffee, G. M., and G. F. Tibbits. Dihydropyridine binding to myocardial sarcolemma: adaptation to exercise. *Clin. Physiol.* 5: 29, 1985.

14. Fitzsimons, D. P., P. W. Bodell, R. E. Herrick, and K. M. Baldwin. Left ventricular functional capacity in the endurance-trained rodent. *J. Appl. Physiol.* 69: 305-312, 1990.

15. Hass, E. E., J. T. Cope, B. Satauffer, J. Blauth, A. M. Semanchick, and R. L. Moore. Effect of endurance training and hypertension on rat cardiac ryanodine receptor number. *Med. Sci. Spts. Exerc.* 24: S20, 1993.

16. Holloszy, J. O. a. E. F. C. Adaptations of skeletal muscle to endurance exercise and their metabolic consequences. *J. Appl. Physiol.* 56: R831-R838, 1984.

17. Lachnit, W. G., M. Phillips, K. J. Gayman, and I. N. Pessah. Ryanodine and dihydropyridine binding patterns and ryanodine receptor mRNA levels in myopathic hamster heart. *Am. J. Physiol.* 267: H1205-H1213, 1994.

18. Lew, W. Y. W., L. V. Hryshko, and D. M. D.M. Bers. Dihydropyridine receptors are primarily functional L-type calcium channels in rabbit ventricular myocytes. *Circulation Res.* 69: 1139-1145, 1991.

19. McGrath, K., and G. F. Tibbits. Exercise-induced alterations in caridac myocyte contractility. *8th International Conference on the Biochemistry of Exercise. Nagoya, Japan, 1991 (abstract).* , 1991.

20. Mikami, A., K. Imoto, T. Tanabe, T. Niidome, Y. Mori, H. Takeshima, S. Narumiya, and S. Numa. Primary structure and functional expression of the cardiac dihydropyridine-sensitive calcium channel. *Nature* 340: 230-233, 1989.

21. Moore, R. L., T. I. Musch, R. V. Yelamarty, R. C. Scaduto Jr., A. M. Semanchick, M. Elensky, and J. Y. Cheung. Chronic exercise alters contractility and morphology of isolated rat cardiac myocytes. *Am. J. Physiol.* 264: C1180-C1189, 1993.

22. Oscai, L. B., P. A. Mole, and J. O. Holloszy. Effects of exercise on cardiac weight and mitochondria in male and female rats. *Am. J. Physiol.* 220: 1944-1948, 1971.

23. Perez-Reyes, E., A. Castellano, H. S. Kim, P. Bertrand, E. Baggstrom, A. E. Lacerda, X. Wei, and L. Birnbaumer. Cloning and expression of a cardiac/brain subunit of the L-type calcium channel. *J. Biol. Chem.* 267: 1792-1797, 1992.

24. Perrault, H., and R. A. Turcotte. Exercise-induced cardiac hypertrophy: Fact or fallacy? *Spts. Med.* 17: 288-308, 1994.

25. Pragnell, M., M. De Waard, Y. Mori, T. Tanabe, T. P. Snutch, and K. P. Campbell. Calcium channel beta-subunit binds to a conserved motif in the I-II cytoplasmic linker of the a1-subunit. *Nature* 368: 67-70, 1994.

26. Sham, J. S. K., L. Cleemann, and M. Morad. Functional coupling of Ca^{2+} channels and ryanodine receptors in cardiac myocytes. *Proc. Natl. Acad. Sci. USA* 92: 121-125, 1995.

27. Srere, P. A. Citrate Synthase. *Meth. Enz.* 13: 3-5, 1969.

28. Sun, X., F. Protasi, M. Takahashi, H. Takeshima, D. G. Ferguson, and C. Franzini-Armstrong. Molecular architecture of membranes involved in excitation-contraction coupling of cardiac muscle. *J. Cell Biol.* 129: 659-671, 1995.

29. Thomas, M. J., and G. F. Tibbits. Endurance exercise training: Effects on Ca^{2+} handling and sarcoplasmic reticulum Ca^{2+} content in rat cardiomyocytes. *Am. J. Physiol. (Cell)* : Cxxx-Cxxx, 1996.

30. Tibbits, G. F., R. J. Barnard, K. M. Baldwin, N. Cugalj, and N. K. Roberts. Influence of exercise on excitation-contraction coupling in rat myocardium. *Am. J. Physiol.* 240: H472-H480, 1981.

31. Tibbits, G. F., H. Kashihara, and K. O'Reilly. Na^{+}-Ca^{2+} exchange in cardiac sarcolemma: modulation of Ca^{2+} affinity by exercise. *Am. J. Physiol.* 256: C638-C643, 1989.

32. Tibbits, G. F., B. J. Koziol, N. K. Roberts, K. M. Baldwin, and R. J. Barnard. Adaptation of the rat myocardium to endurance training. *J. Appl. Physiol.* 44: 85-89, 1978.

33. Tibbits, G. F., K. Philipson, and H. Kashihara. Characterization of myocardial Na^{+}-Ca^{2+} exchange in rainbow trout. *Am. J. Physiol.* 262: C411-C417, 1992.

34. Weyman, M., and G. F. Tibbits. Cardiac Ca-antagonist binding alterations with exercise training. *Med. Sci. Spts. Exer.* 29: S82, 1987.

35. Yu, Z., J. R. McNeill, and G. F. Tibbits. Cellular functions of diabetic cardiomyocytes: contractility, rapid-cooling contracture, and ryanodine binding. *Am. J. Physiol.* 266: H2082-H2089, 1994.

Table 1

Mean values for heart weight, body weight, and protein content in homogenates.

	1M (n=4)	1H (n=8)	2L (n=10)	2LM (n=10)	2M (n=15)
HW (mg)					
C	793 ± 25	772 ± 17	800 ± 20	730 ± 10	740 ± 20
T	823 ± 22	817 ± 12	810 ± 30	800 ± 30	790 ± 10
T%C	104	106	101	110*	107
BW (g)					
C	289 ± 9	275 ± 7	317 ± 3	286 ± 7	292 ± 5
T	282 ± 8	294 ± 5	307 ± 5	295 ± 9	298 ± 4
T%C	98	107	97	103	102
HW/BW (mg/g)					
C	2.75 ± 0.06	2.82 ± 0.11	2.55 ± 0.05	2.57 ± 0.02	2.53 ± 0.06
T	2.92 ± 0.05	2.78 ± 0.02	2.65 ± 0.10	2.71 ± 0.05	2.64 ± 0.04
T%C	106*	99	104	106	104
PROTEIN (mg/g)					
C	113 ± 10	74 ± 4	108 ± 3	99 ± 5	101 ± 5
T	102 ± 13	67 ± 1	97 ± 4	92 ± 4	100 ± 6
T%C	90	91	90	93	99

Values are means ± S.E.M.; HW, ventricular weight; BW, body weight; HW/BW, heart weight to body weight ratio; Protein, protein content of ventricular homogenate per gram wet weight; N, number of animals with one heart per determination; * $p < 0.05$.

TABLE 2

Characteristics of homogenate and SL from the first study.

	Homogenate		Sarcolemma	
	1M	1H	1M	1H
Protein Yield (mg/g heart wt)				
C	112.6 ± 9.9	74.0 ± 3.7	0.6 ± 0.1	0.6 ± 0.1
T	102.0 ± 13.4	67.1 ± 1.4	0.5 ± 0.1	0.7 ± 0.2
K^+-*p*NPPase (µmol/mg/hr)				
C	0.43 ± 0.03	1.08 ± 0.13	9.50 ± 1.40	22.40 ± 2.10
T	0.45 ± 0.08	1.17 ± 0.15	10.75 ± 1.20	19.90 ± 0.90
Purification Index				
C	1	1	22.53 ± 2.77	20.99 ± 1.36
T	1	1	25.13 ± 3.15	17.95 ± 2.49
Recovery (%)				
C	100	100	12.35 ± 1.08	17.01 ± 2.19
T	100	100	13.50 ± 2.73	18.94 ± 4.22

Values are means ± S.E.M. for 8 (homogenate) or 6 (sarcolemma) observations per group; Protein yield is the protein content in the crude homogenate and purified SL, in milligrams per gram heart weight; K^+-*p*NPPase is the SL marker enzyme activity; Purification index is the ratio of K^+-*p*NPPase activity in the SL fraction to that in crude homogenate in µmol/mg/hr; Recovery is the percentage of the total K^+-*p*NPPase activity (µmoles/hr) in the SL fraction compared to the crude homogenate.

Table 3

Maximum specific DHP binding to homogenates.

	1M (n=4)	1H (n=4)	2L (n=10)	2LM (n=10)	2M (n=15)
B_{max} (fmol·mg^{-1})					
C	149 ± 6	185 ± 10	242 ± 28	241 ± 17	175 ± 13
T	173 ± 18	275 ± 11	253 ± 10	227 ± 11	188 ± 12
T%C	116*	149**	105	94	107

Values are means ± S.E.M. of individual curve fits using GRAFIT®; n, number of experiments performed using homogenates prepared from either 8-9 pooled ventricles (1M and 1H) or 1 ventricle per experiment; *$p < 0.05$, **$p < 0.0001$ level.

Table 4

Maximum specific binding to the RyR high affinity site.

	2L (n=10)	2LM (n=10)	2M (n=15)
B_{max} (fmol/mg)			
C	719 ± 67	945 ± 151	635 ± 53
T	742 ± 59	1028 ± 183	785 ± 82
T%C	103	109	124*

Values are means ± S.E.M. of individual curve fits using GRAFIT®; * $p < 0.05$ level; n, number of experiments with one homogenized heart per experiment.

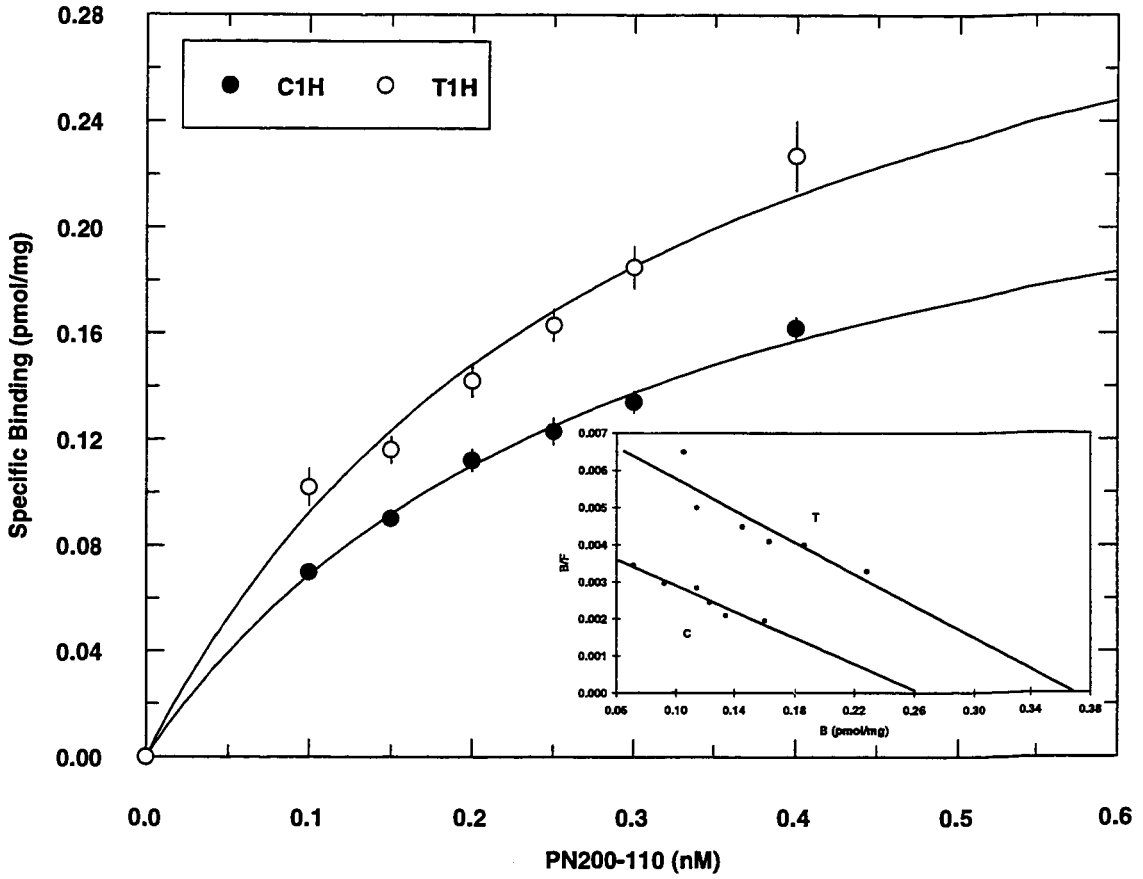

Figure 1 - Specific [^{3}H]-PN200-110 binding to purified sarcolemma (SL) prepared from the hearts of sedentary-control (C1) and treadmill-trained (T1) rats trained under the high (1H) regimen. Training and data collection was performed by M.W. Data represent the mean ± S.E.M. of 4 binding experiments. For each experiment SL was isolated from 8-9 pooled ventricles. Data were fit with a single class of binding sites using non-linear regression (Grafit®). A Scatchard plot of the data is shown in the inset.

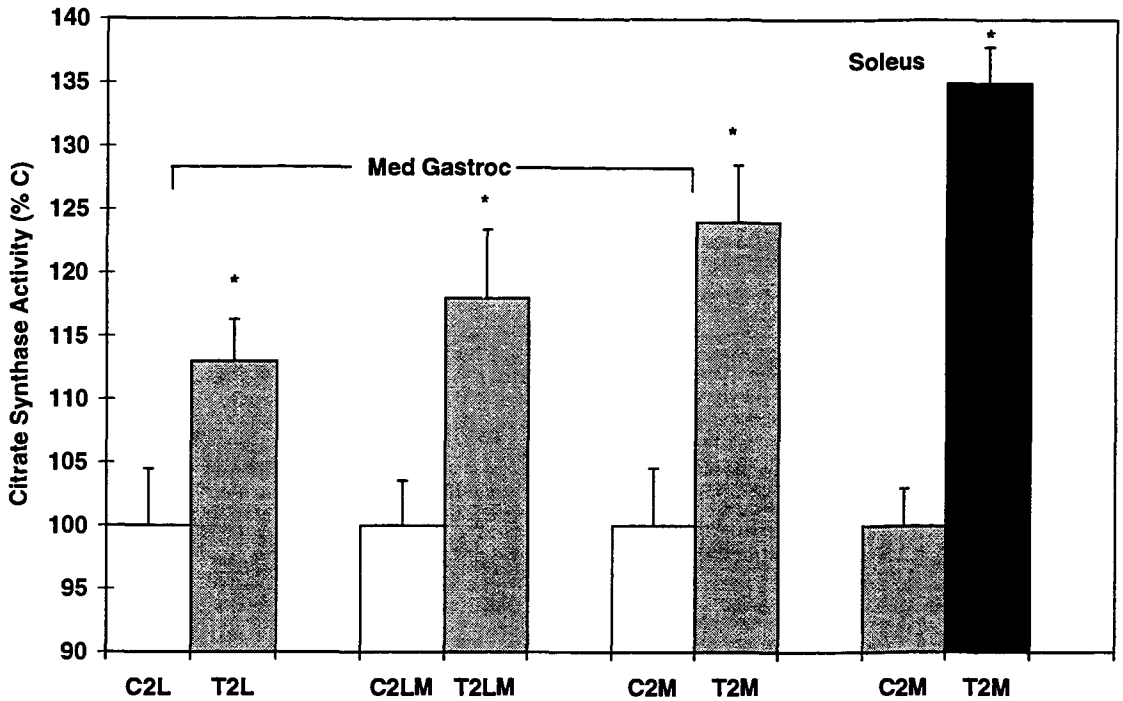

Figure 2. Mean citrate synthase activities from medial gastrocnemius and soleus homogenates isolated from sedentary-control (C2) and treadmill-trained (T2) rats trained under the low (L), low-moderate (LM), and moderate (M) regimens. Data analysis for 2L and 2LM was performed by B.H. Data analysis for 2M (medial gastrocnemius and soleus) was performed by M.T. Data for each group represent the percent increase over control for 10 experiments with one muscle homogenized per experiment. * T2 significantly difference compared to C2, $P < 0.05$.

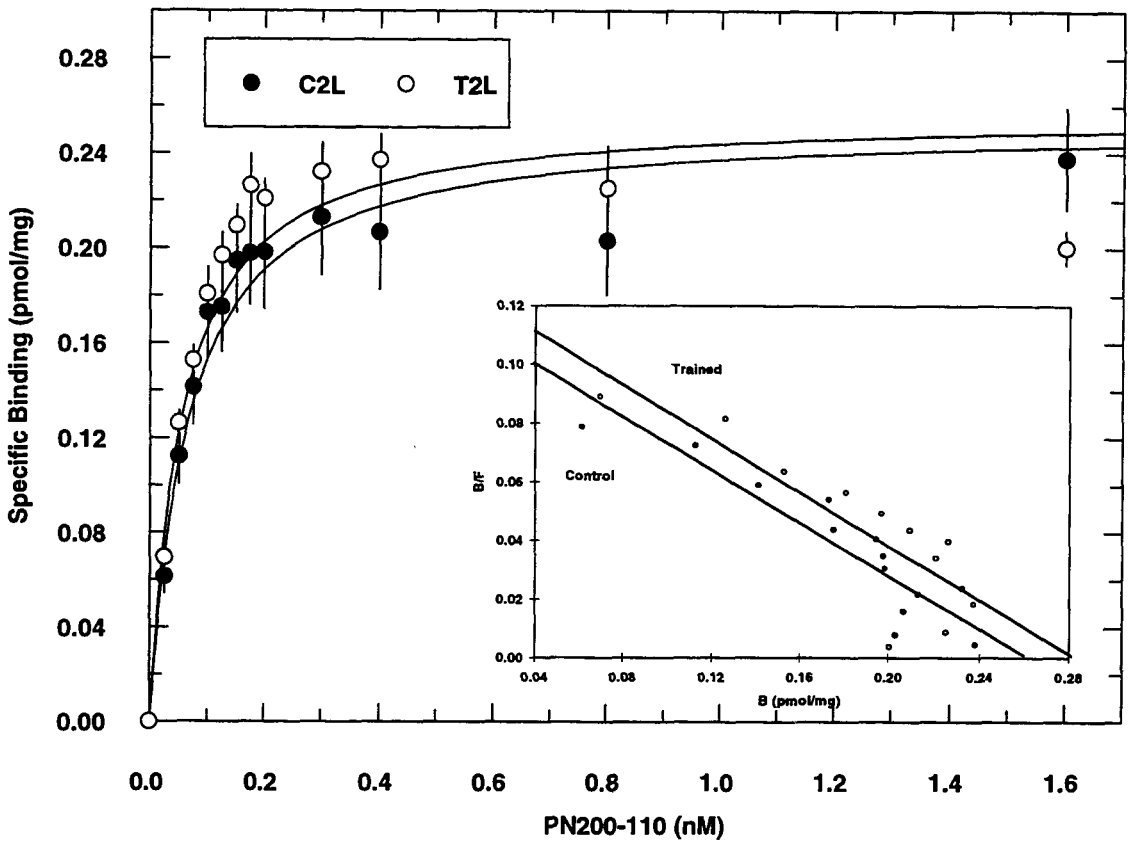

Figure 3. Specific [^{3}H]-PN200-110 binding to crude homogenates prepared from the hearts of sedentary-control (C2) and treadmill-trained (T2) rats trained under the low (L) regimen. Data collection was performed by B.H. and analysis by M.T. Data for each group represent the mean ± S.E.M. of 10 exeriments with one ventricle homogenized per experiment. Non-linear regression (Grafit®) was used to fit the data with a single class of binding sites. A Scatchard plot of the data is shown in the inset.

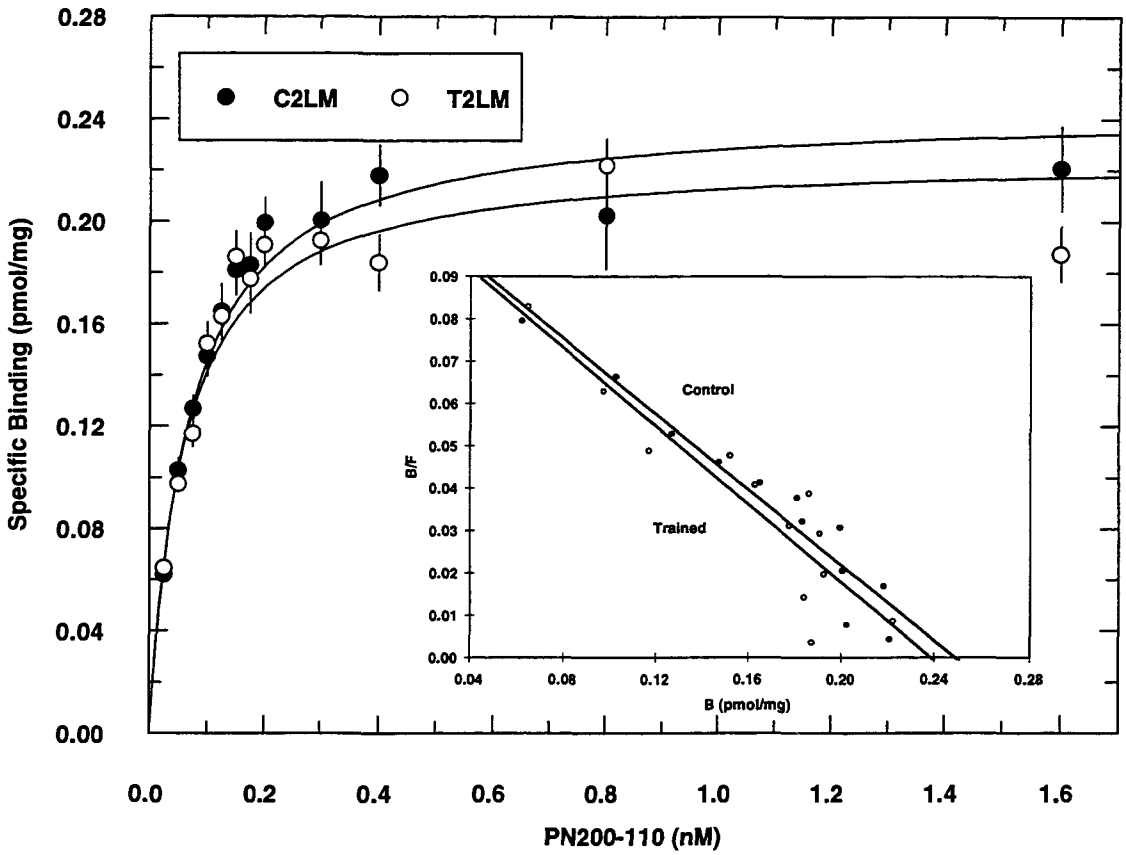

Figure 4. Specific [^{3}H]-PN200-110 binding to crude homogenates prepared from the hearts of sedentary-control (C2) and treadmill-trained (T2) rats trained under the low-moderate (LM) regimen. Data collection was performed by B.H. and analysis by M.T. Data for each group represent the mean ± S.E.M. of 10 exeriments with one ventricle homogenized per experiment. Non-linear regression (Grafit®) was used to fit the data with a single class of binding sites. A Scatchard plot of the data is shown in the inset.

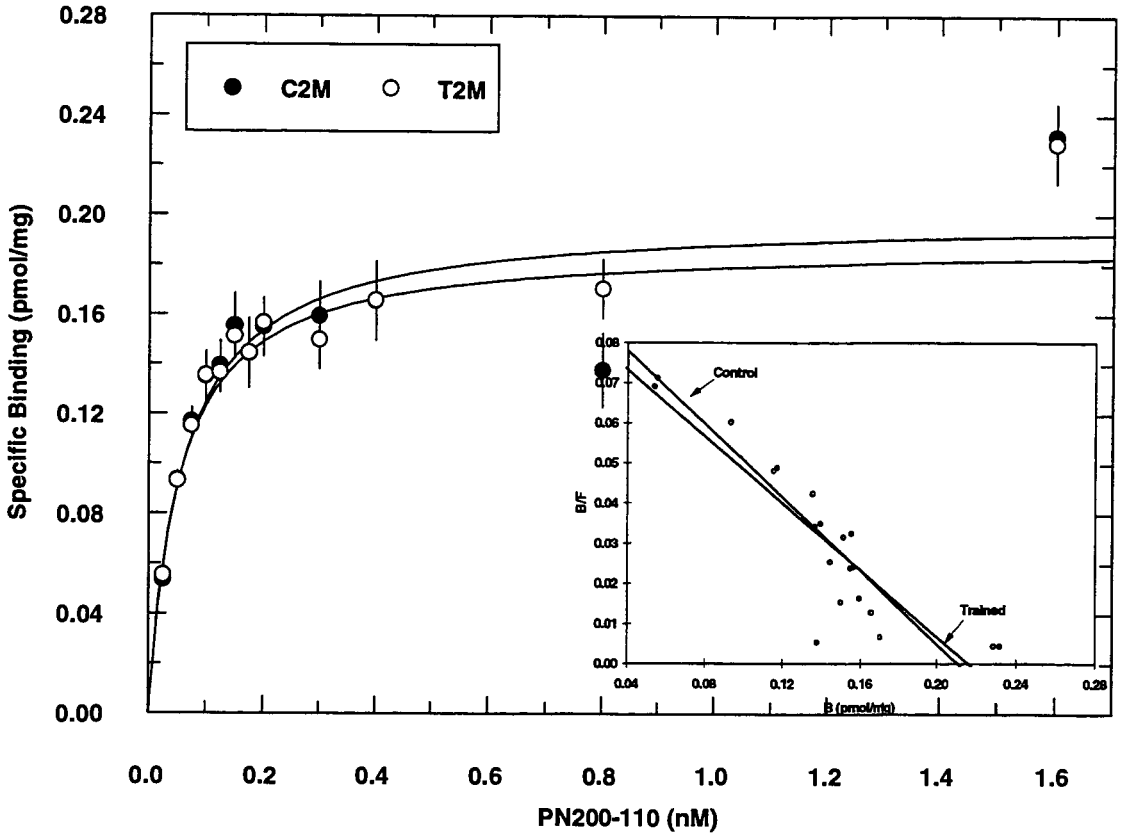

Figure 5. Specific [^{3}H]-PN200-110 binding to crude homogenates prepared from the hearts of sedentary-control (C2) and treadmill-trained (T2) rats trained under the moderate regimen (M). Data collection was performed by B.H. and analysis by M.T. Data for each group represent the mean ± S.E.M. of 15 exeriments with one ventricle homogenized per experiment. Non-linear regression (Grafit®) was used to fit the data with a single class of binding sites. A Scatchard plot of the data is shown in the inset.

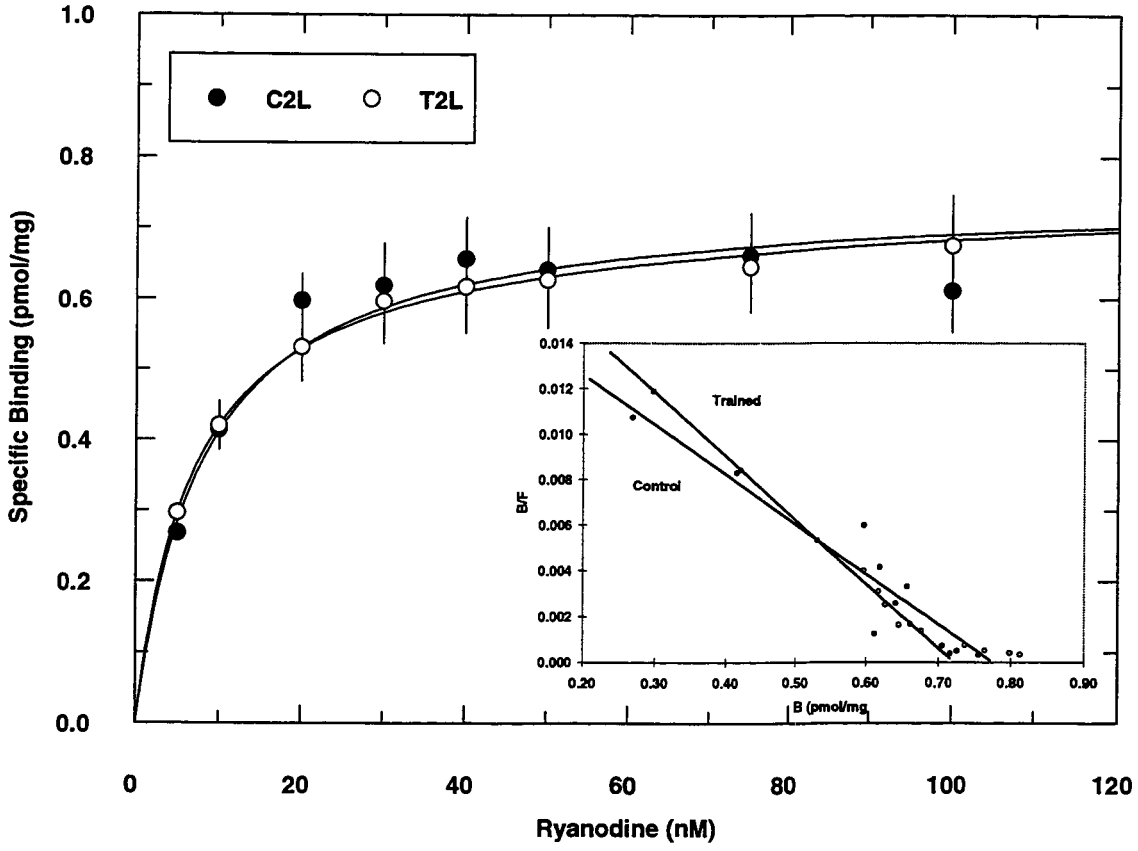

Figure 6. Specific [^{3}H]-ryanodine binding to the same crude homogenates from sedentary-control (C2) and treadmill-trained (T2) rats trained under the low (L) regimen. Data collection and analysis was performed by M.T. Data for each group represent the mean ± S.E.M. of 10 exeriments with one ventricle homogenized per experiment. The homogenate was the same preparation as that used for DHP binding. Non-linear regression (Grafit®) was used to fit the data with a two classes of binding sites over a range of 0 - 500 nM ryanodine. In order to improve the resolution of the high affinity site only data from 0 to 100 nM are shown. A Scatchard plot of the high affinity site is shown in the inset.

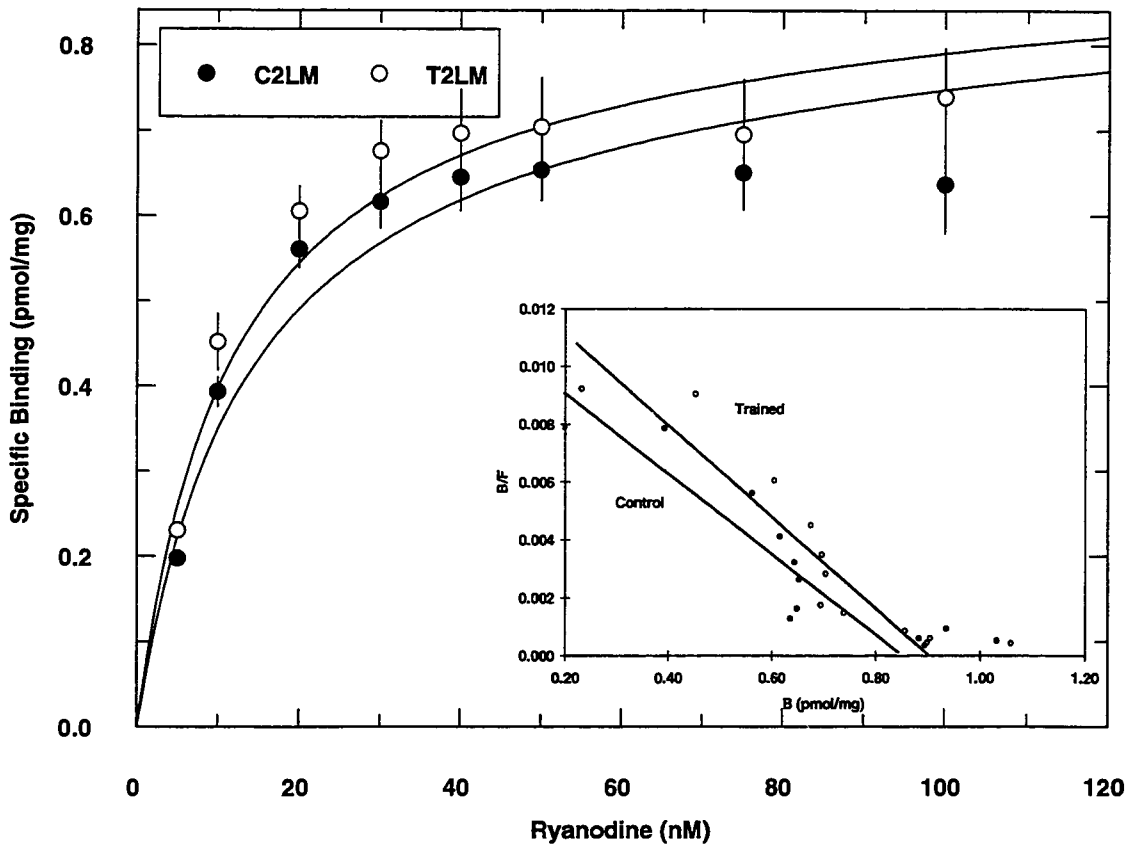

Figure 7. Specific [^{3}H]-ryanodine binding to the same crude homogenates used in the DHP binding from sedentary-control (C2) and treadmill-trained (T2) rats trained under the low-moderate (LM) regimen. Data collection and analysis was performed by M.T. Data for each group represent the mean ± S.E.M. of 10 exeriments with one ventricle homogenized per experiment. Non-linear regression (Grafit®) was used to fit the data with two classes of binding sites over a range of 0 - 500 nM ryanodine. In order to improve the resolution of the high affinity site only data from 0 to 100 nM are shown. A Scatchard plot of the high affinity site is shown in the inset.

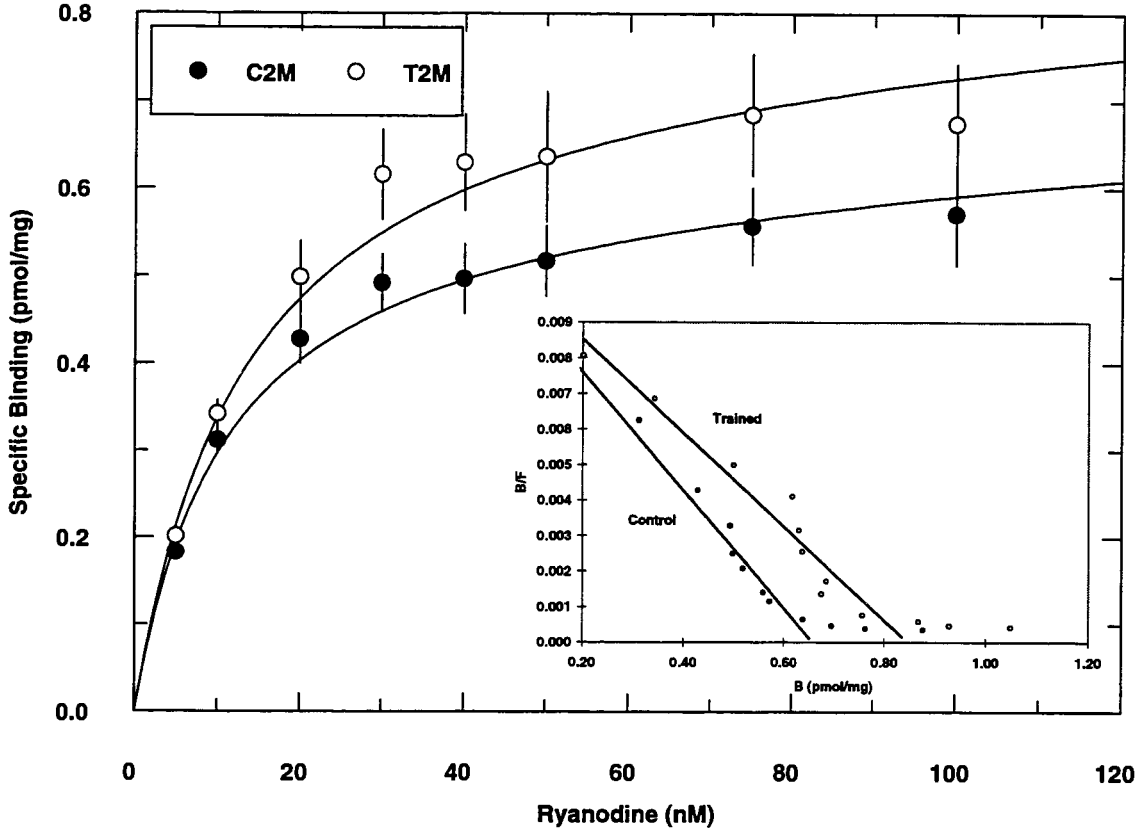

Figure 8. Specific [^{3}H]-ryanodine binding to the same crude homogenates used in the DHP binding from sedentary-control (C2) and treadmill-trained (T2) rats trained under the moderate (M) regimen. Data collection and analysis was performed by M.T. Data for each group represent the mean ± S.E.M. of 10 exeriments with one ventricle homogenized per experiment. Non-linear regression (Grafit®) was used to fit the data with two classes of binding sites over a range of 0 - 500 nM ryanodine. In order to improve the resolution of the high affinity site only data from 0 to 100 nM are shown. A Scatchard plot of the high affinity site is shown in the inset.

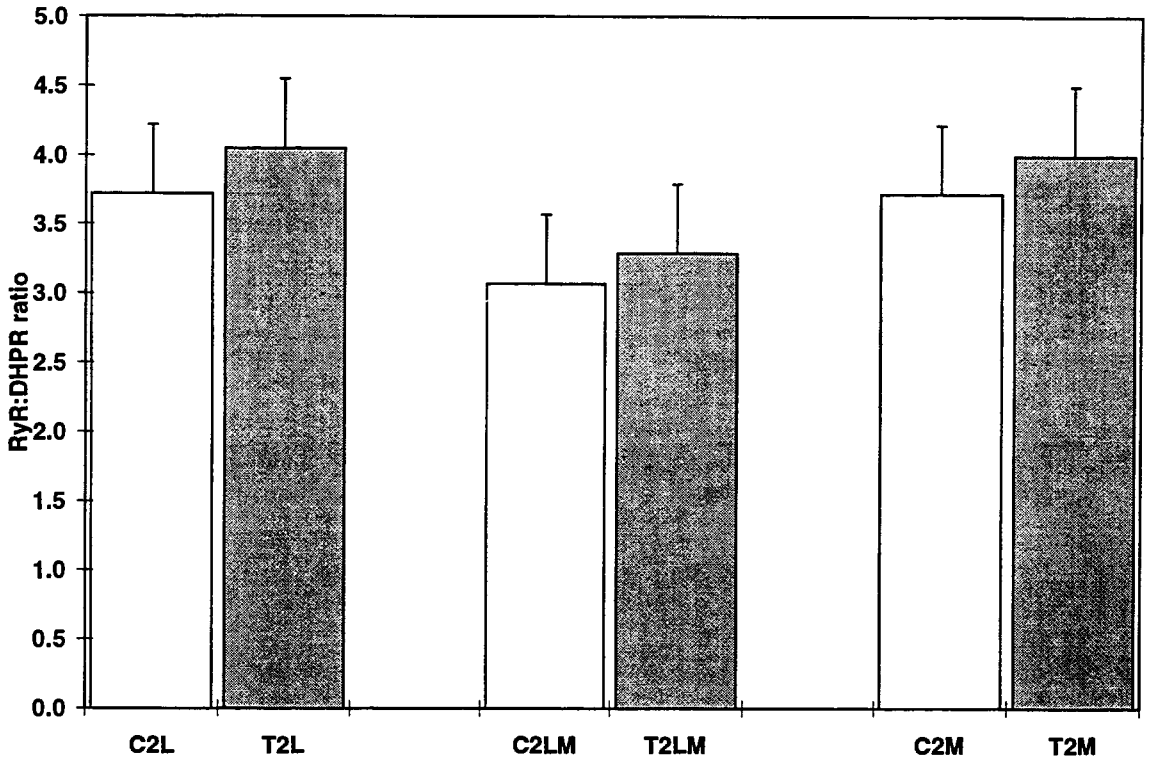

Figure 9. Ratios of B_{max} values for ryanodine receptor (RyR) to dihydropyridine receptor (DHPR) in ventricular homogenates from sedentary control (C2) and treadmill-trained (T2) rats conditioned under the three workrates: low (L), low-moderate (LM) or moderate (M).

CHAPTER 3

ENDURANCE EXERCISE TRAINING: EFFECTS ON Ca^{2+} HANDLING AND SARCOPLASMIC RETICULUM Ca^{2+} CONTENT IN RAT CARDIOMYOCYTES

ABSTRACT

To examine possible exercise-induced alterations in Ca^{2+} handling in the rat cardiomyocyte, indo-1 fluorescence emission (R = ratio 405/480 nm) was monitored simultaneously with changes in cell length during electrically stimulated twitches and rapid cooling contractures (RCCs). Female rats (n=30) were randomly divided into two groups, sedentary-control (C) and treadmill-trained (T). T animals were trained progressively for 14 wks and then maintained for a further 20-28 weeks at 30 m/min, 8% grade, 1 hr/day, 5 days/wk. This training protocol resulted in a 25% increase in soleus muscle citrate synthase activity ($p<0.0001$). Ca^{2+}-tolerant myocytes were enzymatically isolated from C (n=11) and T (n=12) hearts. Unloaded average sarcomere length remained unaltered, 1.90 ± 0.02 μm (n=105 cells) vs 1.88 ± 0.01 μm (n=105 cells) in T vs C, respectively, as a greater number of sarcomeres contributed to the observed 6% increase in cell length, $p<0.05$. Upon field stimulation of T myocytes, maximal extent of shortening, expressed as % change from resting cell length, was significantly ($p<0.05$) greater in T (15.5 ± 0.4 %, n=113 cells) vs C (14.1 ± 0.5 %, n=71 cells). T cells also demonstrated significantly ($p<0.05$) faster peak rates of shortening in T (193 ± 7 μm/s, n=113 cells) vs C (162 ± 6 μm/s, n=71 cells), faster peak rates of relaxation in T (145 ± 5 μm/s, n=113 cells) vs C (127 ± 5 μm/s, n=71 cells) with no change in time-to-peak shortening in T (193 ± 4 msec, n=113 cells) vs C (198 ± 5 msec, n=71 cells). The average R_{rest} in the T group slightly lower compared to C group but was not statistically significant. The maximum rate of rise in R was significantly lower in the T compared to C cells with time to R_{peak} remaining unchanged resulting in a lower R_{peak} (1.13 ± 0.04 vs

1.29 ± 0.05, T (n=29 cells) vs C (n=22 cells)), respectively ($p<0.05$). Inconsistent with greater rates of relaxation during a twitch, T cells (n=29) demonstrated significantly ($p<0.05$) slower time to one-half R decay (290 ± 21 msec) compared to C cells (233 ± 17 ms, n=22 cells). RCCs were used to assess training-induced changes in sarcoplasmic reticulum releaseable Ca^{2+}. Maximal cell shortening during RCCs expressed as % change from initial cell length was not altered as a result of training in T (29.5 ± 0.6 %, n=66 cells) vs C (30.5 ± 0.6 %, n=57 cells). In contrast, R_{peak} during the RCC was significantly ($p<0.05$) reduced in the T group (1.22 ± 0.05, n=15 cells) vs C (1.43 ± 0.10, n=12 cells). The time to one-half relaxation and R decay were significantly faster during rewarming in T compared to C cells, both in the presence and absence of 10 mM caffeine. These results indicate that chronic exercise enhances contractile activation, and this adaptation does not appear to be due to greater Ca^{2+} delivery but rather an increase in contractile element Ca^{2+} sensitivity.

INTRODUCTION

Improvements to the cardiovascular system resulting from endurance exercise training have been well documented in a variety of models (17, 21). Irrespective of the variability of training conditions employed, myocardial functional adaptations are evidenced by greater submaximal and maximum stroke volumes (SV). For a given workload, SV contributes a greater portion to the cardiac output as heart rates are lower (18, 21). While bradycardia may allow for greater filling volumes of the left ventricle under conditions where heart rate and loading conditions were held constant, greater EDV still persisted (33). In addition, evidence for enhanced intrinsic contractile function has also been documented in a variety of preparations including isolated working heart (33), papillary muscle (39) and recently in isolated cardiomyocytes (29).

Intrinsic adapatations may arise from alterations in Ca^{2+} delivery or in the responsiveness of the contractile element to a given amount of Ca^{2+}. Evidence based upon *in vitro* data suggests that increased contractility occurs in the absence of significant alterations to the contractile element (4, 22). However, recent data from intact cell preparations suggest that training may sensitize the contractile element to activation by Ca^{2+} (29). In the trained rat heart, evidence for greater Ca^{2+} delivery is suggested by a prolonged action potential plateau, while papillary muscles generate greater peak isometric twitch tensions (39). Increased SL Ca^{2+} influx may directly activate the myofilaments or trigger an even greater release of Ca^{2+} from the sarcoplasmic reticulum (SR). Recent *in vitro* studies have shown an increase in the DHPR density (20, 43), and Na^{+} /Ca^{2+} exchange affinity for Ca^{2+} (40) with training. Marked changes in the lipid composition of cardiac SL vesicles were also observed in another study (41). However, the consequences of such changes remain to be determined. Finally, virtually nothing is known about the effects of treadmill-training on SR Ca^{2+} content or fractional release.

The purpose of this study was to make a direct assessment of training-induced alterations in Ca^{2+} delivery and removal by measuring intracellular free Ca^{2+} transients (R) in isolated Ca^{2+}-tolerant myocytes using microfluoremetry, and to determined whether these alterations involve relative changes in SR releaseable Ca^{2+} as assessed by rapid-cooling contractures (RCCs). Simultaneous measurement of contractile properties also allowed correlation of changes in Ca^{2+} handling with the functional properties of contraction.

METHODS

Animal Care and Training. Female Wistar rats (n = 30) were randomly divided into exercise-trained (T) and sedentary-control (C) groups. Both groups were housed in a light and temperature controlled room and provided food and water *ad libitum.* Group T participated in a treadmill-training protocol in which the workload was progressively increased for ~10 weeks, until the desired duration, speed and intensity of 5 days per week, 1 hour/day at 30 m/min, 8% grade was achieved. Training at this level was then continued for a further 24 to 32 weeks. Animals were sacrificed during weeks 24 to 32, at the same time each day and at least 24 hours after the last exercise bout to eliminate any acute effects of exercise.

The Cardiomyocyte Model. This study involves the use of enzymatically isolated Ca^{2+}-tolerant cardiomyocytes. This preparation was chosen for a variety of reasons. *In vitro* biochemical analyses, while offering the greatest control of variables, is furthest from the physiological situation and thus extrapolation to the intact organism may often be inappropriate or misleading. Regulatory functions may be lost during the purification of membrane fractions and experimental conditions do not realistically reflect *in vivo* conditions. At the other end of the spectrum is intact cardiac muscle. While these preparations are useful, they present difficulties in controlling membrane potential, and because they also contain nonmyocyte tissue it is difficult to attribute specific activity or property to the myocyte. Isolated single cardiomyocytes are used to study a variety of electrophysiological and biochemical phenomena (7, 12, 13, 34). Putative mechanisms of cardiac adaptation to exercise developed from papillary muscle and cell-free preparations

can now be addressed using a more physiologically relevant model. The isolated cardiac cell offers considerable advantages over other multicellular preparations. Inhomogeneities due to cell-to-cell variations are not masked. Single myocytes are not limited by diffusional spaces nor subject to local accumulation or depletion of substrates and/or pharmacological agents. They are not hindered by series and parallel elastic components. However, it is important to note that the isolated, plated cell is essentially "unloaded" and the mechanical characteristics may not fully represent a functionally intact cell. Also loading the cell with the ester form of Ca^{2+}-sensitive fluorescent indicators may potentially compromise cell viability due to toxic byproducts of the deesterification process. The contractile properties such as changes in length, and rates of shortening and relaxation represent the culmination of a complex series of events. Any changes in these parameters only provides indirect evidence for underlying mechanisms but does help to corroborate evidence obtained from the less physiological biochemical studies. Finally, cardiomyocytes are small with relatively short changes in cell length during a twitch, making quantification of length changes difficult. However, with the use of recently developed video edge detection methods these limitations can be overcome.

Mechanical properties. Mammalian cardiac muscle, in contrast to skeletal muscle, has a very steep sarcomere length-tension relationship. Due to the low intrinsic compliance of the cardiomyocyte, which appears to be related to the cytoskeleton, and the resistance offered by extracellular collagen, the descending limb is essentially absent in cardiac muscle (19). The steepness of the ascending limb has now been attributed to changes in E-C coupling and internal restoring forces as opposed to myofilament overlap.

It is now known that below optimal sarcomere lengths TnC-Ca^{2+} sensitivity decreases and less Ca^{2+} is released from the SR (1, 2, 27).

Indices of contractility. There are many methods that have been used to measure a change in myocardial contractility using a variety of preparations including whole hearts, ventricular strips, papillary muscle and more recently isolated myocytes. A change in contractility, by definition involves length-independent alterations in the amount of work performed during a single cardiac cycle. However, it is virtually impossible to remove all influences of length-dependent changes in tension development. Even the use of isolated cardiomyocytes involves changes in sarcomere length during cell shortening. Characterization of the myocardial contractile process comes from measures of shortening responses such as maximal extent of shortening, rates of shortening and time to peak shortening and these have been used to measure changes in contractility. Tension or force generated by the isolated and intact myocyte is technically difficult to measure. Direct measuremnt of mechanical forces have been achieved, although problems associated with the increased resistance offered by the attachment apparatus can be significant (19, 23).

Ventricular Myocyte Isolation. Ca^{2+}-tolerant myocytes were enzymatically isolated following a modified protocol of Mitra and Morad (28). All solutions were prepared using sterile procedures and aerated before and during use with 100% O_2. Several minutes after an injection of heparin containing sodium pentabarbitol (65 mg/kg and 5 ml/kg heparin ip) the heart was removed and placed into a beaker of ice-chilled buffered minimal essential medium (MEM), pH 7.3 at 23°C. The heart was attached to a

Langendorff apparatus and perfused with MEM (nominally Ca^{2+}-free) at 37°C. After several minutes, the perfusion buffer was changed to a MEM-collagenase solution [1 mg/ml collagenase type II, (Worthington Biochemicals, Freehold, NJ) plus 25 μM Ca^{2+} and 0.5 % bovine serum albumin (BSA; Boehringer Mannheim, fraction V, fatty acid free)].

After ~30 minutes the atria were removed and the venticular cells were gently teased apart, transferred to a water-jacketed beaker (37°C) and subject to a further 3-5 minutes of mechanical digestion. Isolated myocytes were then filtered through a 200 μm nylon mesh. The Ca^{2+} concentration was gradually raised from 0.25 to 1.0 mM in three steps. Step 1 involved pelleting the cells by gravity, removing the supernatant, and resuspending in buffered MEM (7.3 at 23°C) with 1% BSA plus Ca^{2+}. This procedure was repeated three times increasing the Ca^{2+} concentration each time. The fourth and final step involved resuspending cells in buffered medium-199 and 1.8 mM $CaCl_2$ (M199) plus 5% fetal bovine serum (FBS; Gibco). After 1-3 hours recovery at room temperature, myocytes were plated onto laminin-coated (20 μg/ml in M199) glass coverslips (thickness 0.2 mm). All experiments were performed between 3 and 12 hours post-isolation.

Measurement of myocyte dimensions and contractile properties. The plated cells were mounted on the stage of an inverted microscope (Nikon Diaphot-TMD) and continually bathed in a temperature-equilibrated (23°C) modified Tyrode solution containing (in mM): 140 NaCl, 6 KCl, 1.8 $CaCl_2$, 1 $MgCl_2$, 10 glucose, and 5 mM TES buffer (pH

adjusted to 7.3 at 23°C). Myocyte dimensions were routinely made at 2 and 3 hours post-isolation. Selected cells were quiescent in 1.8 mM Ca^{2+}, rod-shaped, had clear striations, visible dark edges, and completely adherent to the coverslip. The focused cell image was captured by a video camera (COHU CCD 4815 series, San Diego, CA) mounted onto the microscope side port (Figure 1). CCD line scan voltage output was passed online to a video edge detector (VED) circuit board (38), and a high resolution monitor (Sony PVW-91). The VED output was also directed to a personal computer, digitized (Tekmar Labmaster board), and viewed on-line using Oscar® [Deltascan Photon Technology International, (PTI)] software at a sampling rate of 50 data points per second. Resting cell length was determined by positioning the left and right VED windows at maximum cell length and recording the voltage output. Maximum cell width was determined in a similar manner after rotating the CCD camera 90° and repositioning the VED windows. Average sarcomere length was determined by dividing the cell length by the number of visually counted sarcomeres.

During motion measurements, myocytes were field-stimulated with platinum electrodes at a frequency of 0.5 Hz (1.5 times threshold), and 5 msec duration using a Grass S11 digital stimulator. In some experiments the frequency was varied between 0.10 and 1.33 Hz. Contractile measurements were taken after 5 minutes of continuous electrical stimulation to ensure cell viability and that a steady state twitch amplitude had been reached without changes in resting length. Only those cells contracting at least 5% of initial length were used. Maximum rates of cell shortening (-dL/dt) and relengthening

(+dL/dt) were determined by derivatizing the motion signal using Oscar® software and converting to units of microns per second.

Measurement of intracellular $[Ca^{2+}]_i$. In chapter 2 pharmacological methods were used to examine two key components of E-C coupling, namely the DHPR and RyR . A more integrated approach to assess the physiological consequences of changes in DHPR and RyR densities is to use isolated Ca^{2+}-tolerant cardiomyocytes. By recording intracellular Ca^{2+} transients under various conditions, a better understanding of the underlying mechanisms which contribute to the known exercise-induced enhancement of contractility may be achieved.

Intracellular Ca^{2+} has been measured in a variety of excitable cells using Ca^{2+}-selective microelectrodes, metallochromic dyes, bioluminescent indicators and more recently fluorescent Ca^{2+} indicators (15). Ca^{2+}-selective microelectrodes generally have a wide dynamic range, but suffer from slow response times making measurements of rapid changes in Ca^{2+} impossible. In addition, Ca^{2+} leakage at the impalement site may lead to inaccurate measurements. In contrast, the metallochromic dyes (i.e., arsenazo III, antipyrylazo III, tetramethylmurexide) and bioluminescent indicators (i.e., aequorin) have significantly faster response times, but have the disadvantages of: 1) motion artifacts, 2) the need for microinjection, 3) inappropriate K_D, 4) low quantum yield, and/or 5) multiple ion sensitivity. The fluorescent Ca^{2+} indicators subsequently developed have overcome many of these drawbacks. In particular, indo-1, has a sufficiently fast response time *in vitro* (tau ~2-14 msec), high quantum yields, and because indo-1 is a derivative of EGTA it is relatively insensitive to Mg^{2+} and temperature. Unlike EGTA, indo-1 is relatively

insensitive to pH. Moreover, indo-1 has a K_D of ~250 nM in the absence of binding to protein and thus is well suited to measure physiological ranges of cytosolic Ca^{2+} (24). Ca^{2+} binding to indo-1 causes a change in the relative intensity of emitted fluorescence at the two wavelengths, 405±10 and 480±10 nm. Indo-1 was chosen for the present experiments because both emission wavelengths can be monitored continuously and simultaneously with myocyte shortening. The ratio of fluoresence emission (405/480 nm) has been used to estimate $[Ca^{2+}]_i$. The ratiometric method eliminates problems associated with variations in emitted light unrelated to Ca^{2+} such as that which would occur due to: 1) variations in excitation light intensity, 2) nonuniform illumination of the optical field, 3) motion artifacts, 4) variable dye concentration, and 5) variations in cell thickness. The effect of fluorescence emission pathlength does not pose a problem in the following experiments. Over the measurement timeframe $[Ca^{2+}]_i$ will be homogeneously distributed throughout the cell. However, interpretation and quantification of the Ca^{2+} transient data has proved difficult for several reasons.

Initial experiments relied upon *in vitro* calibrations in order to estimate $[Ca^{2+}]_i$, and have generally used the free acid form of indo-1. The generation of *in situ* or *in vivo* calibrations, while more appropriate, have been extremely difficult to perform and have not been fully accomplished (8). The difficulties encountered include myocyte contracture at high $[Ca^{2+}]_i$, loss of cellular components including the indicator during equilibration of intra and extracellular media, and interactions between indo-1 and intracellular constituents. The latter can result in altered indicator kinetics and a reduced *in vivo* dynamic range. There is evidence that indo-1 may bind to intracellular proteins

which can decrease its Ca^{2+} affinity by several-fold and lead to underestimations of intracellular Ca^{2+} (3, 8, 14, 26). In addition, high levels (>100 μM) of dye loading may contribute to significant Ca^{2+} buffering effects (6, 30). The use of the actoxymethylester form of indo-1 to load cells with dye further complicates interpretation of the fluorescent signal as it may originate from compartmentalized or incompletely deesterified forms. All these factors place limitations on the quantitation of intracelluar Ca^{2+} during a single contraction. These factors do not, however, prevent relative changes in Ca^{2+}-sensitive fluorescence to be assessed provided care is taken to ensure a viable myocyte preparation is used and dye compartmentation and/or partially deesterified forms are minimized.

Cell loading and Indo-1 Fluorescence Measurements. Cells to be used in fluorescence measurements were loaded with 5 μM indo 1/AM in <0.1% anhydrous DMSO (Molecular Probes, Eugene, OR) for 30 min at 23°C in the dark. After loading, plated cells were washed with M199/FBS and left in the dark for a further 15-20 minutes. This method optimized deesterification and minimized dye compartmentation. Cellular fluorescence emissions were recorded simultaneously with contractile movements as previously described (44). Fluorescence emissions were expressed as the ratio (R) of 405/480 nm and were used to analyze the $[Ca^{2+}]_i$ -transients.

Preliminary experiments, using an excitation wavelength of 350 nm and band pass filters on emission of 405±10 nm and 480±10 nm, determined that a data acquisition rate of 50 pts/sec was the lowest rate that did not compromise signal characteristics while allowing sufficient data storage. Total background fluorescence including autofluorescence accounted for ~4-8% of total fluorescence from loaded cells. While

loading conditions minimized dye compartmentation, pilot experiments in which cells were subject to 1 μM digitonin followed by 1% Triton X-100 revealed that <13% of the total fluorescence counts were contained within intracellular compartments such as mitochondria and SR. In several control experiments, after incubating for 10 min in an inhibition buffer containing 40 mM 2,3 butanedione monoxine and 2 μM carbonyl cyanide p-(trifluoromethoxy)phenylhydrazone, pH 7.5 at 23°C, *in situ* R_{max} was obtained by the addition of $CaCl_2$ (final 4 mM) and ionomycin (final 2 μM, 0.03% DMSO). Several R_{min} values were also obtained by treating the cell with inhibitor buffer plus Ca^{2+}-EGTA (pCa 10) and 2 μM ionomycin or 20 μM digitonin. Finally, the dynamic range of indo-1 *in situ* was slightly lower compared to the *in vitro* calibrations using the free acid form of the indicator (data not shown). Estimates of intracellular free Ca^{2+} ($[Ca^{2+}]_i$) were only made for comparative purposes. There are several reasons why the estimates of $[Ca^{2+}]_i$ may be inappropritate. First, it was not possible owing to the small number of animals remaining at the end of the study to obtain a sufficient number of R_{min} and R_{max} values *in situ*. Second, the interpretation of the results depend upon knowledge of the relative rather than absolute changes in $[Ca^{2+}]_i$. Third, the possibility exists that protein-indo-1 binding decreases the affinity of the indicator for Ca^{2+} (26), thus the binding reaction between Ca^{2+} and indo-1 cannot be considered to be at equilibrium during the transient (34) and thus $[Ca^{2+}]_i$ estimations would not be accurate. The *in situ* K_D value is unknown and has been reported to vary from 0.25-1 μM depending upon the presence of protein, temperature and ionic conditions (3, 8, 26). After data smoothing the

transient signal was derivatized to obtain an estimate of the maximum rate of rise in R (+dR/dt). The time to one-half R decay was obtained by determining the time from R_{peak} to one-half of the difference between R_{pre} and R_{peak} where R_{pre} is R just prior to the rapid R upstroke.

Rapid Cooling Contractures. The protocol used follows Bers *et al.* (12). The indo-1 loaded cells were superfused at ~18-22 ml/min with a modified Tyrode solution containing (in mM): 140 NaCl, 6 KCl, 1.8 $CaCl_2$, 1 $MgCl_2$, 10 glucose, and 5 TES buffer (pH adjusted to 7.3 at 23°C). RCCs were initiated by rapidly switching from a warm (23°C) to cold (1°C) Tyrode solution in less than 2 seconds with the use of minature solenoid valves (Lee Co.). In order to assess potential differences in the relative contribution of Na^+/Ca^{2+} exchange activity to relaxation, 10 mM caffeine was added to the cold and rewarming solutions in some experiments.

The pre-RCC protocol involved 10 stimulated twitches followed by a 10 second rest interval. The influence of rest periods on RCC magnitude has been shown to be species specific (10). The rat myocardium displays a phenomenon of rest potentiation thus optimal time for reproducible loading of the SR with Ca^{2+} prior to each RCC was determined to be 10 seconds. Data collected from the VED output and fluorescence emission were also monitored simultaneously during RCCs at a sampling rate of 50 pts/sec. R_{peak} was taken to be the maximum fluorescence ratio after smoothing and linear regression analysis of the transient data during cold exposure. The relaxation rate during rewarming was taken as the time from the peak of the rewarming spike to one-half of the difference between resting cell length just prior to the RCC and the peak of the

rewarming spike. The R decay rate was determined by the time from R_{peak} to one-half of the difference between R_{rest} prior to RCC and R_{peak}.

Citrate Synthase Assay. The right medial gastrocnemius and soleus muscles from T and C animals were isolated and immediately frozen in liquid N_2. The muscles were subsequently weighed, thawed and homogenized in ice-cold buffer containing (in mM): 20 MOPS (pH 7.2 @ 23°C), 5 EDTA, and 0.1% Triton X-100, then sonicated and re-frozen. On the day of the assay crude homogenates from T and C muscles were thawed in parallel, sonicated and spun at ~13,000 rpm for 5 min. The supernatants were assayed for citrate synthase activity at 37°C as previously described (37).

Statistical Analysis. An independent Student's *t*-test was used to determine the degree of significance between the T and C groups with significance set at $P < 0.05$.

Materials. All reagents were of the highest purity obtained from Sigma Chemical Co. with exceptions as noted.

RESULTS

Training response. Throughout the duration of training no significant differences in total body weights were observed nor were any differences noted at time of sacrifice (338 ± 12 and 362 ± 10 g, in T vs C respectively). In order to preserve cell viability, heart weights were not determined. Indicative of a training effect, this regimen produced marked increases in oxidative marker enzyme activity in both soleus and medial gastrocnemius whole muscle homogenates. Citrate synthase activities were 13% and 25% greater in the medial gastrocnemius and soleus muscles, respectively, from trained compared to control animals (Figure 2). Finally, while no differences were noted in average maximum myocyte width, cells isolated from T hearts were ~6% longer compared to those cells isolated from the control hearts (Table 1). Similarly, T myocytes had a greater number of sarcomeres, $p<0.05$.

Stimulated twitches.

Contractile properties. Both T and C cells displayed a typical negative force-frequency response. During steady-state stimulation (0.5 Hz) maximal extent of cell shortening (L_{max}) was 10% greater in T compared to C cells, $p<0.05$. T myocytes also demonstrated significantly faster rates of shortening and relengthening when compared to C myocytes (Table 2). Overall, however, time-to-peak shortening remained unaltered in these cells.

Ca^{2+}-transients. The exercise training regime used in this study was sufficient to elicit alterations in the time course of the Ca^{2+} transient recorded as the fluorescence emission ratio (R). As shown in Table 3, R_{rest} was slightly lower in the T group but this

difference was not significant. The magnitude of the R_{peak} was significantly lower (~12%) in T compared to C cells, $p<0.05$. In addition, the average Ca^{2+} transients from T cells exhibited a significantly slower maximum rate of rise (+dR/dt) and essentially no change in the time-to-peak R. When R was integrated over the twitch interval no differences were observed in cells from either group. However, the area-to-R_{peak} was significantly less in T vs C myocytes, $p<0.05$. Training did not appear to enhance the rate of Ca^{2+} removal during relaxation as measured by the slower time to one-half R decay (Table 3)

SR releaseable Ca^{2+}. Rapid cooling contractures (RCCs) were used to assess any changes that training may have had in the relative amount of SR releaseable Ca^{2+}. When RCCs were elicited, myocytes from both groups shortened by ~30% of initial cell length (Table 4). In contrast, the amplitude of R_{peak} was significantly lower by ~15% in T compared to C myocytes.

In order to assess the relative contribution of Na^{+}/Ca^{2+} exchange activity to relaxation, 10 mM caffeine was added to the cold and rewarming solutions in some experiments. Similar results were observed in both L_{max} and R_{peak} in the presence and absence of added caffeine. Due to the effects of caffeine on SR function, the time constants for relaxation (τ_{relax}) and ratio decay (τ_{decay}) during rapid rewarming were several-fold higher compared to the same protocol without added caffeine. The τ_{relax} from T cells was 16% and 32% lower in the absence and presence of caffeine, respectively ($p<0.05$). Under the modified Tyrode solution, τ_{decay} from T cells was not

significantly different compared to C cells. However, in the presence of caffeine, τ_{decay} was 42% lower in T vs C cells, $p<0.05$.

DISCUSSION

Training response. The training regime outlined in this study did not produce any significant differences in body weights between the two groups, neither during the time course of training nor at the time of sacrifice. The magnitude of citrate synthase activity increases are consistent with other training studies using similar training intensities demonstrating enhanced contractility (5, 39, 41). The longer cell length measured from T myocytes is accounted for by an increase in sarcomere number. These dimensional changes are also similar to those observed in a previous study using a similar training protocol albeit at a slightly higher intensity (29). The accompanying cell volume increases are also consistent with the slight increase in heart weights of female rodents typically recorded in studies using similar regimens (22, 33, 39). In addition, the longer myocyte lengths may contribute to the observed increases in EDV by increasing the circumferential dimension of the left ventricle. Under conditions of identical heart rate and loading, EDV is increased by 16% in treadmill-trained rats (33). An increase in the chamber volume would be accompanied by less of an increase in myocardial wall stress and consequently a greater SV independent of any changes in contractility or optimization of the sarcomere length-tension relationship.

Stimulated twitch characteristics.

Contractile properties. While the isolated cardiomyocyte provides a more physiological model compared with biochemical analyses, all of the data collected were obtained from cells stimulated well below physiological frequencies, in an unloaded state and at lower temperatures. However, much information can still to be gained and

comparisons made with data collected under similar conditions from other laboratories. When stimulation frequency is changed the force generated by the heart may increase or decrease depending upon species and experimental conditions (10). The features of the force-frequency relationship has been attributed to a transient imbalance between Ca^{2+} influx and efflux. Both T and C myocytes in this study demonstrated a negative force-frequency response typical for rat heart.

In general, the contractile responses of the cardiomyocytes in this study are consistent with those published previously and supports the viability of our cell preparation (35, 36). During steady-state electrical stimulation at 0.5 Hz, T myocytes shortened significantly more than C cells. The peak rates of cell shortening ($-dL/dt_{max}$) and relaxation ($+dL/dt_{max}$) were also significantly faster in the T cells while the time-to-peak shortening remained the same. The greater extent of shortening and unaltered time course of shortening is consistent with similar observations obtained in isolated myocytes from rats trained using a regimen of slightly higher intensity (29). In contrast, we report greater rates of shortening and relengthening. While the reason for this discrepancy remains unclear, the training intensities used in the two studies were somewhat different. The observed training-induced increase in contractile activation as measured by L_{max} does not distinguish between differences in contractile element Ca^{2+} sensitivity or changes in the amount or time-course of Ca^{2+} delivery. The similarity in the +dL/dt over -dL/dt ratio between the two groups does help to rule out alterations arising from the passive components of shortening (19).

A greater response by the contractile element must involve an increase in either the rate or the number of cross bridges being formed. Current *in vitro* evidence is not in favour of a greater rate of cross bridge cycling resulting from training. Alterations in the level of phosphorylated myosin light chain or relative amounts of V_1 myosin isozyme do not occur as the result of treadmill training female rodents (4, 22). Other ways to enhance contractile activation is to: 1) increase the rate of rise in free Ca^{2+} and thus delivery to the myofilaments, 2) prolong the duration of elevated free Ca^{2+}, or 3) increase TnC-Ca^{2+} sensitivity by one of several possible mechanisms. The recording of Ca^{2+} transients attempts to assess any alteration in Ca^{2+} delivery.

Ca^{2+} transients. Individual estimates of intracellular free Ca^{2+} ($[Ca^{2+}]_i$) were not performed for several reasons. It was not possible owing to the small number of animals remaining at the end of the study to obtain a sufficient number of R_{min} and R_{max} values *in situ*. Secondly, the interpretation of the results depends upon knowledge of the relative rather than absolute changes in $[Ca^{2+}]_i$ with the exception that ΔR is not linear with $[Ca^{2+}]_i$ when $[Ca^{2+}]_i >> K_D$. Thirdly, the possibility exists that indo-1 protein binding decreases the affinity of the indicator for Ca^{2+} (26), thus the binding reaction between Ca^{2+} and indo-1 may not be at equilibrium during the transient (34). These factors may lead to erroneous estimations of $[Ca^{2+}]_i$. Under equilibrium conditions, the *in situ* K_D value is currently unknown, but estimates using diferent methodologies have reported values from 0.25-1.0 μM depending upon the presence of protein, temperature and ionic conditions (3, 8, 26). Using reasonable values for K_D, R_{min} and R_{max} (based on pilot

data) and data from Figure 5, an estimation of $[Ca^{2+}]_i$ was made simply for comparative purposes (Figures 6 and 7).

The amplitude of the Ca^{2+} transient is determined by the balance between the rate of cytosolic Ca^{2+} entry and the rate it is removed by binding to various intracellular buffers, SR sequestration, or extrusion from the cell. The binding of Ca^{2+} to TnC and other cytosolic buffers is essentially diffusion limited and occurs within a few milliseconds of the initial rise in cytosolic free Ca^{2+} (31). Thus, if TnC-Ca^{2+} affinity was increased as the result of chronic exercise, one might expect the amplitude of the Ca^{2+} transient to decrease, however, this effect is likely to be very small and probably not observable due to the much larger pool of other Ca^{2+} buffers. While R_{rest} is not significantly different between groups, R_{peak} during an electrically stimulated twitch was 12% lower in the T cells (Table 3, Figure 5). This peak amplitude attenuation has been observed previously in T cells loaded with membrane permeant form of fura-2 (29). A training-induced increase in TnC-Ca^{2+} sensitivity by any one of a number of mechanisms (i.e., increased pH_i buffering, phosphorylation) would provide one explanation for enhanced contractile activation in light of the observed reduction in R_{peak}. Other explanations for the reduced R_{peak} include; 1) greater indo-1 Ca^{2+} buffering, 2) decreased SR release, and/or 3) dilution of Ca^{2+} into a larger cell volume. These factors would not, however, account for greater contractile activation. While intracellular indo-1 concentrations were not determined, it is possible that high levels of dye loading could alter the characteristics of the Ca^{2+} transient in the T cells (6). The loading conditions

used in the present experiments were identical for both groups. No differences were observed in the raw fluorescence values between groups. In another study, intracellular concentration of indo-1 was determined to be on average <50 μM using loading conditions of 10 μM indo-AM, 15 min, room temperature (9). Therefore the loading conditions used (5 μM, 30 min, room temperature) in our study are expected to result in a similar or lower intracellular indo-1 concentration. Concentrations known to affect the transient amplitude and timecourse, have been demonstrated to be >100 μM (6). The best indicator against either differential loading or overloading is the observation that the contractile properties are the same in both loaded and unloaded cells.

In addition to the attenuated amplitude, the time course of the Ca^{2+} transient was altered in the T cells. While this contrasts with previous data (29), the slower rate of rise (+dR/dt) suggest that the kinetics of Ca^{2+} release and/or buffering have been altered as the result of training in the present study. The faster time-to-R_{peak} shown in Table 3 appears to be artifactual as this was not apparent in the averaged traces (Figure 5). Enhanced contractile activation may arise in light of a reduced peak $[Ca^{2+}]_i$ by maintaining the peak $[Ca^{2+}]_i$ concentration for a longer time period or by slowing the rate of $[Ca^{2+}]_i$ removal (16). When the fluorescence ratios were integrated no differences were found in the total area under the average transient, but the area-to-R_{peak} was significantly reduced in the T cells by 15%, $p<0.05$. This suggests that the enhanced contractility is not due to a greater Ca^{2+} delivery. Changes in either the concentration or Ca^{2+} binding affinity of any one or more of the intracellular Ca^{2+} buffers may potentially

explain these results. Further experiments are required to determine if any differences in total intracellular Ca^{2+} buffering exists between cardiomyocytes isolated from trained and sedentary rats.

Finally, during the relaxation phase of the twitch, T myocytes demonstrate significantly slower time to one-half of R decay. The reasons for this result are not known, particularly in light of a faster mechanical relaxation in T compared to C cells. An increase in the affinity of TnC for Ca^{2+} would be expected to decrease the 'off' rate constant of TnC for Ca^{2+} and slow relaxation (16). Alternatively, the slower rate of R decay may be explained by a return to baseline from a lower peak $[Ca^{2+}]_i$. The possibility also exists that TnC-Ca^{2+} affinity is greater during cell shortening and decreases during relengthening. This last point would account for the greater mechanical relaxation observed.

Rapid Cooling Contractures. Rapid cooling of cardiac muscle to $<1^{\circ}C$ in less than a few seconds leads to the release of essentially all of the Ca^{2+} in the SR. At the same time the cold temperatures drastically inhibit other Ca^{2+} transport mechanisms (12). The magnitude of the ensuing contracture is thus believed to reflect the amount of Ca^{2+} which was in the SR just prior to cooling. The relative change in transient magnitude from twitch-R_{peak} to RCC-R_{peak} is considerably less in magnitude compared to the same response in cell shortening (twitch-L_{max} to RCC-L_{max}). One would expect that indo-1 will underestimate free Ca^{2+} during cold exposure due a temperature-dependent increase in the K_D for Ca^{2+} (12). It is also possible that the indo-1 may have become saturated

with Ca^{2+} although this is unlikely because the maximal RCC response is less than R_{max} based on previous *in vitro* calibrations but done at 23°C.

No between group differences were observed in L_{max} during an RCC ellicited under either modified Tyrode or modified Tyrode plus 10 mM caffeine conditions (Table 4). However, the use of L_{max} as an index for SR Ca^{2+} content under maximal SR loading is not valid. Factors limiting L_{max} during an RCC may involve mechanical constraints of the low compliance myocyte (19), the amount of Ca^{2+} released and/or TnC-Ca^{2+} sensitivity. With a thick filament of 1.4 μm and 64 sarcomeres, maximum cell shortening without any thick filament compression/buckling is predicted to be ~25% of resting cell length while RCCs are ~30%. Also, the influence of temperature reduction on cell compliance is not known. Further evidence that the passive components do not appear to be the limiting factor is the presence of the rewarming spike (see Figure 4) typically observed. Rewarming spikes reflect the sudden increase in TnC-Ca^{2+} affinity associated with a rapid increase in temperature. The presence of a rewarming spike also rules out TnC-Ca^{2+} saturation in limiting the extent of shortening. The predominant factor limiting L_{max} is more likely to be the substantial decrease in TnC-Ca^{2+} sensitivity accompanying cold exposure (25). Large amounts of Ca^{2+} would have to be released in order to measure a small change in L_{max}. A better indicator of SR releaseable Ca^{2+} under maximal SR loading is RCC-R_{peak}.

The average R_{peak} during RCCs was significantly reduced in T compared to C cells under modified Tyrode and modified Tyrode plus 10 mM caffeine conditions (Table

4). The possible explanations to account for these results are essentially the same as for the reduced twitch R_{peak} and include: 1) less Ca^{2+} in the SR available for release, 2) greater dilution of the released Ca^{2+}, and/or 3) increased intracellular Ca^{2+} buffering either by indo-1 or other physiological buffers such as TnC. While greater indo-1 buffering does not seem likely, for reasons mentioned above, further experiments are needed to assess the potential contribution by dilution and/or buffering.

Caffeine is known to activate the SR Ca^{2+} release channels preventing SR Ca^{2+} re-uptake (32), thus Ca^{2+} removal and relaxation will occur more slowly and is largely due to Na^{+}/Ca^{2+} exchange (11). In addition, caffeine has multiple effects within the cell, one of which is to enhance myofilament Ca^{2+} sensitivity although both T and C groups are expected to be equally affected (42). Indo-1 fluorescence is also strongly quenched by caffeine, however, this occurs in a wavelength independent manner and thus should not affect the ratio. The absolute values for the time constants of relaxation (τ_{relax}) and fluorescence decay (τ_{decay}) under modified Tyrode conditions were slower than that previously reported in rabbit papillary muscle (11). The faster relaxation times in the latter study may reflect the ~7°C higher rewarming temperatures. Evidence for training-induced alterations in Na/Ca exchange activity is revealed by the subtantially greater reduction in τ_{relax} and τ_{decay} from T cells under the caffeine treatment compared to T cells perfused without added caffeine. These data are consistent with *in vitro* data suggesting enhanced Na^{+}/Ca^{2+} exchange activity with training (40).

Ratio vs $[Ca^{2+}]_i$. The question arises whether or not the reduced R_{peak} recorded during the stimulated twitches and RCCs from T myocytes reflects a true reduction in $[Ca^{2+}]_i$. To address this problem $[Ca^{2+}]_i$ was estimated. A K_D of 400 nM was chosen based upon previous determinations of indo-1 binding to Ca^{2+} in the presence of protein (3, 26). Using the same K_D (400 nM) for both T and C transients (Figure 6), diastolic levels of $[Ca^{2+}]_i$ are reduced in T and the reduction in peak $[Ca^{2+}]_i$ between the average T and C twitch becomes considerably greater than that between the R_{peaks}. It seems unlikely that diastolic $[Ca^{2+}]_i$ would be reduced as the result of training. When a K_D of 755 nM was substitued in T, resting $[Ca^{2+}]_i$ levels were identical and as a result peak $[Ca^{2+}]_i$ were also the same (Figure 7). This analysis suggested that the peak $[Ca^{2+}]_i$ may not be reduced as indicated by the reduced R_{peak}. Even with the differential K_D values it appears that the $[Ca^{2+}]_i$ decay is slower in the average T transient (Figure 7). Extrapolation from these conditions to the normally much higher heart rates should not lead to a rate-dependent rise in diastolic $[Ca^{2+}]_i$ as the decay time constants are known to be condition-dependent (i.e., adrenergic stimulation leads to enhanced uptake of Ca^{2+} by the SR). The change in R (RCC R_{peak} - R_{peak}) between T and C ratios was 0.14 for the average C transient and 0.09 for the average T transient. If the peak $[Ca^{2+}]_i$ transient remained the same, then this would suggest that the K_D of indo-1 for Ca^{2+} is higher in the T compared to cells. Futher experiments are needed to test this hypothesis. One method is to obtain an *in vivo*

calibration curve for both trained and control myocytes with intermediate values between R_{min} and R_{max}.

Functional implications. In summary, we provide evidence that both cardiomyocyte morphology and contractile function are influenced by treadmill training. Longer cell lengths may, at least in part, contribute to the greater EDVs observed after training in a length independent manner. Chronic treadmill training produces enhanced contractile activation in the presence of altered Ca^{2+} dynamics. The data are suggestive that the sensitivity of the contractile element to Ca^{2+} is increased by training. The SR Ca^{2+} content as assessed by RCCs decreases with training. Finally, the greater rates of relaxation during twitches and RCCs and Ca^{2+} transient decay during RCCs support biochemical data (40) for enhanced Na^{+}/Ca^{2+} exchange activity in a more physiological model, the cardiomyoctye.

REFERENCES

1. Allen, D. G., and S. Kuruhara. The effects of muscle length on intracellular calcium transients in mammalian cardiac muscle. *J. Physiol.* 327: 79-94, 1982.

2. Babu, A., E. Sonnenblick, and J. Gulati. Molecular basis for the influence of muscle length on myocardial performance. *Science* 240: 74-76, 1988.

3. Baker, A. J., R. Brandes, J. H. M. Schreur, S. A. Camacho, and M. W. Weiner. Protein and acidosis alter calcium-binding and fluorescence spectra of the calcium indicator indo-1. *Biophys. J.* 67: 1646-1654, 1994.

4. Baldwin, K. M. Effects of chronic exercise on biochemical and functional properties of the heart. *Med. Sci. Spts. Exerc.* 17: 522-528, 1985.

5. Baldwin, K. M., D. A. Cooke, and W. G. Cheadle. Time course adaptations in cardiac and skeletal muscle to different running programs. *J. Appl. Physiol.* 42: 267-272, 1977.

6. Balke, C. W., T. M. Egan, and G. W. Wier. Processes that remove calcium from the cytoplasm during excitation-contraction coupling in intact rat heart cells. *J. Physiol.* 474: 447-462, 1994.

7. Basani, R. A., J. W. M. Basani, and D. M. Bers. Mitochondrial and sarcolemmal Ca^{2+} reduce $[Ca]_i$ during caffeine contractures in rabbit cardiac myocytes. *J. Physiol.* 453: 591-608, 1992.

8. Bassani, J. W. M., R. A. Bassani, and D. M. Bers. Calibration of indo-1 and resting intracellular $[Ca]_i$ in intact rabbit cardiac myocytes. *Biophys. J.* 68: 1453-1460, 1995.

9. Berlin, J. R., J. W. M. Basani, and D. M. Bers. Intrinsic cytosolic calcium buffering properties of single rat cardiac myocytes. *Biophys. J.* 67: 1775-1787, 1995.

10. Bers, D. M. SR Ca loading in cardiac muscle preparations based on rapid-cooling contractures. *Am. J. Physiol.* 256: C109-C120, 1989.

11. Bers, D. M., and J. H. B. Bridge. Relaxation of rabbit ventricular muscle by Na-Ca exchange and sarcoplasmic reticulum calcium pump. *Circ. Res.* 65: 334-342, 1989.

12. Bers, D. M., J. H. B. Bridge, and K. W. Spitzer. Intracellular Ca^{2+} transients during rapid cooling contractures in guinea-pig ventricular myocytes. *J. Physiol.* 417: 537-553, 1989.

13. Bers, D. M., and V. A. Stiffel. Ratio of ryanodine to dihydropyridine receptors in cardiac and skeletal muscle and implications for E-C coupling. *Am. J. Physiol.* 264: C1587-C1593, 1993.

14. Blatter, L. A., and W. G. Wier. Intracellular diffusion, binding, and compartmentalization of the fluorescent calcium indicators indo-1 and fura-2. *Biophys. J.* 58: 1491-1499, 1990.

15. Blinks, J. R. Intracellular [Ca^{2+}] measurements. In: *The heart and cardiovascular system* (Second ed.), edited by H. A. Fozzard, E. Haber, R. B. Jennings and A. M. Katz. New York: Raven Press, Ltd., 1992, p. 1171-1201.

16. Blinks, J. R., and M. Endoh. Modification of myofibrillar responsiveness to Ca^{++} as an inotropic mechanism. *Circ.* 73: 85-98, 1986.

17. Blomqvist, C. G., and B. Saltin. Cardiovascular adaptations to physical training. *Ann. Rev. Physiol.* 45: 169-189, 1983.

18. Booth, F. W., and D. B. Thomason. Molecular and cellular adaptation of muscle in response to exercise: Perspectives of various models. *Physiol. Rev.* 71: 541-571, 1991.

19. Brady, A. J. Mechanical properties of isolated cardiac myocytes. *Physiol. Rev.* 71: 413-428, 1991.

20. Diffee, G. M., and G. F. Tibbits. Dihydropyridine binding to myocardial sarcolemma: adaptation to exercise. *Clin. Physiol.* 5: 29, 1985.

21. Dowell, R. T. Cardiac adaptations to exercise. *Exer. Spt. Sci. Rev.* 11: 99-116, 1983.

22. Fitzsimons, D. P., P. W. Bodell, R. E. Herrick, and K. M. Baldwin. Left ventricular functional capacity in the endurance-trained rodent. *J. Appl. Physiol.* 69: 305-312, 1990.

23. Fozzard, H. A., E. Haber, R. B. Jennings, and A. M. Katz. Isolated myocytes in experimental cardiology. In: *The heart and cardiovascular system.*, edited by P. Stemmer, P. L. Wisler and A. M. Watanabe. New York: Raven Press, 1991.

24. Grynkiewicz, G., M. Poenie, and R. Y. Tsien. A new generation of Ca^{2+} indicators with greatly improved fluorescence properties. *J. Biol. Chem.* 260: 3440-3450, 1985.

25. Harrison, S. M., and D. M. Bers. Temperature dependence of myofilament Ca sensitivity of rat, guinea pig, and frog ventricular muscle. *Am. J. Physiol.* **258**: C274-C281, 1990.

26. Hove-Madsen, L., and D. M. Bers. Indo-1 binding to protein in permabilized ventricular myocytes alters its spectral and Ca binding properties. *Biophys. J.* 63: 89-97, 1992.

27. Kentish, J. C., H. E. D. J. ter Keurs, L. Ricciardi, J. J. J. Bucx, and M. I. M. Noble. Comparison between the sarcomere length-force relations of intact and skinned trabeculae from rat right ventricle. *Circ. Res.* 58: 755-768, 1986.

28. Mitra, R., and M. Morad. A uniform enzymatic method for dissociation of myocytes from hearts and stomachs of vertebrates. *Am. J. Physiol.* 249: H1056-H1060, 1985.

29. Moore, R. L., T. I. Musch, R. V. Yelamarty, R. C. Scaduto Jr., A. M. Semanchick, M. Elensky, and J. Y. Cheung. Chronic exercise alters contractility and morphology of isolated rat cardiac myocytes. *Am. J. Physiol.* 264: C1180-C1189, 1993.

30. Noble, D., and T. Powell. The slowing of Ca^{2+} signals by Ca^{2+} indicators in cardiac muscle. *Proc. R. Soc. Lond. B* 246: 167-172, 1991.

31. Robertson, S. P., J. D. Johnson, and J. D. Potter. The time-course of Ca^{2+} exchange with calmodulin, troponin, parvalbumin and myosin in response to transient increases in Ca^{2+}. *Biophys. J.* 34: 559-569, 1981.

32. Rousseau, E., and G. Meissner. Single cardiac sarcoplasmic reticulum Ca^{2+}-release channel: Activation by caffeine. *Am. J. Physiol.* 256: H328-H333, 1989.

33. Schraible, T., A. Malhotra, G. Ciambrone, P. Buttrick, and J. Scheuer. Combined effects of hypertension and chronic running program on rat heart. *J. Appl. Physiol.* 63: 322-327, 1987.

34. Sipido, K. R., and W. G. Wier. Flux of Ca^{2+} across the sarcoplasmic reticulum of guinea-pig cardiac cells during excitation-contraction coupling. *J. Physiol.* 435: 605-630, 1991.

35. Sollott, S. J., B. D. Ziman, and E. G. Lakatta. Novel technique to load into-1- free acid into single adult cardiac myocytes to assess cytosolic Ca^{2+}. *Am. J. Physiol.* 262: H1941-H1949, 1992.

36. Spurgeon, H. A., M. D. Stern, G. Baartz, S. Raffaeli, R. G. Hansford, A. Talo, E. G. Lakatta, and M. C. Capogrossi. Simultaneous measurement of Ca^{2+}, contraction, and potential in cardiac myocytes. *Am. J. Physiol.* 258: H574-H586, 1990.

37. Srere, P. A. Citrate Synthase. *Meth. Enz.* 13: 3-5, 1969.

38. Steadman, B. W., K. B. Moore, K. W. Spitzer, and J. H. B. Bridge. A video system for measuring motion in contracting heart cells. *I.E.E.E. Trans. Bio. Eng.* 35: 264-272, 1988.

39. Tibbits, G. F., R. J. Barnard, K. M. Baldwin, N. Cugalj, and N. K. Roberts. Influence of exercise on excitation-contraction coupling in rat myocardium. *Am. J. Physiol.* 240: H472-H480, 1981.

40. Tibbits, G. F., H. Kashihara, and K. O'Reilly. Na^{+}-Ca^{2+} exchange in cardiac sarcolemma: modulation of Ca^{2+} affinity by exercise. *Am. J. Physiol.* 256: C638-C643, 1989.

41. Tibbits, G. F., T. Nagatomo, M. Sasaki, and R. J. Barnard. Cardiac sarcolemma: Compositional adaptation to exercise. *Science* 213: 1271-1273, 1981.

42. Wendt, I. R., and D.G. Stephenson. Effects of caffeine on Ca-activated force production in skinned cardiac and skeletal muscle fibers of the rat. *Pflugers Arch.* 398: 210-216, 1983.

43. Weyman, M., and G. F. Tibbits. Cardiac Ca-antagonist binding alterations with exercise training. *Med. Sci. Spts. Exer.* 29: S82, 1987.

44. Yu, Z., J. R. McNeill, and G. F. Tibbits. Cellular functions of diabetic cardiomyocytes: contractility, rapid-cooling contracture, and ryanodine binding. *Am. J. Physiol.* 266: H2082-H2089, 1994.

TABLE 1

Myocyte and sarcomere dimensions

	MYOCYTE			SARCOMERE	
	N	Length (μm)	Width (μm)	sarcomere number	Length (μm)
C	120	120.1 ± 1.5	32.2 ± 0.8	64 ± 1	1.88 ± 0.01
T	110	126.8 ± 1.9	32.5 ± 0.8	67 ± 1	1.90 ± 0.02
T(%C)		106	101	105	101
P-value		<0.01	NS	<0.05	NS

Values are mean ± sem; C, sedentary control; T, treadmill-trained; N, total number of cells from which measurements were taken during 12 (control) and 11 (trained) isolation days. Measurements were taken during quiescence with cells bathed in 1.8 mM Ca^{2+}, 23°C; NS, not significant ($p>0.05$).

TABLE 2

Myocyte contractile chacteristics

	N	L_{max} (% L_o)	TPS (msec)	$-dL/dt_{max}$ (µm/sec)	$+dL/dt_{max}$ (µm/sec)	$\frac{-dL/dt_{max}}{+dL/dt_{max}}$
C	71	14.1 ± 0.5	198 ± 5	162 ± 6	127 ± 5	1.30 ± 0.03
T	113	15.5 ± 0.4	193 ± 4	193 ± 7	145 ± 5	1.35 ± 0.03
T(%C)		110	97	119	114	104
P value		<0.05	NS	<0.005	<0.05	NS

Values are mean ± sem; N, is the total number of cells from which measurements were made over 12 (C) and 11 (T) isolation days; L_{max}, maximum extent of cell shortening expressed as percent resting cell length; TPS, time-to-peak shortening; $-dL/dt_{max}$, peak rate of shortening; $+dL/dt_{max}$, peak rate of relengthening. All measurements were taken during field stimulation at 0.5 Hz, 1.8 mM Ca^{2+}, 23°C. NS, not significant ($p>0.05$).

TABLE 3

Calcium transients during stimulated twitches.

	R_{rest}	R_{peak}	+dR/dt ($x10^{-2}$ sec^{-1})	Time to R_{peak} (msec)	Area to R_{peak}	Time to one-half R_{peak} (msec)
C (n=22)	0.89±0.04	1.29 ± 0.05	5.1 ± 0.5	199 ± 8	11.7 ± 1.0	233 ± 17
T (n=29)	0.81±0.03	1.13 ± 0.04	3.9 ± 0.2	174 ± 9	9.9 ± 1.0	290 ± 21
T (%C)	91	88	76	87	85	125
P value	NS	<0.05	<0.05	<0.05	<0.05	<0.05

Values are mean ± sem; R, fluorescence ratio 405/480 nm during quiescence (R_{rest}); R_{peak}, peak R amplitude during a stimulated twitch; +dR/dt, maximum rate of rise in R expressed in arbitrary units; time-to-R_{peak}, the time from R_{pre} to R_{peak} where R_{pre} is defined as R just prior to onset of the rapid upstroke; Area-to-R_{peak}, represents the integrated fluorescence ratio from R_{pre} to R_{peak} determined by IGOR™ (Wavemetrics, Eugene OR) software; Time to one-half R_{peak}, is the time to one-half of R_{peak} minus R_{pre}. All measurements were taken during field stimulation at 0.5 Hz, 1.8 mM Ca^{2+}, 23°C.

TABLE 4

Rapid cooling contractures

	Cell length		Fluorescence Ratio	
	L_{max} (% chge)	τ_{relax} (sec)	R_{peak}	τ_{decay} (sec)
modified Tyrode solution				
C	30.5±0.6 (57)	9.1±0.7 (62)	1.43±0.10 (15)	7.8±1.1 (22)
T	29.5±0.6 (66)	7.6±0.5 (68)	1.22±0.05 (12)	6.8±0.9 (18)
P value	NS	<0.05	<0.05	NS
modified Tyrode plus 10 mM caffeine				
C	31.0±0.9 (31)	27.2±4.3 (47)	1.59±0.13 (9)	123.8±7.8 (19)
T	31.3±0.6 (42)	18.5±1.2 (64)	1.36±0.07 (16)	71.4±7.1 (18)
P value	NS	<0.05	<0.05	<0.05

Values are mean ± sem; L_{max}, maximum extent of cell shortening during cold exposure expressed as % resting cell length; L_{peak} is peak shortening during the onset of rewarming and encompasses the rewarming spike; τ_{relax}, is the time constant for relaxation in seconds; R_{peak}, peak fluoresence ratio; τ_{decay} is the time constant for fluorescence decay in seconds; Numbers in brackets represent the number of cells from which measurements were taken during the course of 12 (C) and 11 (T) isolation days.

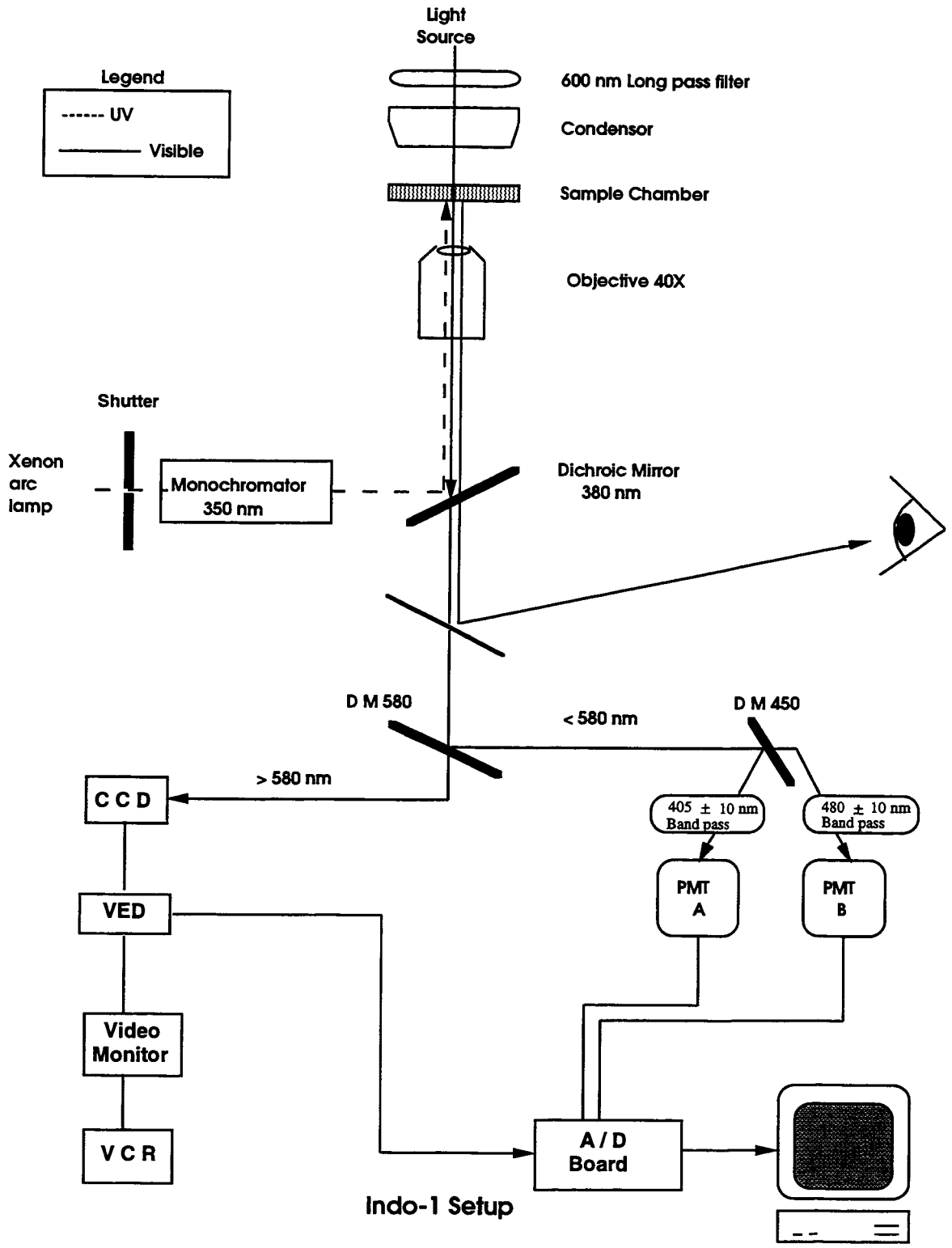

Figure 1. Schematic of contractile and fluorescence monitoring apparatus.

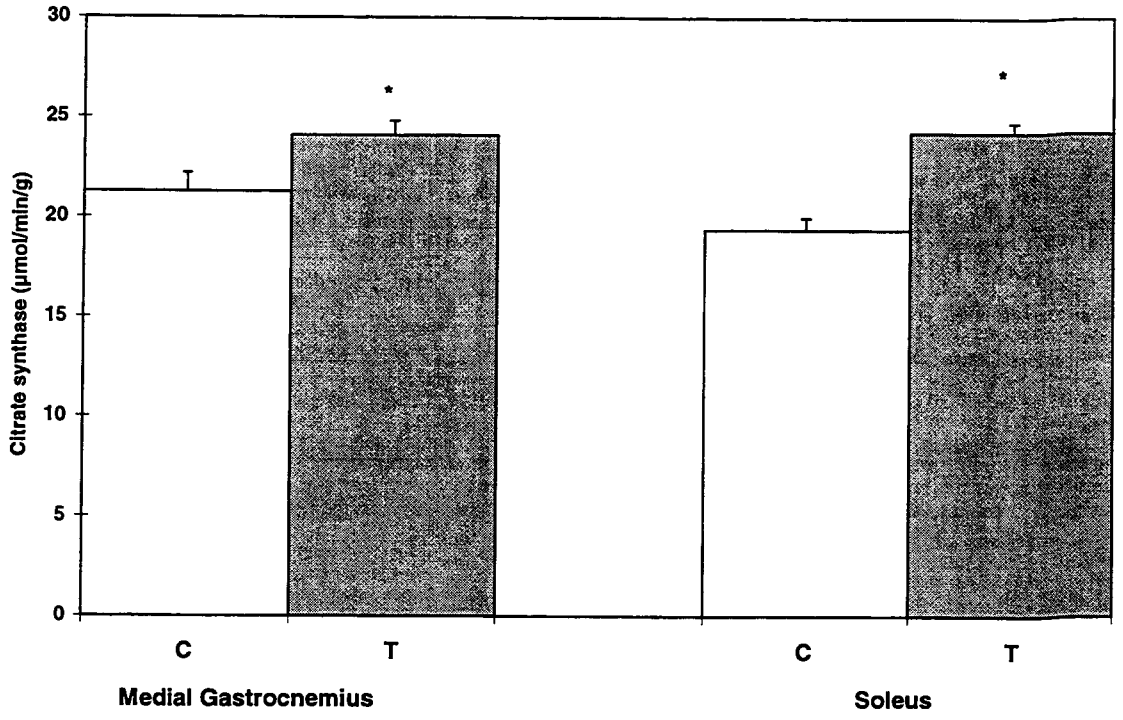

Figure 2. Mean citrate synthase activities in µmoles per minute per gram tissue from medial gastrocnemius and soleus whole muscle homogenages from sedentary-control (C) and treadmill-trained (T) rats. Data for each group represent 10 experiments in which one muscle per experiment was used. *, T significantly greater compared to C, $p<0.05$.

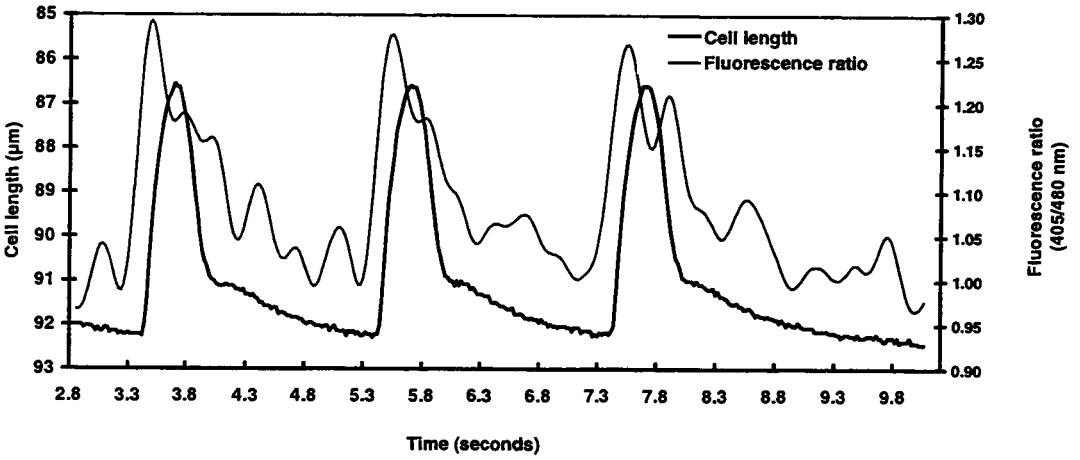

Figure 3. Cell length and fluorescence ratio (R=405/480nm) from a representative control cell. Cells were electrically stimulated at 0.5 Hz and continually bathed in 1.8 mM Ca^{2+} at 23°C.

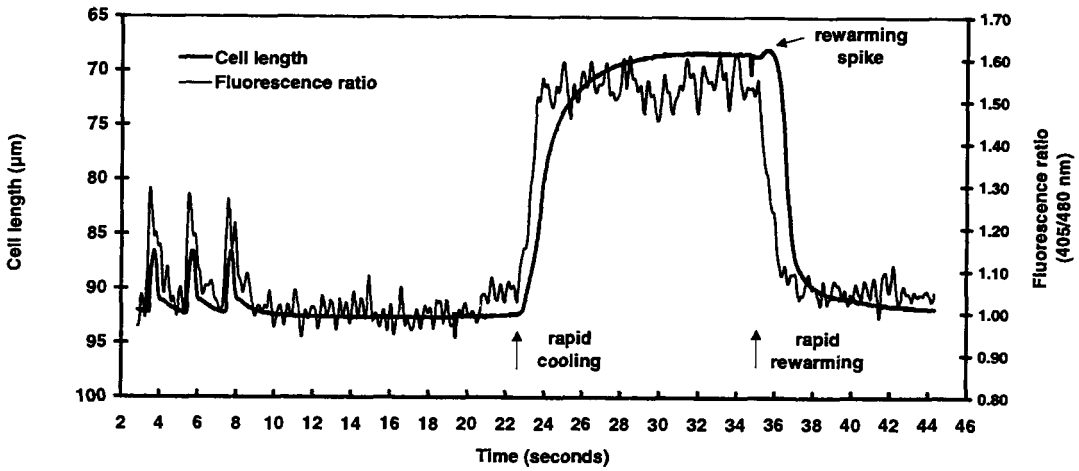

Figure 4. Cell length and fluorescence ratio (R=405/480 nm) recordings during a rapid cooling contracture from a representative control cell.

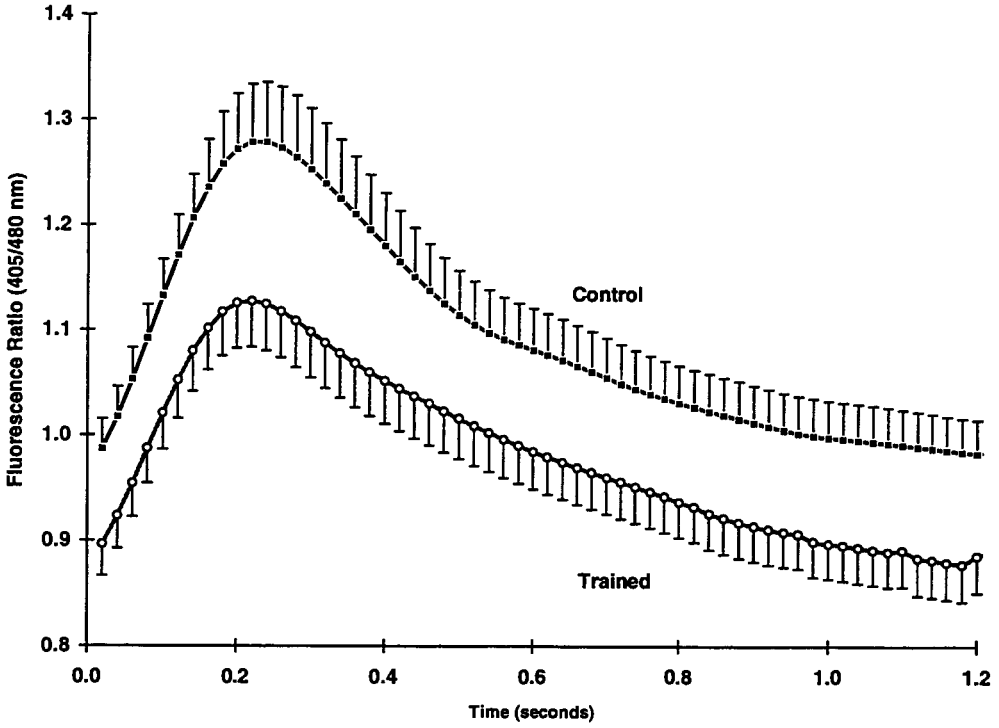

Figure 5. Mean fluorescence ratios during a twitch from C (n=26 cells) and T (n=34 cells) myocytes. Cells were electrically stimulated at 0.5 Hz and continually bathed in 1.8 mM Ca^{2+} at 23°C. In order to superimpose transients from different cells the time scale was normalized starting from 0 seconds and increased by 20 msec for each sampling data point. The fluorescence ratio at 0 seconds was taken as the value just prior to the large upstroke thus the ratio at 0 seconds for T and C cells is defined as R_{pre} to distinguish it from R_{rest}.

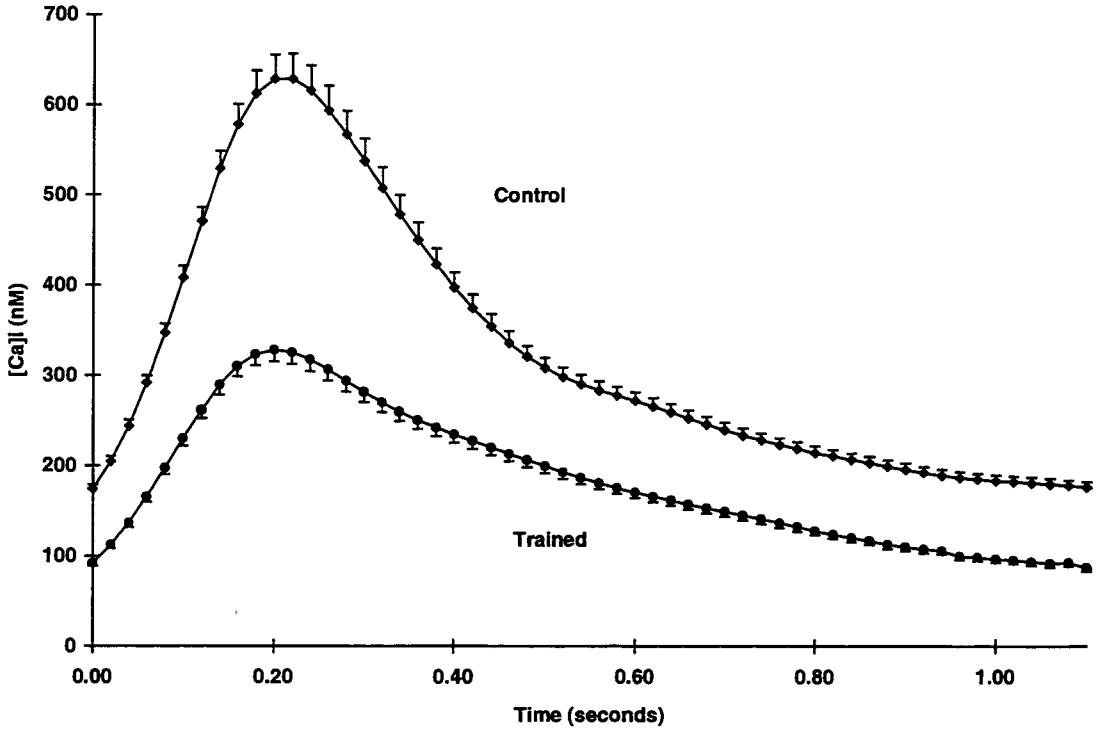

Figure 6. Average $[Ca^{2+}]_i$ estimated during a twitch from C (n=26 cells) and T (n=34 cells) myocytes. The data from Figure 5 was used to estimate the average $[Ca^{2+}]_i$ using the following values: K_D = 400 nM, R_{min} = 0.75, R_{max} = 1.75, and Sf_2/Sb_2 = 1.40 and the equation: $[Ca^{2+}]_i = K_D \times (R-R_{min})/(R_{max}-R) \times Sf_2/Sb_2$ (24).

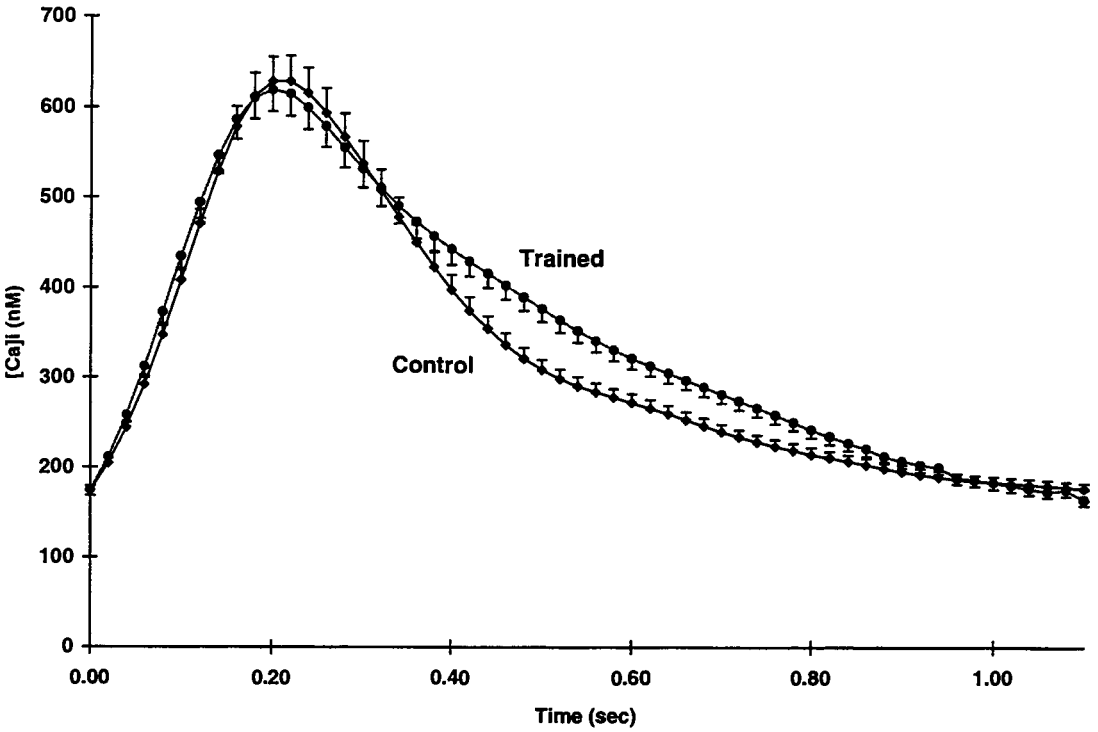

Figure 7. Average $[Ca^{2+}]_i$ estimated during a twitch from C (n=26 cells) and T (n=34 cells) myocytes. The data from Figure 5 was used to estimate the average $[Ca^{2+}]_i$ using the following values: K_D (control) = 400 nM, K_D (trained) = 755 nM, R_{min} = 0.75, R_{max} = 1.75, and Sf_2/Sb_2 = 1.40 and the equation: $[Ca^{2+}]_i = K_D \times (R-R_{min})/(R_{max}-R) \times Sf_2/Sb_2$ (24).

CHAPTER 4

CALMODULIN CONTENT IN SOLUBLE AND MEMBRANE FRACTIONS FROM ENDURANCE-TRAINED RAT HEARTS

Abstract

The possible role of calmodulin (CaM) in mediating exercise-induced enhancement of myocardial contractility was investigated. In two separate but similar training studies, female Sprague-Dawley rats were randomly divided into trained (T) and sedentary control (C) groups. Group T was treadmill-trained until they were capable of running 60 min/day, 5 days/wk at 28-29 m/min on an 8% grade. The effects of calmidazolium, a calmodulin inhibitor, on dihydropyridine (DHP) binding to sarcolemma (SL) isolated from T and C was assessed. The calmidazolium inhibition of DHP binding was significantly greater in SL from T. There was, in general, little indication of a change in the relative amounts of myocardial protein between groups as determined by SDS PAGE. However, in T the level of a SL protein with an apparent M_r of 186 kDa was 60% of C ($p<0.05$), while the level of a protein with a M_r of 16 kDa was 170% of C ($p<0.001$). When CaM was quantified using an ELISA, no significant differences were noted. The total CaM content was 284 and 238 μg/g heart weight for the T and C groups, respectively. These values are ~6 times greater than those reported previously in mammalian cardiac tissue using different methodology. The differences observed in calmidazolium inhibition of DHP binding, densiometric analysis of SL proteins and a trend towards greater amounts of CaM suggests that CaM may be involved in exercise adaptation but its role requires further study.

Introduction

Myocardial contraction is initiated by small influx of Ca^{2+} through voltage sensitive, L-type Ca^{2+} channels located on the sarcolemma (SL). This influx of Ca^{2+} is believed to trigger the release of a greater amount of Ca^{2+} from the sarcoplasmic reticulum (SR) via SR Ca^{2+} release channels (6). The increase in cytosolic [Ca^{2+}] leads to cross bridge formation, tension development and subsequent contraction. The amount of tension developed is modulated, in large part, by gradations in Ca^{2+} delivery to the myofilaments (33). Relaxation occurs when the cytosolic Ca^{2+} concentration is lowered by SR Ca^{2+} uptake and extrusion from the cell by the Na^{+}/Ca^{2+} exchanger. The importance of Ca^{2+} as an intracellular modulator of myocardial contractility is demonstrated not only by the multiplicity of systems that have evolved for Ca^{2+} transport but also by the fact that these systems are under complex regulatory control (7). In addition, evidence exists that chronic exercise may improve the intrinsic contractile performance of the heart, possibly by mechanisms that involve Ca^{2+} transport (35).

Calmodulin (CaM), a highly conserved Ca^{2+} binding protein, appears to be involved in the regulation of ion channels. For example, Ca^{2+}-dependent Na^{+} channel activity in excised patches of *Paramecium* plasma membranes is restored by CaM in the absence of ATP (31). The lack of an ATP requirement suggests that CaM acted either by direct binding to the channel or an associated membrane component without CaM kinase. There is some evidence to suggest that SL Ca^{2+} channels may also be modulated by CaM

in a similar manner. In chick heart cell reaggregates, CaM antagonists inhibited the activation of naturally-occurring slow Ca^{2+} action potentials, while the addition of CaM restored the action potentials (1). A class of Ca^{2+} channel blockers, the dihydropyridines (DHP), bind to a site that is located on the α_1 subunit of the SL Ca^{2+} channel (24). High affinity binding of radiolabelled DHP is known to be strongly Ca^{2+}-dependent (13, 15, 23). In addition, CaM antagonists were found to inhibit DHP binding (23). Collectively, these results suggest the presence of a Ca^{2+} binding protein that regulates specific DHP binding and possibly SL Ca^{2+} channel function. More recently, several studies have implicated a role for CaM in modulation of the cytosolic Ca^{2+}-transient in cardiac myocytes (9, 28). The CaM inhibitor, W7, decreased the amplitude of both the Ca^{2+}-transient and twitch in rat ventricular myocytes. Evidence was presented suggesting that this negative inotropy was due, at least in part, to a reduction in SR Ca^{2+} content and myofilament Ca^{2+} sensitivity (9). Clearly, results to date implicate multiple roles for CaM in the regulation of contractility which involves both Ca^{2+} transport and myofilament Ca^{2+} sensitivity.

A potential CaM binding site has been identified in the recently cloned cardiac SL Na^+/Ca^{2+} exchange protein (26). However, there are no reports of CaM directly affecting SL Na^+/Ca^{2+} exchange activity. In contrast, in the absence of Ca^{2+}, CaM inhibits the activity of the SL Ca^{2+}-ATPase by direct association (39). SR Ca^{2+}-ATPase activity is modulated indirectly by CaM through phosphorylation of an associated regulatory

protein, phospholamban (14). The cardiac SR Ca^{2+} release channel also appears to be highly regulated by CaM (12, 32) by both direct binding and indirectly via Ca^{2+} CaM dependent kinases acting at a multitude of sites (20, 21). The potential thus exists for exercise-mediated adaptations involving either Ca^{2+} transport directly or regulatory control mechansims.

Published data about exercise-induced cardiac adaptations involving CaM are limited. There is only one report of cardiac CaM being quantified in partially purified membrane particles from trained and sedentary rats (29). While no differences were noted in the amount of CaM as determined by radioimmunoassay, the amounts cited were several orders of magnitude lower than those typically reported for heart (18). The possibility exists that a significant amount of CaM may have remained in the particulate fraction (16). CaM has also been implicated in training-induced enhancement of SR Ca^{2+} uptake in microsomes from swim-trained rat hearts (22).

CaM is found in virtually every tissue and species with reported amounts varying from approximately 40 mg/kg wet weight in skeletal and heart muscle to about 600 mg/kg wet weight in brain (18). While located primarily in the cytosol, a smaller amount of CaM remains tightly associated with membrane fractions even in the absence of Ca^{2+} (18). The only published estimate of SL associated CaM in cardiac tissue is 7.5 ng/mg SL protein which corresponds to approximately 27 ng/g wet weight (4).

Problems associated with CaM quantification involve difficulty in liberating membrane bound CaM during heat treatment. It has been estimated that as much as 70% of total CaM may remain associated with particulate fractions (16). Techniques to

quantify CaM have involved subjecting partially purified, heat-treated tissue extracts to electrophoresis and quantifying the resulting protein bands using densitometry, or solubilizing portions of the stained gel and analyzing the solution using spectrophotometry. However, these methods suffer from a lack of sensitivity. Another method takes advantage of CaM's ability to stimulate phosphodiesterase (PDE) activity. The PDE assay can lead to underestimates of CaM content if CaM is not in a biologically active form or bound to other proteins and thus unavailable (3). A third and more recent method uses polyclonal antibodies in a radioimmunoassay (RIA). The RIA is generally thought to be more sensitive and less vulnerable to the problems mentioned above. In rat heart, values for CaM that are 3-fold greater than values obtained using the PDE assay have been reported (3).

The putative role for CaM in the physiological regulation of cytosolic Ca^{2+} and the potential for exercise adaptations in the amount of CaM provided the impetus for further investigation into exercise-induced alterations in the amount of CaM in rodent heart. The purpose of the present study was to 1) characterize further the role of CaM in DHP binding, 2) develop a method to reassess cardiac CaM content in the heart, and 3) determine if these amounts are altered as the result of chronic exercise. In the first training study, specific DHP binding to highly-purified SL was assessed in the presence and absence of a CaM antagonist, calmidazolium. In a second training study, CaM was quantified in various fractions collected during SL isolation.

Material and methods

Animal training

In order to test this hypothesis, two separate but similar treadmill training regimens were conducted. The first study was conducted by G.D. and the second study by M.T. In both studies, female Sprague Dawley rats were randomly divided into treadmill-trained (T) and sedentary control (C) groups. Group T was trained progressively until after 10 weeks the animals were capable of running 60 min/day, 5 days/wk at 28-29 m/min on an 8% grade. A period of 48-72 hours was allowed between the last running bout and animal sacrifice.

Sarcolemmal (SL) isolation

In both studies SL was isolated from the hearts of T and C in parallel as described previously (38) and outlined in Figure 2. All steps were carried out at 4°C and all solutions were made without any added $CaCl_2$. The hearts were removed and perfused retrogradely through the aorta with ice-cold homogenizing medium (HM) containing: 280 mM sucrose and 10 mM 3-(N-morpholino) propanesulfonic acid (MOPS) buffer, pH 7.4. Hearts were trimmed of atria, connective tissue, blotted and weighed. For each SL isolation, 8-9 ventricles from each group were pooled in ice-cold HM, minced with scissors and homogenized with a Tekmar Tissuemizer (Cincinnati, Ohio) at a setting of 40 for two bursts of 3 sec each. The homogenate was then filtered through two layers of steel mesh and brought to a volume of 51.4 ml. One aliquot of 1 ml was set aside for biochemical analyses. A final volume of 56 ml was obtained by the addition of 5.6 ml of KCl (100 mM), sodium pyrophosphate (25 mM) to the remaining homogenate. After a

10 min incubation the suspensions were centrifuged at 177,000 g (Ti-50.2 rotor) for 1 hr. After removing the supernatant (S1) containing primarily myofilament protein, the pellet was homogenized in 20 ml of HM using a Wheaton glass homogenizer and motor controlled (Black & Decker drill press) Teflon pestle. The suspension was then spun at 2,000 g (J21C rotor) for 10 min. The supernatants were removed carefully from the pellet (P2) and spun again for 1 hr at 177,000 g and the supernatant (S3) removed. The pellets were resuspended in 5 ml of 45% sucrose, layered on top with a discontinuous sucrose gradient and then spun at 122,000 g for 16 hr in a swinging bucket rotor (SW-28). Four membrane fractions labeled F1 through F4 were collected. All fractions were diluted with decreasing concentrations of NaCl until equilibrated with 140 mM NaCl and 10 mM MOPS, pH 7.4. The suspensions were then spun for 1.5 hr at 177,000 g after which the supernatants (S5F1-F4) were removed and the pellets (F1-F4) resuspended in 1-1.5 ml of 140 mM NaCl, 10 mM MOPS. A small aliquot was removed from each fraction for biochemical characterization (see below) and the remainder frozen in liquid N_2. Samples from pellets (P2) and supernatants (S1, S3, and S5F1-F4) were stored at -80°C.

Sarcolemmal characterization

Protein was determined by the method of Bradford (2) using bovine serum albumin as the standard. The SL marker enzyme activity, K^+-stimulated *p*-nitrophenylphosphatase (K^+-*p*NPPase), was assayed in the crude homogenate and all fractions derived from the sucrose gradient. The purification index is defined as the ratio of the specific activity of K^+-*p*NPPase in the SL fraction to that in the crude homogenate.

Recovery is defined as the percent of total K^+-*p*NPPase activity in the SL fraction compared with that in the crude homogenate.

[^{3}H]PN200-110 binding

[^{3}H]PN200-110 (PN) binding was measured in the highly-purified SL fraction (F2) harvested from the sucrose gradient. For the binding, unless indicated otherwise, tubes were prepared with PN (78 Ci/mmol, New England Nuclear) concentrations ranging from 0.15 to 0.50 nM, 2.5 mM $CaCl_2$, 50 mM MOPS (pH 7.4@37°C), 0.5% v/v absolute (95-100%), 10-40 μg protein and deionized (Millipore) water to bring the tubes to a final volume of 5 ml. In separate experiments, $CaCl_2$ was varied between 0.002-5.0 mM and CaM was varied between 10 to 1000 nM. The concentrations of the CaM antagonists were varied between 0.05 to 2.0 μM for calmidazolium (R24571) and 5 to 200 μM for trifluoperazine (TFP). All assay tubes were incubated for 90 min at room temperature.

Gel electrophoresis and densitometry

All samples taken in the second study were subjected to sodium dodecyl sulfate-polyacrylamide gel electrophoresis (SDS-PAGE) and the stained protein bands quantified by densitometry. Mini-protean II system and reagents obtained from Bio-Rad® were used for SDS-PAGE. Preparation of 4% stacking and 5-20% linear gradient separating gels followed the manufacturer's protocol. Samples were prepared by dilution in sample dilution buffer containing 40% (w/v) glycerol, 12% SDS, 25 mM Tris/glycine (pH 8.8

@21°C), 0.4% 2-mercaptoethanol and 0.1% bromophenol blue. The diluted samples were then boiled for 5 min, cooled and 5 µl (10-25 µg protein) was applied per lane. Known molecular weight standards including CaM (Sigma Chemical Co.) were also prepared and loaded onto each gel. After electrophoresis, the gels were stained, destained and then scanned using a Hoefer GS 300 densitometer (Hoefer Scientific). Transmittance at 585 nm was recorded.

Antibody production and IgG purification

Rabbit polyclonal antibodies were produced at the University of B.C. Animal Care Facility using standard immunization protocols. Three female New Zealand rabbits (Geobet Rabbits Ltd, Abbotsford, B.C.) were immunized with highly purified bovine brain CaM (Zoion Research) while another three were immunized with ovalbumin-conjugated CaM. Ovalbumin was conjugated to CaM with a molar ratio of 3 CaM:1 Ovalbumin using the carbodiimide method (10). All procedures were carried out under essentially Ca^{2+} free conditions. After sacrifice and whole body bleeding of the immunized rabbits, IgG was purified from a pool of heat inactivated serum. Using a combination of caprylic acid precipitation followed by ammonium sulfate precipitation and final clean up on a DEAE Sephacel column. Specific IgG was then affinity-purified using a CaM-linked Sepharose (Pharmacia) column. In order to minimize the cross reaction with troponin C (TnC), the affinity purified antibody was back-absorbed on a TnC-Sepharose column prepared using TnC and CNBr-activated Sepharose 4B CL (Pharmacia).

ELISA

A non-competitive enzyme-linked immunosorbent assay (ELISA) was developed using either the rabbit anti-bovine brain CaM or sheep anti-rat testes CaM as the primary antibody. All unknown samples tested for CaM were diluted in coating buffer containing 0.1 M carbonate buffer, pH 9.5, plus 100 mM EGTA and boiled for 5 min then cooled on ice. Purified bovine brain CaM (6-800 ng/ml) and unknown sample protein (20-30,000 ng/ml) were added to 96-well microtest plates using a serial dilution method. Several methods were tried in an attempt to solubilize membrane CaM including boiling and treatment of detergents such as 1% digitonin, 0.5% sodium-cholate with 0.2% Emulgen 911, and 1% Lubrol PX. In each case, significant amounts of CaM were still detected in the pellet after centrifugation at 10,000 g for 30 min. The centrifugation step was subsequently omitted.

Various types of flat bottom 96-well plates were tested as were several methods for plate activation such as MeOH and glutaraldehyde fixation. Nunc Immuno II - high binding polystyrene plates without any pre-treatment were found to give the best results. After coating overnight at 4°C, unbound antigen was removed by inverting the plates and striking vigorously against a paper towel several times. Unbound sites were blocked by the addition of a blocking buffer containing phosphate buffered saline (PBS), pH 7.4, plus 0.3% (w/w) gelatin (Knox) and incubated with gentle agitation at 37°C for 1 hr. Plates were then inverted and washed three times with wash buffer containing PBS plus 500 mM NaCl and 0.05% Tween-20 detergent. Primary antibody diluted with PBS plus 0.3% gelatin was added to each well and the plates were incubated at 37°C for 2 hr with gentle agitation. The plates were then washed and the secondary antibody (diluted 1 in

3000 with PBS plus 0.3% gelatin) was added followed by incubation at 37°C for another 2 hr. Depending upon which primary antibody was used, either horse-radish peroxidase conjugated goat anti-rabbit $F(ab')_2$ or rabbit anti-sheep $F(ab')_2$ (Tago, Inc.) was used as the secondary antibody. After washing off excess antibody, substrate solution containing 2.2 mM OPD (o-phenylenediamine), 0.01% hydrogen peroxidase in 0.1 M sodium citrate buffer, pH 5.0 was added. The reaction was quenched by the addition of 4 M H_2S0_4. Absorbance at 490 nm was read with the use of an ELISA plate reader (Biotech). Non-specific binding was subtracted out by not coating the first and last column of wells with antigen and subtracting these absorbance values from sample absorbance values of CaM standards and tissue samples. The validity of the assay was demonstrated by adding known amounts of CaM to pure epoxide hydrolase and using the assay to determine CaM content.

Statistical analysis

Results are expressed as means ± SEM and were analyzed using the Student's *t*-test. Differences that had a p value of < 0.05 were considered to be statistically significant.

Results

As shown in Table 1, the effect of this training paradigm on the heart to body weight ratio (HW/BW) was an increase of ~4% and is similar to our other studies using this protocol. The training regimens used in the two studies did not reveal any significant differences between T and C groups with respect to total SL protein, SL marker enzyme (K^+-*p*NPPase) analysis, percent recovery or relative purification (Table 2).

In the first study, it was determined that the specific binding of the radiolabelled dihydropyridine, [^{3}H]PN200-110 (PN), was inhibited by the CaM antagonist, calmidazolium, in a dose-dependent manner. The presence of calmidazolium had little effect on the non-specific binding. Because of the potential ambiguity in the interpretation of this result, we tested the effect of exogenously added CaM to the PN binding. In general, the effect of CaM (over the range of 10-1000 nM) was to increase specific binding slightly. However, within this range there was a peak at 50 nM added CaM. At this concentration the specific binding of PN to SL was enhanced approximately two-fold and was associated with an increase in total and a decrease in non-specific binding (results not shown). The reason for the decreased non-specific binding is unclear. In the presence of 0.20 to 2.0 μM calmidazolium, maximal inhibition of PN binding (0.41 nM) was increased significantly in SL isolated from T compared to C hearts (Figure 1).

In the second study, SL was subjected to electrophoresis on a 5-20% gradient polyacrylamide gel and quantified by densitometry. With the exception of the SL fraction, there was in general, little change in the relative amounts of myocardial protein in any of the pellet or supernatant fractions obtained during the SL isolation procedure

from either group. In the SL fraction a protein with a M_r of ≅186 kD was significantly less abundant (60% of C), while a protein with a M_r of ≅16 kD was significantly more (170% of C) in the T samples, $p<0.05$ (Figure 3).

A non-competitive ELISA to quantitate CaM was developed using either rabbit anti-CaM IgG or sheep anti-CaM IgG as the primary antibody. Several unsuccessful attempts were made to develop a western blot method. During development of the ELISA several important observations were noted. First, the rabbit antibodies were found to be non-precipitating. Second, the use of bovine serum albumin in the blocking buffer prevented antibody access to CaM. Third, 0.3% gelatin was used successfully in blocking the non-specific sites. Fourth, the rabbit antibodies recognized soluble and bound CaM with differing affinities thus prohibiting the development of a competitive ELISA. The antibody from rabbits immunized with purified bovine brain CaM reacted more strongly than antibody obtained from rabbits immunized with ovalbumin-conjugated CaM. Affinity purified rabbit antibody that was back-absorbed against TnC yielded values for total CaM which were several fold greater for both T and C groups than values obtained using the sheep antibody. However, when compared to the sheep antibodies, the rabbit antibodies demonstrated a comparable detection limit of 1-2 ng and less TnC cross reactivity to TnC, ie. 200-fold less sensitive compared to 20-fold for the sheep Ab. With both antibodies there was a trend towards an increased amount of CaM in each of the T fractions compared with C fractions sampled during different stages of the SL isolation (data not shown).

Therefore, the levels of CaM presented in Table 3 were measured using the sheep antibody. Because CaM was initially quantified using the rabbit antibody there was

insufficient samples for some fractions from the T group remaining in order to repeat the assay using the sheep antibody. Approximately 4.5 % of the homogenate protein was determined to be CaM (Table 3). The CaM level in the various fractions from the C group ranged from 0.84 ± 0.11 to 2.71 ± 0.24 %. When the S1-TnC fraction, which is known to contain substantial amounts of TnC, was excluded the total amount of CaM was 284 and 238 μg/g heart wgt in T and C, respectively. Table 4 shows values obtained for total CaM in both rat heart and rat brain homogenate compared with that found in the literature. While a mean of approximately 560 μg/g heart wgt obtained from rat brain was similar to previous reports (3, 11, 16, 17, 40), the CaM amount for rat heart was several-fold higher compared to literature values (3, 11, 16, 17, 34).

Discussion

Training protocols similar to the one used in this study using treadmill-trained female rats have been well documented previously (8, 25, 35-37). There was a small but significant increase of 4% in the HW/BW ratio in T relative to C (Table 1). This is consistent with studies of similar regimens and thus our protocol did not produce a substantial amount of cardiac hypertrophy. These studies have also consistently induced a significant increase in skeletal muscle mitochondrial oxidative marker activity of 20-35% and gives further indication of a training effect (25, 35). Also typical is the fact that no differences between the T and C groups with respect to total protein, SL marker enzyme activity, percent recovery or SL purity were observed during the isolation of SL.

The apparent inhibition of PN binding in the presence of calmidazolium, was dose-dependent and is in agreement with Luchowski *et al* (23). However, the inhibition of PN binding by calmidazolium may also be due to a non-specific effect. To address this, exogenous CaM at concentrations ranging from 10 to 1000 nM was added. The degree to which CaM potentiated specific PN binding was dose-specific. While CaM increased specific PN binding slightly at most CaM concentrations, 50 nM CaM significantly increased specific PN binding by more than 100%. These data suggest an involvement of CaM in DHP binding to the SL. Another observation was that between 0.20 and 2.0 μM calmidazolium, specific PN binding (at 0.41 nM PN) to SL isolated from T hearts was inhibited to a significantly greater extent compared to the C group (Figure 1). This is reflected to an even greater extent when one compares absolute values. In the absence of calmidazolium, the absolute specific PN binding was about 35% greater in T vs. C. Several possibilities exist to account for the exercise-induced

increase in calmidazolium sensitivity. It is possible that more CaM is partitioned in the SL in the T heart and associated with the DHP receptor. As a corollary to this, perhaps less CaM is depleted from the SL of group T during the isolation procedure. Alternatively, there may simply be a change in the distribution of CaM within the SL such that more of the existing SL-bound CaM is associated with the DHP receptor either directly or via some associated component. Because of the possibility that training may increase the amount of SL-bound CaM it was decided to reassess CaM content in heart tissue from treadmill-trained and sedentary control rats.

In study two, all samples taken during the SL isolation were subjected to gradient polyacrylamide gel electrophoresis and prominent protein bands were quantified by densitometry (Figure 3). There was no significant difference in the level of any major protein band between T and C samples with the exception of the SL fraction. In this fraction, the amount of protein from two distinct bands from T hearts were significantly different with respect to C. The amount of a protein with a M_r of 186 kDa was decreased to approximately 60% of C, while a band with a M_r of 16 kDa, was increased by approximately 170% in the SL fraction from T samples. Due to the limitations of SDS-PAGE, we are not able to identify these two protein bands unequivocally. However, the SL Ca^{2+} channel α_1 subunit and CaM are known to be 170-195 and 16-18 kDa, respectively. Protease inhibitors were not used as previous experiments demonstrated they have not had any effect. In addition, our CaM standard migrated the same distance as the 16 kDa band. These data suggest that SL-bound CaM may be increased after training. However, the relative lack of sensitivity associated with denaturing gel electrophoresis and densitometry presents difficulty with such an interpretation. The

possibility also exists that the protein bands may contain proteolytic fragments from other proteins.

A CaM tissue content of 300-600 μg/g wet weight has been reported for brain and amounts of 20-40 μg/g heart wet wt have been cited for cardiac muscle (11, 16, 34, 40). While a value of approximately 560 μg/g wet wt for rat brain obtained in this study is within the range previously reported, the values obtained for rat heart are several fold greater. Reasons for this discrepancy are unknown. It is possible that a greater proportion of cardiac CaM may be in a form unable to activate PDE. A previous study compared the amount of CaM in rat heart and brain obtained by RIA and the PDE assay. The CaM content was ~300% and ~40% greater using the RIA compared to the PDE assay in rat heart and rat brain, respectively (3). This suggests that the PDE assay underestimates CaM content to a greater extent in heart tissue compared to brain. Another possibility, although unlikely, is that CaM may have been overestimated in heart tissue due to the presence of another Ca^{2+} binding protein such as S100. Recently, a new isoform, S100C, has been identified in heart tissue (27). The comparative values from both the PDE and CaM ELISA in brain suggest that S100, highly enriched in brain (1,000-10,000 fold), does not cross react with our Abs. Previous RIA experiments have revealed little if any crossreactivity with several S100 proteins using either mono- and polyclonal Abs raised against CaM (30). Although it is not known which fractions may contain S100C, nor how much is present, it is possible that the CaM antibodies used in the present study may have recognized a common epitope on S100C. By omitting the TnC containing fraction, S1-TnC, cross reactivity with TnC and thus TnC did not contribute to an overestimation of CaM, except in the crude homogenate determination.

A range of approximately 17 to 27 μg/g heart wt for membrane-bound CaM in the SL fraction from both T and C groups is three orders of magnitude greater than previously determined using RIA (4). Reasons may involve variations in the isolation and purification of SL membranes and the treatment of SL membrane samples prior to RIA. While no information is given with respect to % recovery and relative purification of SL membranes in the previous study, differential loss of specific SL proteins is known to occur during SL isolation (5, 19). In addition, when tissue extracts are subjected to heat treatment and centrifugation, not all of the membrane-associated CaM may be released into the supernatant which is used in the quantitation of CaM. As much as 70% of particulate CaM was released after heat treatment with 1% Lubrol PX detergent in samples from various rat and bovine tissues (16). In the present study CaM was detected in particulate fractions even after boiling in the presence of Lubrol PX. Therefore, CaM was quantified using the whole suspension.

In order to assess % recovery of CaM, CaM determinations were also made in the crude HG. In the C group, 4.5% of the protein, or 4155 μg/g heart wt was determined to be CaM. However, this sample contained approximately 12 times more TnC than CaM. When the value for HG content of CaM was corrected for the presence of TnC taking into account the 20-fold lower antibody sensitivity, a revised value of 1745 μg/g heart wt was obtained. Thus, approximately 14% of the CaM determined in all the fractions (excluding S1-TnC) was recovered from crude homogenate. Although it is unknown to what extent S100C may have contributed to the possible overestimation in this value, it appears that significant amounts of CaM may be lost or degraded during the SL isolation procedure.

In conclusion, based upon the results from this study, it appears that previous reports of 20 to 40 μg/g heart wet wt. may have underestimated CaM content in heart. The true value may be closer to 240 μg/g heart wet wt. When the latter value is expressed as a percent of total protein, 0.32% is obtained and is not inconsistent with the amount found in a variety of vertebrate tissues (18). No significant differences in the absolute amounts of CaM with training were found. Further investigations are needed to address the relative contribution of S100C to the CaM determination. The observations of greater inhibition of PN binding by calmidazolium, the trend towards increased amounts of CaM and the differences in electrophoretic and densiometric analysis of SL proteins are suggestive that the SL undergoes compositional changes in response to exercise training and this may include alterations in the amount of SL-bound CaM.

References

1. Bkaily, G., and N. Sperelakis. Calmodulin is required for full activation of the calcium slow channels in heart cells. *J. Cyclic Nucleo. Prot. Phos. Res.* 11: 25-34, 1986.

2. Bradford, M. A rapid and sensitive method for the quantitation of microgram quantities of protein utilizing the principle of protein-dye binding. *Anal. Biochem.* 72: 248-254, 1976.

3. Chafouleas, J. G., J. R. Dedman, R. P. Munjaal, and A. R. Means. Calmodulin: Development and application of a sensitive radioimmunoassay. *J. Biol. Chem.* 254: 10262-10267, 1979.

4. Cros, G., A. Molla, and S. Katz. Does calmodulin play a role in the regulation of cardiac sarcolemmal adenylate cyclase activity? *Cell Calcium* 5: 365-375, 1984.

5. DePover, A., I. L. Grupp, G. Grupp, and A. Schwartz. Diltiazem potentiates the negative inotropic action of nimodipine in heart. *Biochem. biophys. Res. Commun.* 114: 922-929, 1983.

6. Fabiato, A. Calcium-induced release of calcium from the cardiac sarcoplasmic reticulum. *Am. J. Physiol.* 245: C1-C14, 1983.

7. Famulski, K. S., and E. Carafoli. Calmodulin-dependent protein phosphorylation and calcium uptake in rat liver microsomes. *Eur. J. Biochem.* 141: 15-20, 1984.

8. Fitzsimons, D. P., P. W. Bodell, R. E. Herrick, and K. M. Baldwin. Left ventricular functional capacity in the endurance-trained rodent. *J. Appl. Physiol.* 69: 305-312, 1990.

9. Frampton, J. E., and C. H. Orchard. The effect of a calmodulin inhibitor on intracellular [Ca^{2+}] and contraction in isolated rat ventricular myocytes. *J. Physiol.* 453: 385-400, 1992.

10. Goodfriend, T. L. Antibodies to bradykinin and angiotensin: A use of carbodiimides in immunology. *Science* 144: 1344-1346, 1964.

11. Grand, R. J. A., and S. V. Perry. Calmodulin-binding proteins from brain and other tissues. *Biochem. J.* 183: 285-295, 1979.

12. Hain, J., H. Onoue, M. Mayrleitner, S. Fleischer, and H. Schindler. Phosphorylation modulates the function of the calcium release channel of sarcoplasmic reticulum from cardiac muscle. *J. Biol. Chem.* 270: 2074-2081, 1995.

13. Hess, P., and R. W. Tsien. Mechanism of ion permeation through calcium channels. *Nature* 309: 453-456, 1984.

14. James, P. M., M. Inui, M. Tada, M. Chiesi, and E. Carafoli. Nature and site of phospholamban regulation of the calcium pump of sarcoplasmic reticulum. *Nature* 342: 90-92, 1989.

15. Janis, R. A., J. G. Sarmiento, S. C. Maurer, G. T. Bolger, and D. J. Triggle. Characteristics of the binding of [^{3}H]NTP to rabbit ventricular membranes: modification by other calcium channel antagonists and by the calcium channel agonist Bay K8644. *J. Pharm. Exp. Ther.* 231: 8-15, 1984.

16. Kakiuchi, S., S. Yasuda, R. Yamazaki, Y. Teshima, K. Kanda, R. Kakiuchi, and K. Sobue. Quantitative determinations of calmodulin in the supernatant and particulate fractions of mammalian tissues. *J. Biochem.* 92: 1041-1048, 1982.

17. Klamut, H. J., K. P. Strickland, and C. H. Lin. Calmodulin content and Ca-activated protease activity in dystrophic hamster muscles. *Ms. Nerve* 6: 436-441, 1983.

18. Klee, C. B., and T. C. Vanaman. Calmodulin. *Adv. Prot. Chem.* 35: 213-319, 1982.

19. Lachnit, W. G., M. Phillips, K. J. Gayman, and I. N. Pessah. Ryanodine and dihydropyridine binding patterns and ryanodine receptor mRNA levels in myopathic hamster heart. *Am. J. Physiol.* 267: H1205-H1213, 1994.

20. Lee, H. C., R. Aarhus, R. Graeff, M. E. Gurnack, and T. F. Walseth. Cyclic ADP ribose activation of the ryanodine receptor is mediated by calmodulin. *Nature* 370: 307-309, 1994.

21. Lee, H. C., R. Aarhus, and R. M. Graeff. Sensitization of calcium-induced calcium release by cyclic ADP-ribose and calmodulin. *J. Biol. Chem.* 270: 9060-9066, 1995.

22. Levine, S. N., and G. T. Kinasewitz. Exercise conditioning increases rat myocardial calcium uptake. *J. Appl. Physiol.* 60: 1673-1679, 1986.

23. Luchowski, E. M., F. Yousif, D. J. Triggle, S. C. Maurer, J. G. Sarmiento, and R. A. Janis. Effects of Metal Cations and Calmodulin Antagonists on [^{3}H] Nitrendipine Binding in Smooth and Cardiac Muscle. *Jn. Pharm. Exp. Ther.* 230: 607-613, 1984.

24. Mikami, A., K. Imoto, T. Tanabe, T. Niidome, Y. Mori, H. Takeshima, S. Narumiya, and S. Numa. Primary structure and functional expression of the cardiac dihydropyridine-sensitive calcium channel. *Nature* 340: 230-233, 1989.

25. Moore, R. L., T. I. Musch, R. V. Yelamarty, R. C. Scaduto Jr., A. M. Semanchick, M. Elensky, and J. Y. Cheung. Chronic exercise alters contractility and morphology of isolated rat cardiac myocytes. *Am. J. Physiol.* 264: C1180-C1189, 1993.

26. Nicoll, D. A., S. Longi, and K. D. Philipson. Molecular cloning and functional expression of the cardiac sarcolemmal Na^{+}-Ca^{2+} exchanger. *Science* 250: 562-565, 1990.

27. Ohta, H., T. Sasaki, M. Naka, O. Hiraoka, C. Miyamoto, Y. Furuichi, and T. Tanaka. Molecular cloning and expression of the cDNA coding for a new member of the S100 protein family from porcine cardiac muscle. *FEBS lett.* 295: 93-96, 1991.

28. Okazaki, K., T. Ishikawa, M. Inui, M. Tada, K. Goshima, T. Okamoto, and H. Hidaka. KN-62, a specific Ca^{++}/calmodulin-dependent protein kinase inhibitor, reversibly depresses the rate of beating of cultured fetal mouse cardiac myocytes. *J. Pharm. Exp. Ther.* 270: 1319-1324, 1994.

29. Palmer, W. K., and S. Doukas. Cyclic AMP phosphodiesterase activity in the hearts of trained rats. *Can. J. Physiol. Pharmacol.* 61: 1017-1024, 1983.

30. Sacks, D. B., S. E. Porter, J. H. Ladenson, and J. M. McDonald. Monoclonal antibody to calmodulin: Development, characterization, and comparison with polyclonal anti-calmodulin antibodies. *Analy. Biochem.* 194: 369-377, 1991.

31. Saimi, Y., and K. Y. Ling. Calmodulin activation of calcium-dependent sodium channels in excised membrane patches of *Paramecium. Science* 249: 1441-1444, 1990.

32. Smith, J. S., E. Rousseau, and G. Meissner. Calmodulin modulation of single sarcoplasmic reticulum Ca^{2+}-release channels from cardiac and skeletal muscle. *Circ. Res.* 64: 352-359, 1989.

33. Solaro, R. J., R. M. Wise, J. S. Shiner, and F. N. Briggs. Calcium requirements for cardiac myofibrillar activation. *Circ. Res.* 34: 525-530, 1974.

34. Teo, T. S., T. H. Wang, and J. H. Wang. Purification and properties of the protein activator of bovine heart cyclic AMP phosphodiesterase. *J. Biol. Chem.* 248: 588-595, 1973.

35. Tibbits, G. F., R. J. Barnard, K. M. Baldwin, N. Cugalj, and N. K. Roberts. Influence of exercise on excitation-contraction coupling in rat myocardium. *Am. J. Physiol.* 240: H472-H480, 1981.

36. Tibbits, G. F., H. Kashihara, and K. O'Reilly. Na^{+}-Ca^{2+} exchange in cardiac sarcolemma: modulation of Ca^{2+} affinity by exercise. *Am. J. Physiol.* 256: C638-C643, 1989.

37. Tibbits, G. F., B. J. Koziol, N. K. Roberts, K. M. Baldwin, and R. J. Barnard. Adaptation of the rat myocardium to endurance training. *J. Appl. Physiol.* 44: 85-89, 1978.

38. Tibbits, G. F., M. Sasaki, M. Ikeda, K. Shimada, T. Tsuruhara, and T. Nagatomo. Characterization of rat myocardial sarcolemma. *J. Molec. Cell. Cardiol.* 13: 1051-1061, 1981.

39. Vorherr, T., P. James, J. Krebs, A. Enyedi, D. J. McCormick, J. T. Penniston, and E. Carafoli. Interaction of calmodulin with the calmodulin binding domain of the plasma membrane Ca^{2+} pump. *Biochem.* 29: 355-365, 1990.

40. Watterson, D. M. Structural similarities between Ca2+-dependent regulatory proteins of 3':5'-cyclic nucleotide phosphodiesterase and actomyosin ATPase. *J. Biol. Chem.* 251: 4501-4513, 1976.

TABLE 1

Comparison of heart and body weights in treadmill-trained and sedentary control rats (Study 2)

sample	control	trained
HW (mg)	765 ± 11	822 ± 13*
BW (g)	308 ± 4	318 ± 5
HW/BW (mg/g)	2.49 ± 0.03	2.60 ± 0.04*

Each value is a mean ± S.E.M. of 36 (C) or 35 (T) rats; HW, heart weight in mg; BW, body weight in g; HW/BW, ratio of ventricular weight to body weight in mg/g; *, mean value of T group is significantly different ($p<0.05$) from that of C group.

TABLE 2

Characterization of purified rat heart sarcolemma (Study 2)

	control	trained	units
HG protein	73.40 ± 5.50	73.97 ± 4.30	mg/g heart wt
SL protein	0.23 ± 0.03	0.28 ± 0.06	mg/g heart wt
SA (HG)	1.02 ± 0.06	0.93 ± 0.09	µmol/mg protein/hr
SA (SL)	14.90 ± 0.75	14.17 ± 0.81	µmol/mg protein/hr
recovery	4.65 ± 0.96	6.25 ± 1.72	%
purification index	14.45 ± 0.35	15.62 ± 1.90	

Each value is a mean ± S.E.M. of 4 separate isolations where 9 hearts were pooled per isolation; HG protein is the total protein in the crude homogenate; SL protein is expressed as the total protein in the SL fraction; SA (HG) is the specific activity of K^+-*p*NPPase in the crude homogenate; SA (SL) is the specific activity of K^+-*p*NPPase in the SL fraction; Recovery is defined as the percentage of the total K^+-*p*NPPase activity (µmoles/hr) in the SL fraction compared to the crude homogenate; Purification index is the SA(SL) / SA(HG) ratio.

TABLE 3

Absolute and relative CaM levels in fractions collected during the SL isolation procedure (study 2).

		Abs. [CaM] (μg/g heart wt)		Rel. [CaM] (% of total CaM)	
Fraction	n	Control	Trained	Control	Trained
HMG	2	4155.4	-	4.54	-
		(437.8)	-	(0.03)	-
S1-TnC	4	960.4	1086.7	1.95	2.31
		(46.3)	(329.2)	(0.13)	(0.68)
P2	4	76.2	79.5	2.71	3.09
		(14.3)	(8.7)	(0.24)	(0.29)
S3	2	45.7	45.8	1.11	1.15
		(1.8)	(5.0)	(0.11)	(0.20)
F2	4	16.6	27.1	2.08	3.03 *
		(1.4)	(13.0)	(0.12)	(0.46)
F3	4	9.2	18.7	1.56	2.22
		(3.7)	(14.6)	(0.70)	(1.42)
F4	4	77.4	98.7	1.45	1.71
		(9.9)	(16.3)	(0.11)	(0.30)
S5F4	2	12.8	14.5	0.84	0.99
		(1.4)	(0.9)	(0.11)	(0.20)

Each value represents the mean (±S.E.M.) of n CaM ELISA determinations. Each CaM ELISA determination was performed on samples from 1 of 4 separate isolations where 9 hearts were pooled per isolation. *, mean value of T group is significantly different ($p<0.05$) from that of C group. HMG, crude homogenate, S1-TnC, is the TnC containing fraction of the first supernatant, P refers to pellet and S to supernatant, and F refers to fraction as outlined in Figure 2. F2 represents the purified SL fraction.

TABLE 4

Total CaM: comparison with previously published values.

tissue	previously reported (µg/g heart wt)	present study 2* (µg/g heart wt)
heart	40 [28,31]	240
brain	300-600 [21,30]	560

* CaM values obtained in the present study represent the sum of the mean CaM values for each fraction from the 4 determinations. The CaM content of the S1-TnC fraction was excluded due to the presence of TnC. The CaM content for rat brain was determined for 4 separate preparations of crude homogenate. CaM content previously reported were determined using more indirect methods involving gel densitometry and Ca^{2+}-CaM activation of phosphodiesterase activity.

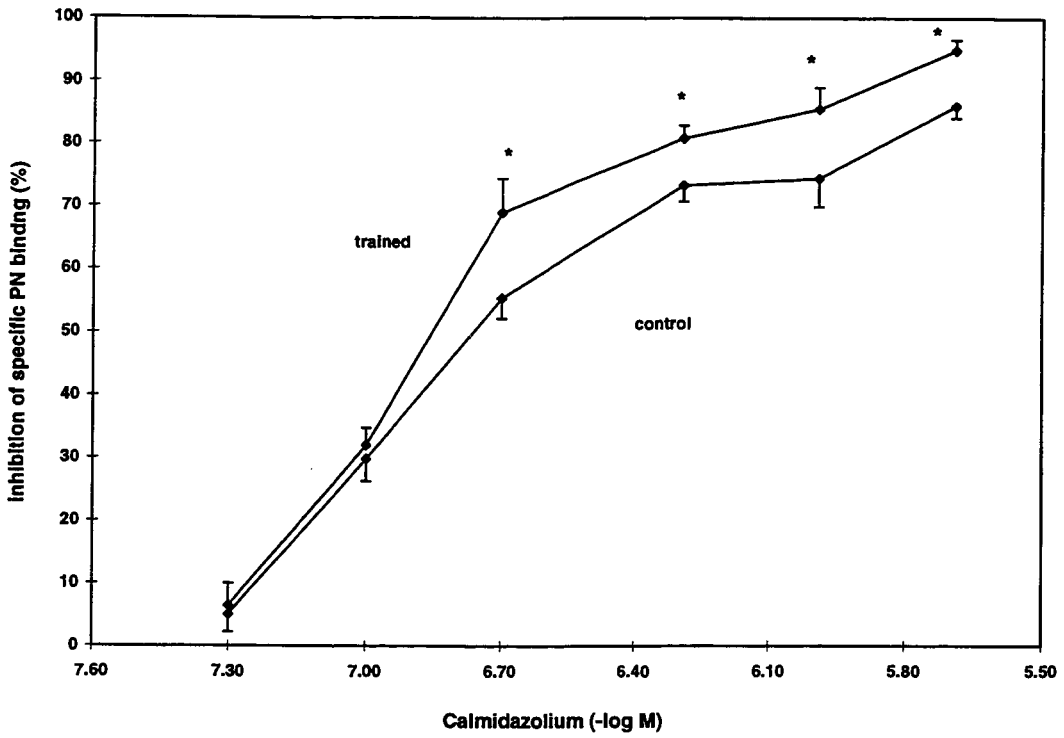

Figure 1. Relative (%) inhibition of PN200-110 specific binding as a function of calmidazolium concentration (-log[M]) in highly-purified sarcolemma isolated from T and C groups in study 1. Data collection and analysis by G.D. The PN200-110 concentration was 0.41 nM. Calmidazolium concentrations were varied between 0.05 to 2.0 μM. Extravesicular buffer concentration was 50 mM and the incubation time was 90 min at 23°C. Bars represent ± S.E.M.

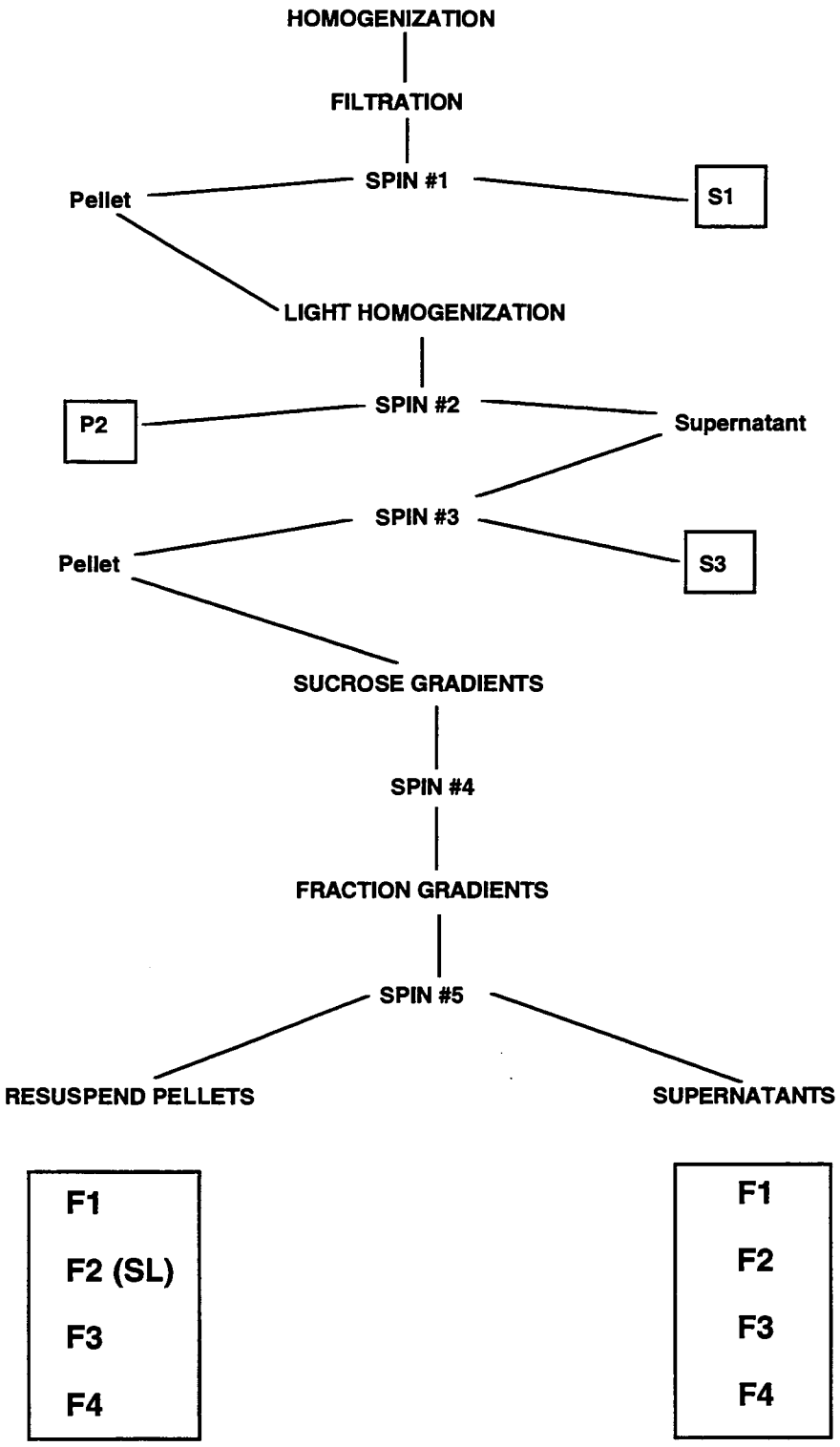

Figure 2. Schematic of the sarcolemmal (SL) isolation procedure. Samples subject to CaM determination are identified in the boxes.

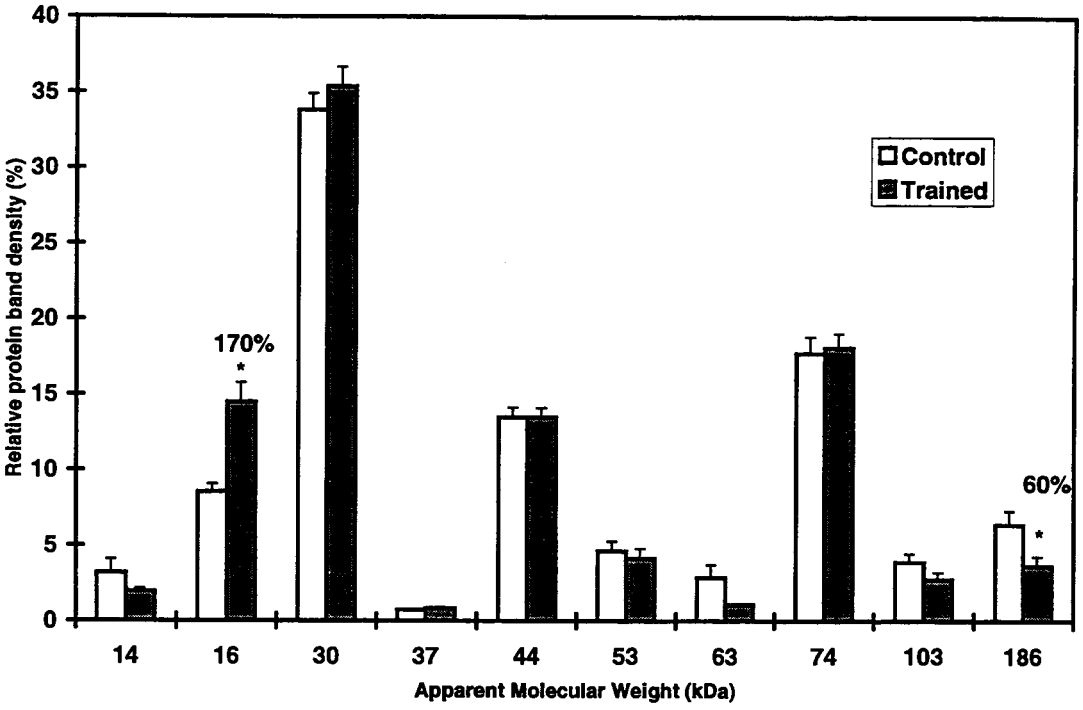

Figure 3. Histogram of the relative densities of sarcolemmal (SL) protein bands in kDa separated during 5-20% gradient polyacrylamide gel electrophoresis and quantified by densitometry in study 2. The asterisk represents a significant difference between the mean values and are expressed as a percentage of the control value.

CHAPTER 5

DIHYDROPYRIDINE AND RYANODINE BINDING IN VENTRICLES FROM RAT, TROUT, DOGFISH AND HAGFISH

ABSTRACT

In the adult mammalian heart, the majority of Ca^{2+} required for contraction is released from the sarcoplasmic reticulum (SR) via the Ca^{2+}-release channel or ryanodine receptor (RyR). Such release is initially dependent upon a relatively small influx of Ca^{2+} entering the cell across the sarcolemma (SL) by means of the L-type Ca^{2+} channel or the dihydropyridine receptor (DHPR). In lower vertebrates, there is indirect evidence suggesting that Ca^{2+} influx across the SL may be sufficient to support contraction, in the absence of Ca^{2+} release from the SR. This apparent difference in myocardial excitation-contraction (E-C) coupling was investigated further by determining DHPR and RyR densities in ventricular homogenate preparations from rat, trout, dogfish and hagfish. DHPR B_{max} values (means ± s.e.m.) were highest in rat (0.30±0.02 pmol/mg) and dogfish (0.27±0.03 pmol/mg), lower in trout (0.16±0.01 pmol/mg), and slightly above the level of detection in hagfish (0.03±0.01 pmol/mg). The DHPR dissociation constants (K_d), 40-70 pM in these species were similar. RyR binding revealed both high- and low- affinity sites in all species. RyR B_{max} for the high affinity site was greatest in the rat (0.68 pmol/mg), lower in trout (0.19 pmol/mg), dogfish (0.07 pmol/mg) and lowest in hagfish (0.01 pmol/mg). The RyR K_{d1} values for the high-affinity sites were comparable in all preparations (range 12-87 nM). The quantitative expression of RyRs in these species is consistent with the relative amount of SR present as indicated by electron microscopy and the relative insensitivity to ryanodine. Taking into consideration myocyte morphology of teleost and elasmobranch species, the data are consistent with a greater reliance on Ca^{2+} influx across the SL during E-C coupling in lower vertebrates, although a functional role for Ca^{2+} release from the SR in the more active species awaits further investigation.

INTRODUCTION

Fishes have developed cardiovascular systems which must function under very different physiological conditions. Environmental factors, such as varying temperature, place unique demands on myocardial Excitation-Contraction (E-C) coupling mechanisms. In mammals, myocardial contraction is initiated with an influx of Ca^{2+} through the sarcolemmal (SL) L-type Ca^{2+} channels, otherwise known as dihydropyridine receptors (DHPRs). This influx of Ca^{2+} is believed to trigger the release of a greater amount of Ca^{2+} from the sarcoplasmic reticulum (SR) (13) via the SR Ca^{2+}-release channels or ryanodine receptors (RyRs) (31). Although the magnitude of Ca^{2+} influx through SL Ca^{2+} channels varies between species (2), estimates that take into account the total amount of Ca^{2+} required for twitch generation, including intracellular Ca^{2+} buffering, suggest that it varies from 10 to 40% of this total (48). Studies using ryanodine, an agent known to block the SR Ca^{2+}-release channel, provide evidence that Ca^{2+} released from the SR is the major source of Ca^{2+} for contraction in adult mammalian hearts (40).

In lower vertebrates, a role for SR Ca^{2+} release in myocardial tension generation is generally dismissed for several reasons. In several fish species, electron microscopy reveals a relative paucity of SR relative to the amount found in mammals, as well as a lack of organizational complexity (35). In addition, ryanodine does not reduce contractile force in ventricular strips from a number of fishes at physiological temperatures (10-15°C) and stimulation frequencies above 0.2 Hz (10).

Experiments probing the mechanisms of E-C coupling in the hearts of lower vertebrates are also complicated by the varying temperatures to which poikilotherms are subject. Myofibrillar Ca^{2+} sensitivity in both endo- and ectotherms is reduced at lower temperatures (8, 20). However, amphibian (*Rana pipiens*) and rainbow trout hearts demonstrate a greater Ca^{2+}-sensitivity at lower temperatures than mammals suggesting that poikilotherms have developed some degree of thermal adaptation. To complicate matters, the total amount of Ca^{2+} required by the contractile element, taking into account the degree of intracellular Ca^{2+} buffering, has yet to be determined in fish. In the assessment of Ca^{2+} buffering, the temperature- and pH-dependence of the K_d values of the various intracellular Ca^{2+} binding sites would also have to be determined.

Despite the lack of information regarding temperature-dependencies of Ca^{2+} binding, there are a number of observations suggesting that the hearts of lower vertebrates place a greater reliance on SL Ca^{2+} influx to support tension generation than do the hearts of higher vertebrates (42). As with mammalian preparations, isometric force increases as extracellular Ca^{2+} concentration ($[Ca^{2+}]_o$) is raised in agnathan, elasmobranch and teleost ventricular strips (10). While the characteristics of the cardiac action potential may vary considerably among poikilotherms, the action potential is generally longer lasting and has a more pronounced plateau phase than that of the mammalian ventricle (44). In the frog and trout heart, a longer action potential duration is correlated with greater time-to-peak tension. In addition, both amphibian (2) and teleost (sea raven and cod) ventricles (10) are relatively insensitive to ryanodine at concentrations known to block SR Ca^{2+} release in mammals (40). Shark (*Squalus Acanthias*) ventricular myocyte contractions and I_{Ca} both demonstrate a bell-shaped dependence on voltage

which are completely supressed by nifedipine (5 μM) (30). The smaller myocyte diameters observed in amphibians, teleosts and elasmobranchs would also serve to reduce diffusional distances and substantially increase the SL surface area relative to cell volume (35). In addition to the absence of T-tubules and relatively sparse SR (5, 35), the DHPR density has been reported to be significantly higher in trout hearts than in mammalian preparations (41). However, owing to variability among species with respect to the degree of SR development, environmental parameters and experimental conditions used, a physiological role for the SR cannot, as yet, be ruled out. Therefore, in this study, we have attempted to characterize the key components of E-C coupling by determining the relative densities of DHPRs and RyRs in species phylogenetically distinct from mammals.

MATERIALS AND METHODS

Animal care. Female Wistar rats (290-324 g) were obtained from the University of British Columbia and kept in a temperature- and light- controlled vivarium (23°C, 12/12 hr light/dark cycle). Rainbow trout [*Oncorhynchus mykiss* (Walbaum)] weighing 600-800 g were obtained from West Creek Trout Farm, Aldergrove, British Columbia, and maintained locally at approximately 12°C for a minimum of 1 week outside during the summer months. Pacific hagfish [*Eptatretus stoutii* (Lockington)] and spiny dogfish [*Squalus acanthias*(Linnaeus)] were obtained and held in outdoor tanks (approximately 8°C) during the summer at the Bamfield Marine Station, Bamfield, British Columbia. Dogfish and hagfish binding experiments were carried out in a laboratory at this marine research station. Rat and trout experiments were conducted at Simon Fraser University.

Ventricular homogenate preparation. Animals were killed by standard protocols including lethal injection of sodium pentabarbitol (rat), a sharp blow to the head (trout), pithing (dogfish) or decapitation (hagfish). The hearts were rapidly excised and placed into a beaker of ice-cold homogenization medium (HM) containing 250 mM sucrose, 20 mM MOPS, pH 7.4 at 37°C. After rinsing, the ventricle(s) were isolated, blotted, weighed, and further rinsed in ice-cold HM. After mincing 0.5-1.7 g of tissue in approximately 5 ml HM, the tissue was homogenized using a Tekmar Tissumizer (five times 3 s on setting 40) and filtered through two layers of wire (nos. 30 and 40 stainless steel) mesh. The homogenate was then brought to a final volume of 15-20 ml per gram wet mass. Protein was determined using the Bradford method with bovine serum albumin as the standard.

Sarcolemma isolation. In two additional studies, SL was isolated from rat and trout hearts using techniques described previously (42, 45). Isolating trout SL involves several important modifications to existing purification steps employed for the rat. Owing to the relative fragility of the trout heart, reductions in both the duration and speed of homogenization as well as omission of the deoxyribonuclease incubation were required to enhance the recovery of SL. Briefly, pooled trout ventricles (at least 5.3 g) were minced with scissors in approximately 10 ml of ice-cold HM containing 280 mM sucrose and 20 mM *N*-tris (hydroxymethyl)methyl-2-aminoethanesulphonic acid (TES), pH 7.8 at 21°C. Homogenization and filtration through two layers of stainless-steel mesh (nos. 30 and 40) were followed by the addition of 1.0 M KCl and 250 mM sodium pyrophosphate to solubilize contractile proteins. Subsequent steps involved differential centrifugation and discontinuous sucrose gradient fractionation. The resultant pellets containing various membrane fractions were resuspended in 140 mM NaCl and 10 mM TES, pH 7.8 at 21°C, and frozen in liquid N_2. Protein was determined from a small sample taken prior to freezing. The sarcolemmal marker enzyme, K^+-stimulated *p*NPPase, was measured as described previously (42, 45).

[^{3}H]DHP binding assay. All binding experiments were performed using [^{3}H](+)PN200-110 (PN), as the stereospecific DHP ligand and the same ventricular homogenate preparations used for the [^{3}H]ryanodine binding experiments (see below). All PN binding experiments were performed by B. Hamman. Specific binding was determined by varying the amount of PN (0.025 to 1.6 nM) added to tubes containing 150-160 µg of protein (diluted in 25 mM MOPS, pH 7.4 at 23°C), and 2.5 mM $CaCl_2$ in a final volume of 5 ml. Non-specific binding was determined in separate tubes containing the same solution as that for specific binding plus 1 µM nifedipine.

After incubation at room temperature in the dark for 90 minutes, the separation of free from bound ligands was achieved by rapid filtration of a 2.25 ml sample using Whatman GF/C glass-fibre filters. Each filter was washed three times with 4.5 ml of ice-cold 25 mM MOPS buffer. The filters were then dried in liquid scintillation vials, after which 5 ml of Beckman Ready Protein liquid scintillant was added followed by 2 hours of orbital shaking at 200 rev/min to solubilize the protein. Vials were then counted (Beckman LS 7000) using standard liquid scintillation procedures.

[^{3}H]Ryanodine binding assay. To determine specific ryanodine binding varying amounts (0 to 495 nM) of unlabelled ryanodine (Calbiochem) plus 5 nM [^{3}H]ryanodine were added to tubes containing 150 mM KCl, 20 mM MOPS (pH 7.4 at 23°C), and 100 μM $CaCl_2$ in a final volume of 2 ml. Non-specific binding was measured by adding a 100-fold excess of unlabelled ryanodine to separate tubes. After the addition of 500 μg of ventricular homogenate protein, tubes were incubated at room temperature for 2 hours to allow the binding to reach a maximum. Duplicates were taken for each of the 12 points. Separation of bound and free ligand was achieved by rapid filtration using Whatman GF/C filters, followed by rinsing twice with 4 ml of ice-cold buffer (containing 150 mM KCl, 20 mM MOPS, 100 μM $CaCl_2$) and once with 4 ml of ice-cold 10% ethanol. After drying filters overnight in scintillation vials, 5 ml Beckman Ready Protein liquid scintillant was added followed by 2 hours of orbital shaking at 200 rev/min to solubilize the protein. Vials were then counted using standard liquid scintillation procedures.

Data and statistical analyses. DHPR binding data were analyzed by iterative non-linear regression and Scatchard analysis using LIGAND (Munson and Rodbart, NIH) to determine the maximum receptor density (B_{max}) and the dissociation constant (K_d) for each preparation. RyR

binding data were analyzed using an iterative non-linear regression method using GRAFIT (Erithacus Software Ltd, UK). The goodness-of-fit of the predicted value from several different equations to the data sets were determined by χ^2 analysis. Between group comparisons were made by performing the Bonferonni (Dunn) t-test, with the significance level set at $p < 0.05$.

Materials. All reagents used were of the highest purity and purchased from Sigma unless specified otherwise. Radioisotopes were purchased from New England Nuclear (Du Pont, St. Laurent, Quebec, Canada).

RESULTS

The wet mass of the ventricles used in preparing homogenates of the four species and the protein yields are given in Table 1. The protein content in both dogfish and hagfish was considerably lower than typically observed in either mammals or teleosts. Specific binding of DHP at different concentrations of PN200-110 to ventricular homogenate is shown in Figure 1. At 0.10 nM [^{3}H](+)PN200-110, the specific binding accounted for more than 70% of the total binding for all species. Over the more than two orders of magnitude of [^{3}H](+)PN200-110 concentrations used in this study (0.025-1.6 nM), the data fit a single class of high affinity binding sites as exemplified by linear Scatchard plots and low values of χ^2 in the appropriate regression equation. Scatchard analyses of the fitted data are shown in Figure 2 and yielded B_{max} and K_d values listed in Table 2. Both the B_{max} and K_d values for the trout and dogfish were comparable to those for mammals. The calculated densities of receptors (sites per μm^3 cell volume) are given in Table 4. In all species, except the hagfish, the DHPR density was within the range (0.08-0.3 pmol/mg) observed in mammals. The derived B_{max} for the DHPR in hagfish was 0.03 pmol/ mg and was about an order of magnitude lower than that observed in the other species. Because the hagfish values were so low, barely above the limit of detection, one cannot be confident of the derived B_{max} and K_d.

Homogenates were used in this study because this preparation represents the entire pool of channels without the loss that occurs with membrane isolation. An example of the problems that can arise from membrane isolation is shown in Figure 3. This demonstrates the differential loss of DHPRs relative to marker enzyme activity in rat sarcolemmal fractions compared with

those of trout. In rat, the increase in specific DHP binding over the levels found in homogenates is markedly lower compared with the increase in SL marker enzyme activity. In contrast, the trout demonstrates comparable purification of both DHPRs and SL marker enzyme activity.

Figure 4 shows specific [^{3}H]ryanodine binding to the same preparations used for the DHPR binding assays. When the RyR data from all lower vertebrate species were linearized in a Scatchard plot, they generated neither straight nor concave lines. Consistent with this result is the fact that neither a one- nor a two- site ligand binding equation fit the data well. Because the RyR specific binding as a function of ryanodine concentration (over the range 0-75 nM) consistently demonstrated sigmoidicity, a two-site Adair equation was also used to fit the data. This resulted in clearly the best fit both by eye and in the χ^2 analysis. In order to observe the high-affinity site better, data are shown for concentrations ranging from 0 to 75 nM ryanodine (Figure 4). With the full range of ryanodine concentrations used, the presence of at least two separate independent binding sites were observed (Figure 5). At 30 nM total ryanodine, the specific binding accounted for more than 70% of total binding for all species. After fitting the data to one of several different equations, the two-site Adair equation gave the best results for the high-affinity and the one-site equation gave the best results for the low affinity sites. The B_{max} and K_d values obtained are listed in Table 3. The number of high-affinity sites is significantly reduced in the trout, dogfish and hagfish compared to rat. However, the K_d values remained comparable to values for mammalian preparations. The calculated densities (sites per μm^3 cell volume) are given in Table 4. The rat which relies most heavily on Ca^{2+} release from the SR had by far the greatest density of RyRs. In contrast, the hagfish which is the most primitive species

studied, had the lowest density of RyRs. Table 4 shows the ratios of RyR/DHPR densities in the various species.

DISCUSSION

DHPR and RyR densities were determined in ventricular preparations from phylogenetically distinct species to characterize further the key components in E-C coupling in lower vertebrates.

Protein content. The protein content of ventricular homogenates is significantly lower for dogfish and hagfish than rat and trout. A value of approximately 100 mg · g wet mass^{-1} is typically observed in mammals (25). Reference values for ventricular protein content in elasmobranch or hagfish species is not available. This difference may reflect the fact that the myocardium of dogfish, *Squalus acanthias*, contains a high percentage, approximately 80%, of spongy trabeculae and the hagfish systemic heart is composed exclusively of spongiosa (14). Previous studies indicated that spongy trabeculae from frog (39), teleost (36), elasmobranchs (36, 46) and hagfish (26) ventricles have more extracellular space (ECS) than the compact myocardium of mammals (17).

DHPR binding. In mammalian hearts, the α_1 subunit of the SL Ca^{2+} channel contains both the DHP binding domain and Ca^{2+} conductance capabilities when expressed in oocytes (29). The α_1 subunit from trout has a similar M_r of 185 and K_d for DHP binding to those of mammals (Tuana, BS, BJ Murphy, J Wigle, C Pratt, and GF Tibbits in preparation). The K_d values reported in Table 2 for both rat and trout are in agreement with these data. The K_d value in the dogfish preparation is comparable with the values for the rat and trout, suggesting that at least the DHP binding domain may be the same in this species. In contrast, the trout cardiac α_2 subunit appears to be quite different in both size and nucleotide sequence from the mammalian form (ibid.).

The densities of DHPRs were calculated for three of the four species and recorded in Table 4. Values not measured were taken from the literature or estimated, as noted. The calculated densities rely on three assumptions. The first assumption is that all DHPRs are from myocyte sarcolemma. Because myocyte protein represents $\geq$50% of homogenate protein the maximum purification of DHPR is 200% (3). The finding that DHP binding in isolated myocytes from rabbit heart is ~180% of that in whole-muscle homogenates suggests that the number of DHPRs in non-myocyte tissue is minimal (3). The second assumption is that the relative contribution of ECS measured in the trout is the same for dogfish. Quantitative analysis using stereological measurements has indicated that the amount of total tissue occupied by ECS in rat heart is approximately 28% including T-tubules (17). The only quantitative information available on the extent of the ECS in fish is a figure of approximately 32%. This value was obtained by isotopic measurements of ECS in the *in situ* perfused trout heart (15) and was used to calculate DHPR density for both trout and dogfish. The third assumption is that all of the intracellular volume is made up of myocytes. While there are many cell types in the heart, the much larger myocytes account for approximately 75-90% of the cell volume (1). The calculated DHPR densities, in sites per μm^3 cell volume (Table 4), were 29 for rat, 18 for trout, 13 for dogfish and 2 for hagfish. The value for rat is high for mammalian cardiac muscle, but this is almost completely due to the observed difference in B_{max} rather than the assumptions made (3). A possible explanation may be that, for reasons unknown, fewer receptors were damaged or degraded during the present experiments on rat. DHPR densities for the trout and dogfish, while somewhat lower than the density for the rat, still remain well within the mammalian range (3, 25). Using previously published data from DHP binding in homogenized rat cardiomyocytes, a density of

approximately 12 sites per μm^3 is calculated (3) which is comparable to the densities calculated in this study for rat, trout and dogfish. The densities of DHPRs in the hagfish were almost an order of magnitude lower than that observed for the other species in this study. However, previous experiments on ventricular strips from the Atlantic hagfish still show a sensitivity to $[Ca^{2+}]_o$ (34).

In a previous report (42), the B_{max} of purified SL preparations from the trout was determined to be 3.06 pmol/mg SL protein. This value is an order of magnitude higher than values reported for mammalian SL of similar purity (9, 25). It was concluded from these observations that DHPR density is greatly increased in the trout compared with the mammalian heart (42). This conclusion turns out to be erroneous, as shown by the present data using ventricular homogenates (Table 2). This discrepancy may be explained by a differential DHPR purification during the SL isolation in the two species. Examination of Figure 3 shows that during SL purification, the percentage increase of DHP binding and of SL marker enzyme (K^+-stimulated *p*NPPase) are not proportional in the rat, suggesting that DHPRs are being lost during purification, presumably to denser fractions. Similar results have also been reported in canine heart (9) and more recently, in cardiomyopathic hamsters (25). This apparent loss of DHPRs from the SL may be due to the tight coupling between the junctional SR RyR and the DHPR in the mammalian T-tubule (18). Since DHPRs are known to be clustered in the T-tubules in mammals (47), a differential loss of T-tubule DHPRs over DHPRs not associated with RyRs would lead to an underestimation of mammalian B_{max} values. In contrast, the DHPR loss is not as apparent in the trout (Figure 3). DHPR binding increases approximately 12-fold during trout SL purification, which is comparable to the approximately 15-fold increase in SL marker activity

(42). The lack of T-tubules and the relatively sparse SR found in the trout suggest that the RyRs and DHPRs may be more loosely coupled, which may explain these results.

While DHPR densities in trout and dogfish are comparable to those of mammals, it is not known whether the total amount of Ca^{2+} entering the cell in each of these species is also of the same magnitude. Using a whole-cell patch-clamp technique, an L-type Ca^{2+} current (I_{Ca}) density of >3 $\mu A/cm^2$ (in 1.8 mM $CaCl_2$ at 23°C) has been obtained in frog ventricular myocytes (27). This falls somewhat below the lower end of the 10-30 $\mu A/cm^2$ range of I_{Ca} densities typically observed in mammalian species under similar recording conditions (27). However, I_{Ca} density does not take into account the extent of Ca^{2+}-dependent channel inactivation. Lower I_{Ca} densities are known to inactivate more slowly; thus the $[Ca^{2+}]_i$ could potentially be the same or even greater. In another study, $[Ca^{2+}]_i$-transients detected with aequorin recorded from salamander ventricular strips were prolonged relative to $[Ca^{2+}]_i$-transients from mammalian myocardium (19). If one assumes that the intracellular Ca^{2+}-buffering capacity is similar to that in mammals and that DHPRs represent functional L-type Ca^{2+} channels (16), then Ca^{2+} entry of similar magnitude could provide a greater rise in $[Ca^{2+}]_i$ for the trout and dogfish myocytes simply because of the smaller myocyte diameters. In addition, the mammalian I_{Ca} amplitude is extremely temperature-dependent with a Q_{10} of approximately 3 (7). Without some sort of evolutionary selection with regard to the temperature-dependence of Ca^{2+} channel function, the contractility of the hearts of these lower species may be profoundly impaired. The temperature dependence of I_{Ca} amplitude in lower vertebrates is not known. Clearly, precise measurements

of Ca^{2+} current density integrated over time and the effects of temperature on both the electrophysiological and Ca^{2+}-buffering processes are required to determine the extent of SL Ca^{2+} entry.

Finally, the potential contribution of mitochondrial Ca^{2+} has been ruled out in mammals by a variety of pharmacological and kinetic arguments (13). However, these experiments have not yet been done in lower vertebrates where Ca^{2+} cycling may be considerably slower.

RyR Binding. The presence of both high- and low-affinity ryanodine binding sites in all of the species in this study is consistent with current knowledge of the mammalian cardiac RyR. Conventional analysis, however, did not yield good results with respect to curve-fitting of the fish data. We were, therefore, forced to try several different approaches. The best results were obtained (lowest χ^2 and best fit by eye) when the high-affinity data were fitted with the two-site Adair equation. When microscopic dissociation constants are not equal, the Adair equation will describe the cooperative ligand binding that was observed in the different fish species. It also became apparent (see Fig. 5B-D) that in the poikiolotherm preparations, particularly the trout, this cooperativity was positive. A recently proposed sequential model of ryanodine binding in both mammalian skeletal and cardiac SR demonstrates negative cooperativity among the four putative binding sites (33). While further investigation involving kinetic and equilibrium measurements is needed, these preliminary results suggest that ryanodine binding in the lower vertebrates may reflect a functionally distinct cardiac RyR isoform.

To date there has been only one RyR isoform (RyR_2) identified in cardiac tissue (28). The mammalian cardiac RyR is a polypeptide with a calculated M_r of approximately 560 as determined by cloning and sequencing of full-length cDNA (31). Electron microscopy and

biochemical studies have demonstrated that RyR *in vitro* exists as a homotetramer (28). Single-channel recordings of isolated RyRs incorporated into lipid bilayers demonstrate an open subconductance state in the presence of nanomolar concentrations of ryanodine, while micromolar concentrations close the channel completely (38). A negative cooperativity between the subunits is also demonstrated in this study by the presence of high- and low-affinity ryanodine binding. In each of the species examined, the K_{d1} values for the high-affinity site were within the range found in mammals under similar conditions and temperature (28). The comparable ryanodine binding affinities observed in this study suggest that the ryanodine binding domains of the SR Ca^{2+}-release channel is similar to that found in mammalian myocardium. However, the presence of positive cooperativity within the high-affinity binding suggests that there may be some subtle differences in the fish RyR. While further investigation is required to elucidate the precise mechanisms underlying this positive cooperativity, the physiological implications may involve some sort of functional adaptation in the RyR, allowing the SR to participate in E-C coupling to a greater extent under certain conditions.

Maximum [^{3}H]ryanodine binding to the high affinity site was greatest in rat and decreased considerably in the order trout > dogfish > hagfish (Figure 4). Overall, the maximum binding and calculated densities (Table 4) correlate with the phylogenetic development of SR in these species (35). The SR accounts for approximately 3.5 % of myocyte volume in rat (32), and considerably less, <0.3 %, in amphibians (5). While limited information is available for fish, electron microscopic observations show that the SR tends to be better developed in teleosts than in either amphibians or agnathans, and is least developed in elasmobranchs (21, 46). A possible explanation as to why the elasmobranch has less total SR but more ryanodine binding than the

hagfish may be related to the relative abundance of peripheral couplings or junctional SR, with which the RyR is known to be associated. More quantitative information is needed to resolve this issue. It is also not known whether there are differences between spongy and compact myocardium with respect to content of RyR or complexity of SR.

The calculated RyR receptor densities shown in Table 4 were 65 for rat, 21 for trout, 3 for dogfish, and <1 for hagfish. The value of 65 sites/μm^3 for rat is comparable to a previous report of 0.83 pmol/mg myocyte protein which corresponds to approximately 53 receptors/μm^3 after correcting for 0.6 mg myocyte protein per mg homogenate and 127 mg homogenate protein per cm^3 (3). The lower number obtained from the myocyte study may be a reflection of greater receptor degradation due to the higher incubation temperatures used. The lower RyR densities for trout, dogfish and hagfish clearly reflect the reduced volume of SR hence the contribution of SR Ca^{2+} in these species, as indicated by light and electron microscopy (35).

The presence of high-affinity RyRs at room temperature (Figure 4) in trout, dogfish and hagfish, although in smaller numbers than in rat, suggests that functional RyRs may exist in the SR of these species. There is an abundance of evidence correlating the relative amount of SR with both the extent of [^{3}H]ryanodine binding and the ability of ryanodine to suppress tension development in mammals and amphibians (2, 47). Ryanodine is known to depress twitch tension by varying degrees depending upon species, tissue and development (2, 47). The frog heart is relatively insensitive to ryanodine and has considerably less total SR than mammalian heart (2). In the rat heart, a profound change in E-C coupling occurs during ontogeny (47). Active tension generation in ventricular strips from the neonate is suppressed by the dihydropyridine nifedipine while being relatively insensitive to ryanodine. Conversely, the ability of ryanodine to suppress

tension is greatly increased in the adult, while dihydropyridine-sensitivity is diminished. The amount of SR is known to increase during ontogeny and is associated with a concomitant increase in [^{3}H]ryanodine binding (47).

In assessing the apparent effects of ryanodine, knowledge of the experimental conditions, especially incubation time and temperature, is of critical importance. Ryanodine binding is extremely slow and is both [Ca^{2+}]- and temperature-dependent with a Q_{10} of 4 (6). Therefore, experiments using ryanodine at concentrations known to block SR Ca^{2+} release in mammals may not show an effect at the lower temperatures used in the fish preparations. In addition, cooling from 23 to 5-10°C increases the open probability of sheep RyRs reconstituted into lipid bilayers from 0.1 to 0.7 (38). Rapid cooling to below 5°C in isolated mammalian myocytes induces a rapid cooling contracture (RCC) which is caused, apparently, both by the opening of the SR Ca^{2+} release channel in response to the cold and by the inability of Ca^{2+} removal systems to operate at the lower temperatures. In the Amphibia, only very small RCCs can be elicited partly because of the sparseness of SR and also because other Ca^{2+} transport mechanisms, such as the Na^+/Ca^{2+} exchanger, continue to function at lower temperatures (4). If the SR Ca^{2+}-release channel maintains a mammalian temperature-dependence, the SR may be rendered non-functional at the lower temperatures experienced by some species.

Owing to the relative paucity of SR and the general lack of ryanodine-sensitivity in lower vertebrates, the role of SR Ca^{2+} release in contractile activation has usually been dismissed. However, under certain conditions, it is possible to induce SR Ca^{2+} release in several poikilotherms (10-12). Post-rest potentiation (PRP), a phenomenon ascribed to greater SR Ca^{2+}

release after a prolonged rest interval, while nonphysiological and temperature-dependent, has been demonstrated in ventricular strips from skate at 10°C and trout at 15°C (10, 12). In addition, ryanodine at concentrations known to block SR Ca^{2+} release in mammals abolished the potentiated force in the trout. The inability of ryanodine to suppress force under more physiologically relevant conditions may have been due to the lower temperatures used. In a more recent study, contractility was substantially reduced by ryanodine in atrial strips from skipjack tuna at 25°C (24). Further evidence of a role for SR in regulating contractility in trout myocardium comes from observations on the influence of temperature on both ryanodine-sensitivity and force-frequency relationships in trout heart (22). In contrast to mammals and the frog, which show a decrease in force when temperatures are raised (37), ventricular strips from trout are able to maintain twitch force (0.2 Hz) at temperatures between 15 and 25°C (22). This may be because there was a greater contribution of SR Ca^{2+} release at the higher temperature. This is supported by the finding that the ability of ryanodine to suppress both the twitch force and PRP was significantly greater at 25°C than at 15°C. In both cases, the reduction in force induced by ryanodine was due to a lower maximum rate of force generation while time-to-peak force was not altered. In agreement with a greater contribution of Ca^{2+} release from the SR is the observation that the concentration of ryanodine required to reduce contractile force by half ($K_{1/2}$) is raised substantially at lower temperatures. The $K_{1/2}$ at 25°C agrees with the K_d values obtained in all the species compared in this study at the same temperature. The current evidence thus suggests that the RyR has not undergone any evolutionary selection for improved function at

lower temperatures. Therefore, it seems possible that at higher temperatures, in some fish species, SR Ca^{2+} release may contribute to the regulation of contractility.

RyR/DHPR Ratios. The RyR/DHPR ratios given in Table 4 reflect the relative density of receptors per μm^3 cell volume as assessed by binding of radiolabelled ligand. Optimal binding conditions, in terms of [Ca^{2+}], time and temperature, were determined for both assays. The 2 hr incubation time at room temperature for RyR represents a trade-off between maximum specific binding due to the slow binding kinetics of ryanodine and receptor degradation (6). With these limitations in mind, the lower trout and dogfish ratios reflect primarily a reduction in numbers of RyRs. The rat RyR:DHPR ratio shows twice as many RyRs as DHPRs and reflects the large contribution of SR Ca^{2+} release to E-C coupling in this species. However, this ratio is lower than the 4 to 7 typically observed for this species. A high PN B_{max} of 3.0 pmol/mg contributed to the lower RyR:DHPR ratio. The range in heart rate from 300-600 beats/min requires an extremely rapid cycling of Ca^{2+}. In contrast, the heart rates of lower vertebrates are considerably slower; thus, the need for rapid cycling of Ca^{2+} is greatly reduced. A RyR:DHPR ratio of <1 may reflect an alteration in E-C coupling to one of reduced reliance on SR Ca^{2+} release and a greater reliance on Ca^{2+} entry across the SL in these species.

Implications For E-C Coupling. In mammalian cardiac muscle, a small amount of Ca^{2+} enters the cell triggering the release of a much larger amount of Ca^{2+} from the SR. While the relative roles of each Ca^{2+} source may vary between mammalian species, the SR remains the largest contributor to contractile activation. A greater involvement of SR in Ca^{2+} cycling would serve to increase the speed of contraction and relaxation. The hagfish is a relatively sedentary species, in

which, heart rates rarely exceed 35 beats/min, output pressures are low and myocardial tension development is slow (14, 23). Thus there is no apparent need to develop a rapid Ca^{2+} cycling system involving the SR. The long cardiac action potentials, often approximately 1 second in duration, support the idea of an almost exclusive reliance on SL Ca^{2+} influx (23). However, because DHP binding was negligible in this species, SL Ca^{2+} influx may occur by another mechanism, such as Na^{+}/Ca^{2+} exchange. In contrast, both the dogfish (*Squalus acanthias*) and rainbow trout (*Oncorhynchus mykiss*) are more active and capable of generating much greater cardiac outputs and heart rates. As a consequence, there is a need to develop more rapid Ca^{2+} cycling, at least under certain conditions, in these species. Biochemical studies performed on compact and spongy myocardium support the idea that the development of a compact myocardium is a morphological adaptation related to the activity level of the fish species (36).

Finally, the reduced SR content in the lower vertebrates studied would necessitate a fundamentally different relative contribution to Ca^{2+} removal during relaxation. While little is known about the SL Ca^{2+}-ATPase in lower vertebrates, the SL Na^{+}/Ca^{2+} exchanger is known to be relatively active even at the lower physiological temperatures of both trout and amphibians (4, 43).

In conclusion, the results of this comparative study of DHPR and RyR binding in ventricular homogenates from mammalian, teleost, elasmobranch and agnathan species are consistent with current evidence indicating that heart contraction in lower vertebrates is largely dependent upon trans-sarcolemmal Ca^{2+} entry although Ca^{2+} release from the SR may also make a contribution, depending upon species and environmental factors such as temperature.

REFERENCES

1. Anversa, P., G. Olivetti, M. Melissari, and A. V. Loud. Morphometric study of myocardial hypertrophy induced by abdominal aortic stenosis. *Lab. Invest.* 40: 341-349, 1979.

2. Bers, D. M. Calcium influx and sarcoplasmic reticulum Ca release in cardiac muscle activation during postrest recovery. *Am. J. Physiol.* 248: H366-H381, 1985.

3. Bers, D. M., and V. A. Stiffel. Ratio of ryanodine to dihydropyridine receptors in cardiac and skeletal muscle and implications for E-C coupling. *Am. J. Physiol.* 264: C1587-C1593, 1993.

4. Bersohn, M. M., R. Vemuri, D. S. Schuil, and K. D. Philipson. Effect of temperature on Na^{+}-Ca^{2+} exchange in sarcolemma from mammalian and amphibian hearts. *Biochimica et Biophysica Acta* 1062: 19-23, 1991.

5. Bossen, E. H., and J. R. Sommer. Comparative stereology of the lizard and frog myocardium. *Tissue & Cell* 16: 173-178, 1984.

6. Carroll, S., J. G. Skarmeta, X. Yu, K. D. Collins, and G. Inesi. Interdependence of ryanodine binding, oligomeric receptor interactions, and Ca^{2+} release regulation in junctional sarcoplasmic reticulum. *Archs. Biochem. Biophys.* 290: 239-247, 1991.

7. Cavalie, A., T. F. McDonald, D. Pelzer, and W. Trautwein. Temperature-induced transitory and steady-state changes in the calcium current of guinea pig ventricular myocytes. *Pflugers Arch.* 405: 294-296, 1985.

8. Churcott, C. S., C. D. Moyes, B. H. Bressler, K. M. Baldwin, and G. F. Tibbits. Temperature and pH effects on Ca^{2+} sensitivity of cardiac myofibrils: a comparison of trout and mammals. *Am. J. Physiol.* 267: R62-R70, 1994.

9. DePover, A., I. L. Grupp, G. Grupp, and A. Schwartz. Diltiazem potentiates the negative inotropic action of nimodipine in heart. *Biochem. biophys. Res. Commun.* 114: 922-929, 1983.

10. Driedzic, W. R., and H. Gesser. Differences in force-frequency relationships and calcium dependency between elasmobranch and teleost hearts. *J. Exp. Biol.* 140: 227-241, 1988.

11. Driedzic, W. R., and H. Gesser. Energy metabolism and contractility in ectothermic hearts: hypoxia, acidosis, and low temperature. *Physiol. Rev.* 74: 221-258, 1994.

12. El-Sayed, M. F., and H. Gesser. Sarcoplasmic reticulum, potassium, and cardiac force in rainbow trout and plaice. *Am. J. Physiol.* 257: R599-R604, 1989.

13. Fabiato, A. Calcium-induced release of calcium from the cardiac sarcoplasmic reticulum. *Am. J. Physiol.* 245: C1-C14, 1983.

14. Farrell, A. P., and D. R. Jones. The heart. In: *Fish Physiology*, edited by W. S. Hoar, D. J. Randall and A. P. Farrell. San Diego, CA: Academic Press, Inc., 1992, p. 1-73.

15. Farrell, A. P., and C. L. Milligan. Myocardial intracellular pH in a perfused rainbow trout heart during extracellular acidosis in the presence and absence of adrenaline. *J. Exp. Biol.* 125: 347-359, 1986.

16. Flockerzi, V., H. Oeken, F. Hofmann, D. Pelzer, A. Cavalie, and W. Trautwein. Purified dihydropyridine-binding site from skeletal muscle T-tubules is a functional calcium channel. *Nature* 323: 66-68, 1986.

17. Frank, J. S., and G. A. Langer. The myocardial interstitium: Its structure and its role in ionic exchange. *J. Cell Biol.* 60: 586-601, 1974.

18. Franzini-Armstrong, C., and A. O. Jorgensen. Structure and development of E-C Coupling units in skeletal muscle. *A. Rev. Physiol.* 56: 509-534, 1994.

19. Gwathmey, J. K., and J. P. Morgan. Calcium handling in myocardium from amphibian, avian, and mammalian species: the search for two components. *J. Comp. Physiol.* 161: 19-25, 1991.

20. Harrison, S. M., and D. M. Bers. Temperature dependence of myofilament Ca sensitivity of rat, guinea pig, and frog ventricular muscle. *Am. J. Physiol.* 258: C274-C281, 1990.

21. Helle, K. B., and A. Storesund. Ultrastructural evidence for a direct connection betwen the myocardial granules and the sarcoplasmic reticulum in the cardiac ventricle of *Myxine glutinosa* (L.). *Cell Tiss. Res.* 163: 353-363, 1975.

22. Hove-Madsen, L. The influence of temperature on ryanodine sensitivity and the force-frequency relationship in the myocardium of rainbow trout. *J. Exp. Biol.* 167: 47-60, 1992.

23. Jensen, D. The aneural heart of the hagfish. *Ann. N. Y. Acad. Sci.* 127: 443-458, 1965.

24. Keen, J. E., A. P. Farrell, G. F. Tibbits, and R. W. Brill. Cardiac dynamics in tunas. II. Effect of adrenaline, calcium and ryanodine on force-frequency relationships in atrial strips from skipjack tuna, *Katsuwonus pelamis. Can. J. Zool.* 70: 1211-1217, 1992.

25. Lachnit, W. G., M. Phillips, K. J. Gayman, and I. N. Pessah. Ryanodine and dihydropyridine binding patterns and ryanodine receptor mRNA levels in myopathic hamster heart. *Am. J. Physiol.* 267: H1205-H1213, 1994.

26. Leak, L. V. Electron microscopy of cardiac tissue in a primitive vertebtate *Myxine glutinosa. J. Morph.* 128: 131-158, 1969.

27. McDonald, T. F., S. Pelzer, W. Trautwein, and D. J. Pelzer. Regulation and modulation of calcium channels in cardiac, skeletal, and smooth muscle cells. *Physiol. Rev.* 74: 365-507, 1994.

28. Meissner, G. Ryanodine receptor/Ca^{2+} release channels and their regulation by endogenous effectors. *Ann. Rev. Physiol.* 56: 485-508, 1994.

29. Mikami, A., K. Imoto, T. Tanabe, T. Niidome, Y. Mori, H. Takeshima, S. Narumiya, and S. Numa. Primary structure and functional expression of the cardiac dihydropyridine-sensitive calcium channel. *Nature* 340: 230-233, 1989.

30. Nabauer, M., and M. Morad. Modulation of contraction by intracellular Na^+ via Na^+-Ca^{2+} exchange in single shark (*Squalus Acanthias*) ventricular myocytes. *J. Physiol.* 457: 627-637, 1992.

31. Otsu, K., H. F. Willard, V. K. Khanna, F. Zorzato, N. M. Green, and D. H. MacLennan. Molecular cloning of cDNA encoding the Ca^{2+} release channel (ryanodine receptor) of rabbit cardiac muscle sarcoplasmic reticulum. *J. Biol. Chem.* 265: 13472-13483, 1990.

32. Page, E. Quantitative ultrastructural analysis in cardiac membrane physiology. *Am. J. Physiol.* 235: C147-C158, 1978.

33. Pessah, I. N., and I. Zimany. Characterization of multiple [^{3}H]ryanodine binding sites on the Ca^{2+} release channel of sarcoplasmic reticulum from skeletal and cardiac muscle: Evidence for a sequential mechanism in ryanodine action. *Molec. Pharmac.* 39: 679-689, 1991.

34. Poupa, O., J. A. Ask, and K. B. Helle. Absence of calcium paradox in the cardiac ventricle of the atlantic hagfish (*Myxine glutinosa*). *Comp. Biochem. Physiol.* 78A: 181-183, 1984.

35. Santer, R. M. Morphology and innervation of the fish heart. *Adv. Anat. Embryol. Cell Biol.* 89: 1-102, 1985.

36. Santer, R. M., and M. G. Walker. Morphological studies on the ventricle of teleost and elasmobranch hearts. *J. Zool., Lond.* 190: 259-272, 1980.

37. Shattock, M. J., and D. M. Bers. Inotropic response to hypothermia and the temperature-dependence of ryanodine action in isolated rabbit and rat ventricular muscle: Implications for excitation-contraction coupling. *Circ. Res.* 61: 761-771, 1987.

38. Sitsapesan, R., R. A. P. Montgomery, K. T. MacLeod, and A. J. Williams. Sheep cardiac sarcoplasmic reticulum calcium-release channels: Modification of conductance and gating by temperature. *J. Physiol., Lond.* 434: 469-488, 1991.

39. Sommer, J. R., E. A. Johnson, N. R. Wallace, and R. Nassar. Cardiac muscle following quick-freezing: Preservation of in vivo ultrastructure and geometry with special emphasis on intercellular clefts in the intact frog heart. *J. Molec. Cell. Cardiol.* 20: 285-302, 1988.

40. Sutko, J. L., and J. L. Kenyon. Ryanodine modification of cardiac muscle responses to potassium-free solutions. *J. Gen. Physiol.* 82: 385-404, 1983.

41. Tibbits, G. F., L. Hove-Madsen, and D. M. Bers. Calcium transport and the regulation of cardiac contractility in teleosts: a comparison with higher vertebrates. *Can. J. Zool.* 69: 2014-2019, 1991.

42. Tibbits, G. F., H. Kashihara, M. J. Thomas, J. E. Keen, and A. P. Farrell. Ca^{2+} transport in myocardial sarcolemma from rainbow trout. *Am. J. Physiol.* 259: R453-R460, 1990.

43. Tibbits, G. F., C. D. Moyes, and L. Hove-Madsen. Excitation-contraction coupling in the teleost heart. In: *Fish Physiology*, edited by W. S. Hoar, D. J. Randall and A. P. Farrell. San Diego, CA: Academic Press, 1992, p. 267-304.

44. Tibbits, G. F., K. Philipson, and H. Kashihara. Characterization of myocardial Na^{+}-Ca^{2+} exchange in rainbow trout. *Am. J. Physiol.* 262: C411-C417, 1992.

45. Tibbits, G. F., M. Sasaki, M. Ikeda, K. Shimada, T. Tsuruhara, and T. Nagatomo. Characterization of rat myocardial sarcolemma. *J. Molec. Cell. Cardiol.* 13: 1051-1061, 1981.

46. Tota, B. Myoarchitecture and vascularization of the elasmobranch heart venticle. *J. Exp. Zool. (Suppl.)* 2: 122-135, 1989.

47. Wibo, M., G. Bravo, and T. Godfraind. Postnatal maturation of excitation-contraction coupling in rat ventricle in relation to the subcellular localization and surface density of 1,4-dihydropyridine and ryanodine receptors. *Circ. Res.* 68: 662-673, 1991.

48. Wier, W. G. Cytoplasmic $[Ca^{2+}]_i$ in mammalian ventricle: Dynamic control by cellular processses. *Ann. Rev. Physiol.* 52: 2440-2447, 1990.

TABLE 1

VENTRICULAR CHARACTERISTICS IN THE DIFFERENT SPECIES.

	Rat	Trout	Dogfish	Hagfish
VENTRICULAR MASS (g)	0.80 (0.02)	0.48 (0.03)	1.70 (0.17)	0.46 (0.04)
PROTEIN CONTENT (mg/g)	107.7 (2.5)	116.8 (9.9)	49.6 (3.3)*	66.3 (6.3)*
N	10	6	6	6

Values are means (S.E.M.). VENTRICULAR MASS, wet mass of trimmed ventricle in grams. PROTEIN CONTENT, milligrams of protein per gram wet mass of ventricle. N, number of assays performed with one assay on each ventricle for rat, trout and dogfish, and 2-6 ventricles pooled for each assay for the hagfish. Multiple comparisons were made using the Bonferroni (Dunn) t-test. * Values for dogfish and hagfish are significantly ($P < 0.05$) different from values for both rat and trout.

TABLE 2

COMPARISON OF DHP BINDING IN DIFFERENT SPECIES.

	Rat	Trout	Dogfish	Hagfish[a]
B_{max} (pmol/mg)	0.30 (0.02)	0.16 (0.01)*	0.27 (0.03)	0.03*
K_d (nM)	0.07 (0.01)	0.04 (0.01)	0.07 (0.01)	0.42
N	10	6	6	5

Values are means (S.E.M.). B_{max} is the maximum density of dihydropyridine binding sites determined by Scatchard analysis; K_d is the dissociation constant determined by Scatchard analysis; N is the number of assays performed (with one assay on each ventricle for rat, trout and dogfish, and 2-6 ventricles pooled for each assay for hagfish). Multiple comparisons were made using the Bonferroni (Dunn) t-test. * Values significantly different from those of the rat ($P<0.05$). [a] Analysis performed on composite data. All PN binding experiments were performed by B.H..

TABLE 3

COMPARISON OF RYANODINE BINDING IN DIFFERENT SPECIES.

	Rat	Trout	Dogfish	Hagfish
HIGH AFFINITY SITE:				
B_{max} (pmol/mg)	0.68	0.19	0.073	0.011
	(0.53-0.87)	(0.09-0.23)	(0.04-0.23)	(0.00-0.05)
K_{d1} (nM)	33	87	67	12
K_{d2} (nM)	2	57	240	155
LOW AFFINITY SITE:				
B_{max} (pmol/mg)	0.92	1.61	0.42	0.12
K_d (nM)	43	779	130	474
N	10	6	6	5

Values for the high-affinity site were obtained through non-linear regression analysis using the two-site Adair equation provided in the computer program GRAFIT (Erithacus Software Ltd, UK) and for the mean binding data obtained over the range 0-75 nM ryanodine. The range for the high affinity B_{max} values are indicated below in brackets. Values for the low-affinity site were obtained using the same method, a one-site ligand binding equation and binding data for 100-500 nM ryanodine. All analyses were performed on the composite data for each species. N is the number of assays performed (with one assay on each ventricle for rat, trout and dogfish and 2-6 ventricles pooled for each assay for hagfish.

TABLE 4

CALCULATIONS OF DHPR AND RyR DENSITIES.

	Rat	Trout	Dogfish	Hagfish
DHPR B_{max} [a] (pmol/mg)	0.30	0.16	0.27	0.03
RyR B_{max} [b] (pmol/mg)	0.68	0.19	0.073	0.011
Protein content[c] (mg/cm^3)	114	124	53	70
ECS[d] (%)	28[e]	32[f]	32[f]	32[f]
DHPR density[g] (sites/μm^3 cell vol.)	29	18	13	2
RyR density[h] (sites/μm^3 cell vol.)	65	21	3	<1
RyR : DHPR	2.3	1.2	0.2	0.5

DHPR, dihydropyridine receptor; RyR, ryanodine receptor.

[a] Mean DHPR B_{max} values taken from Table 2.

[b] Mean RyR high-affinity site B_{max} values taken from Table 3.

[c] Homogenate protein in mg per gram wet weight x muscle density (1.06 g/cm^3).

[d] Percentage of total tissue occupied by extracellular space (ECS).

[e] Taken from Frank and Langer (1974).

[f] Taken from Farrell and Milligan using trout heart (1986).

[g] DHPR density = DHPR B_{max} x protein content x ECS correction x 6.02×10^{23}

[h] RyR density = RyR (high-affinity) B_{max} x protein content x ECS correction x 6.02×10^{23}

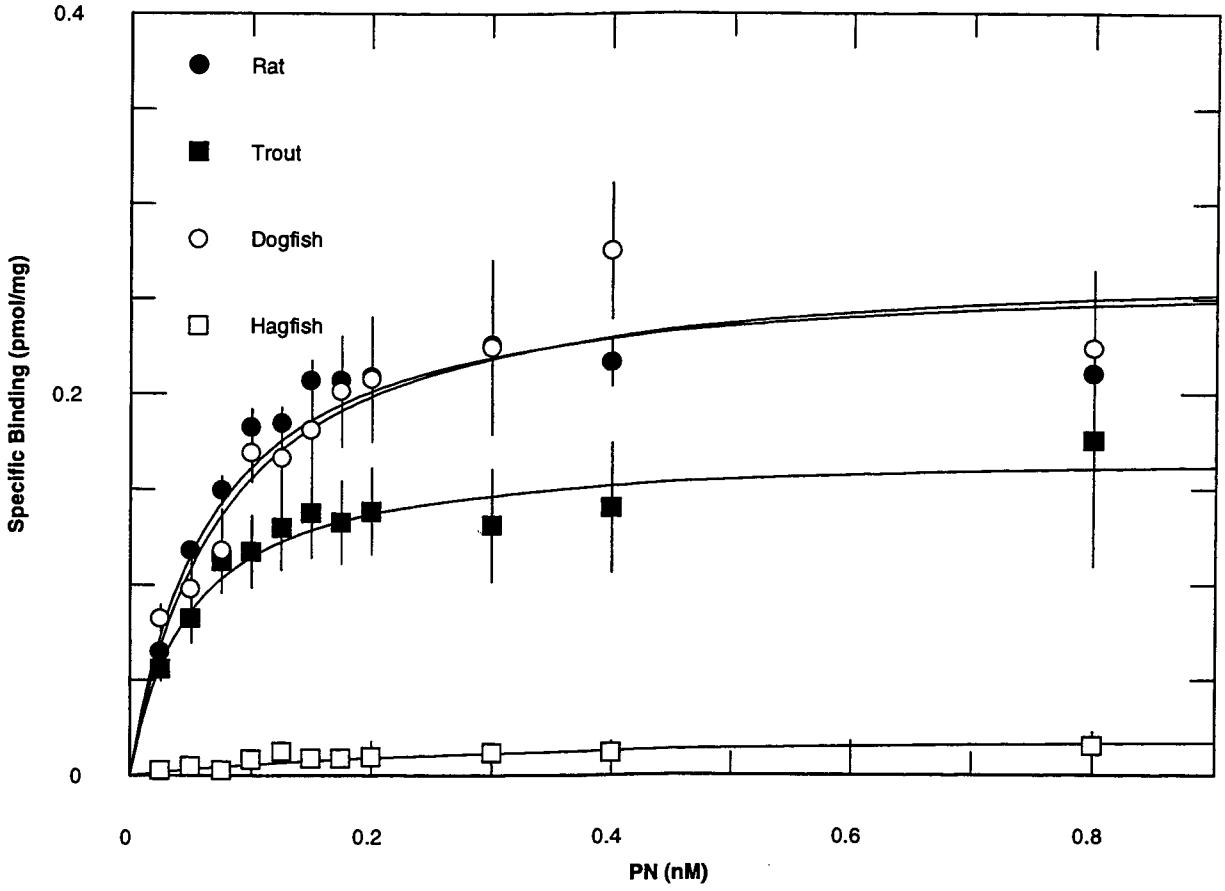

Figure 1. Specific [^{3}H](+)PN200-110 binding as a function of total PN200-110 concentration to ventricular homogenates in rat (filled circles, n=10), trout (filled squares, n=6) dogfish (open circles, n=6) and hagfish (open squares, n=5). Data are represented as mean ± S.E.M.. PN binding was determined as outlined in MATERIALS AND METHODS.

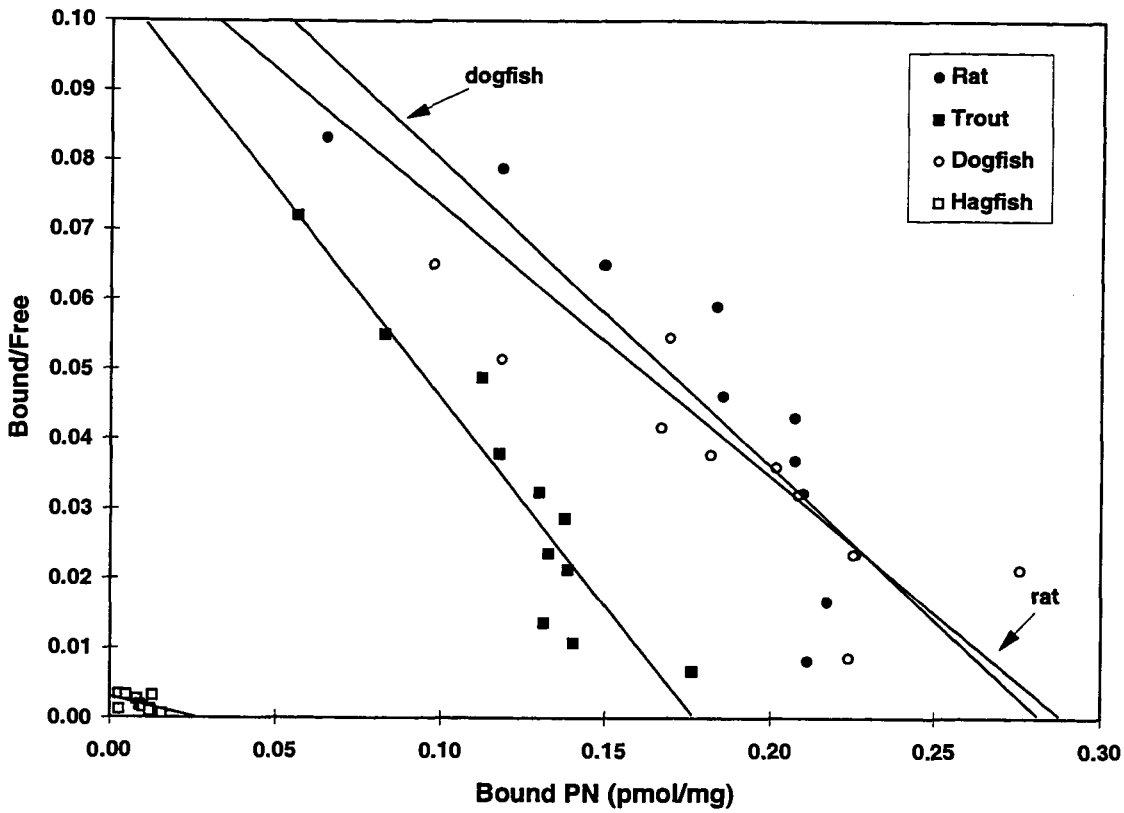

Figure 2. Scatchard analysis of specific [^{3}H](+)PN200-110 (PN) binding in each species. Specific binding for rat (filled circles, n=10), trout (filled squares, n=6), dogfish (open circles, n=6) and hagfish (open squares, n=5) are shown as a function of free ligand concentration. Bound PN is specific PN binding in pmoles per mg protein. Bound/Free is specific PN binding in pmol/mg divided by free PN in pmol/mg.

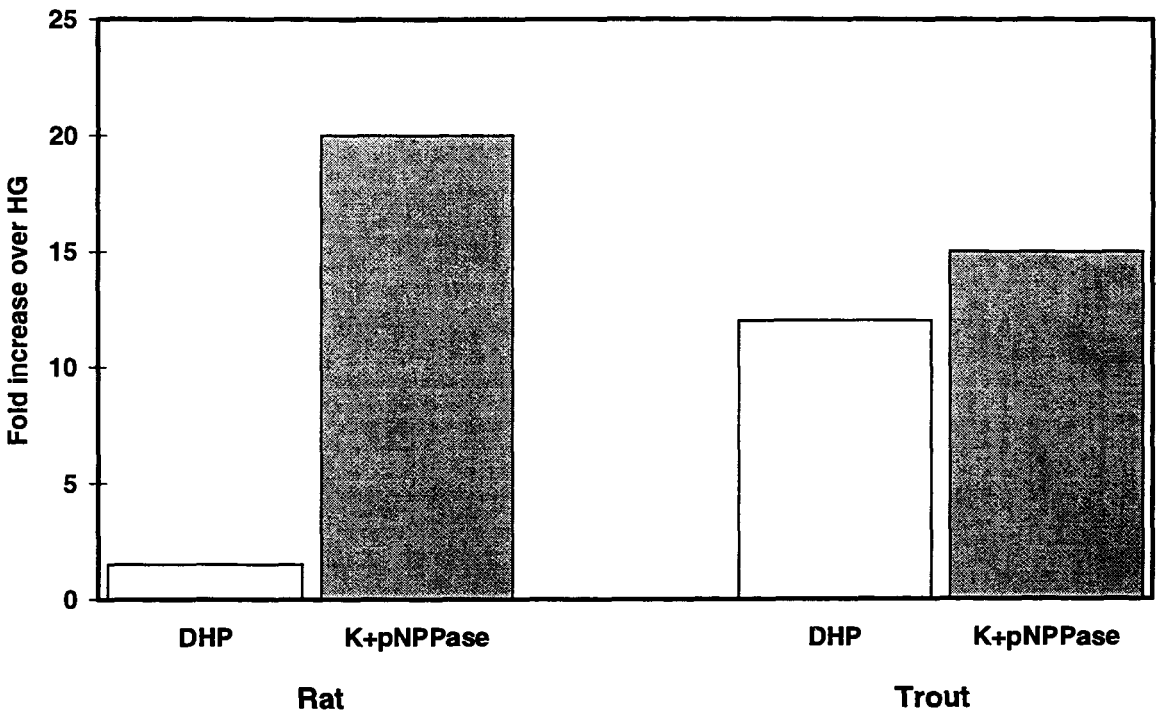

Figure 3. Specific [^{3}H](+)PN200-110 (PN) binding and sarcolemmal marker enzyme activity (K^+*p*NPPase) in SL from rat and trout heart. Maximum PN binding and K^+*p*NPPase activity are normalized to the respective homogenate values. PN binding was determined as outlined in MATERIALS AND METHODS.

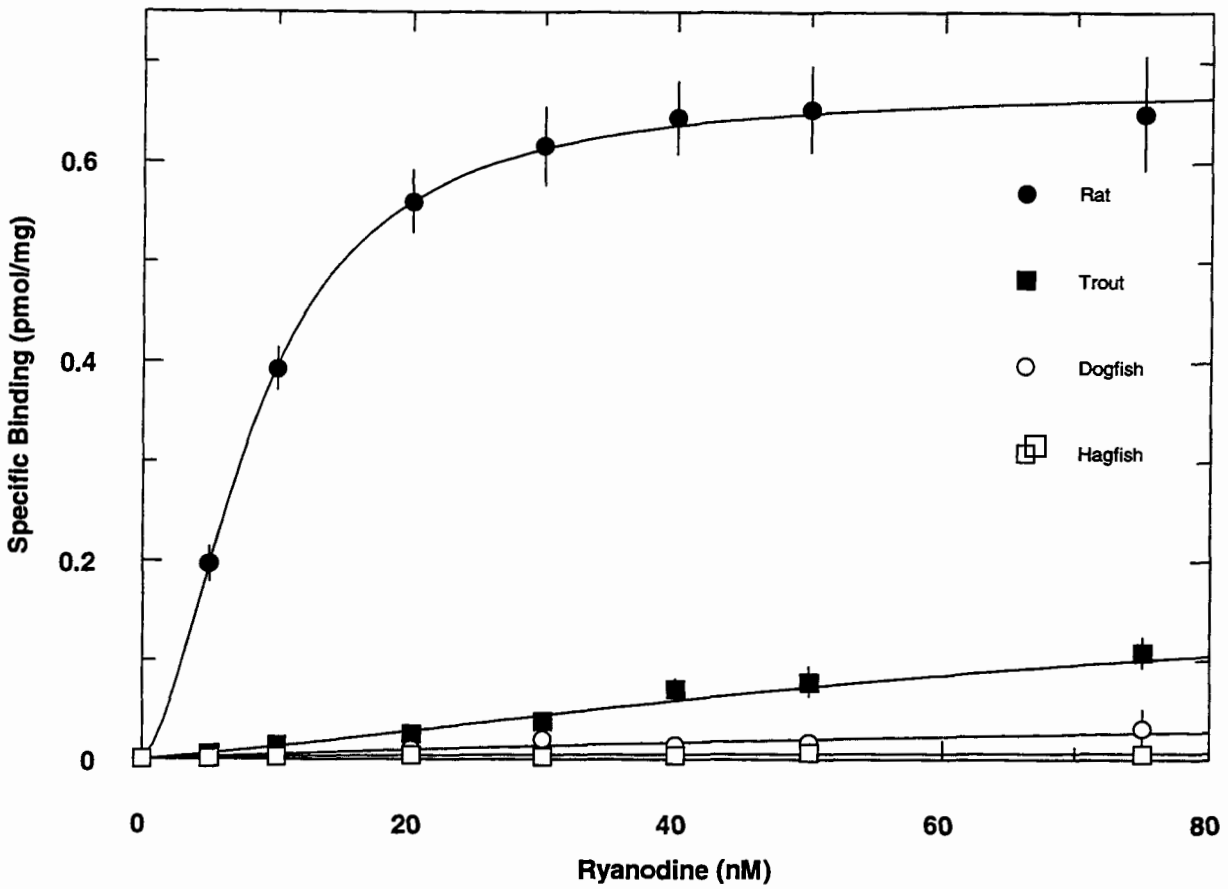

Figure 4. Specific [^{3}H]ryanodine binding as a function of total ryanodine concentration to ventricular homogenates from rat, trout, dogfish and hagfish hearts. Only the high-affinity sites (0-75 nM) are shown for simplicity. Each data set represent the mean values with error bars ± S.E.M. of separate rat (filled circles, n=10), trout (filled squares, n=6), dogfish (open circles, n=6) and hagfish (open squares, n=6) binding assays, with each experiment consisting of individual (rat, trout, dogfish) or pooled (hagfish) ventricles. Ryanodine binding was determined as outlined in MATERIALS AND METHODS.

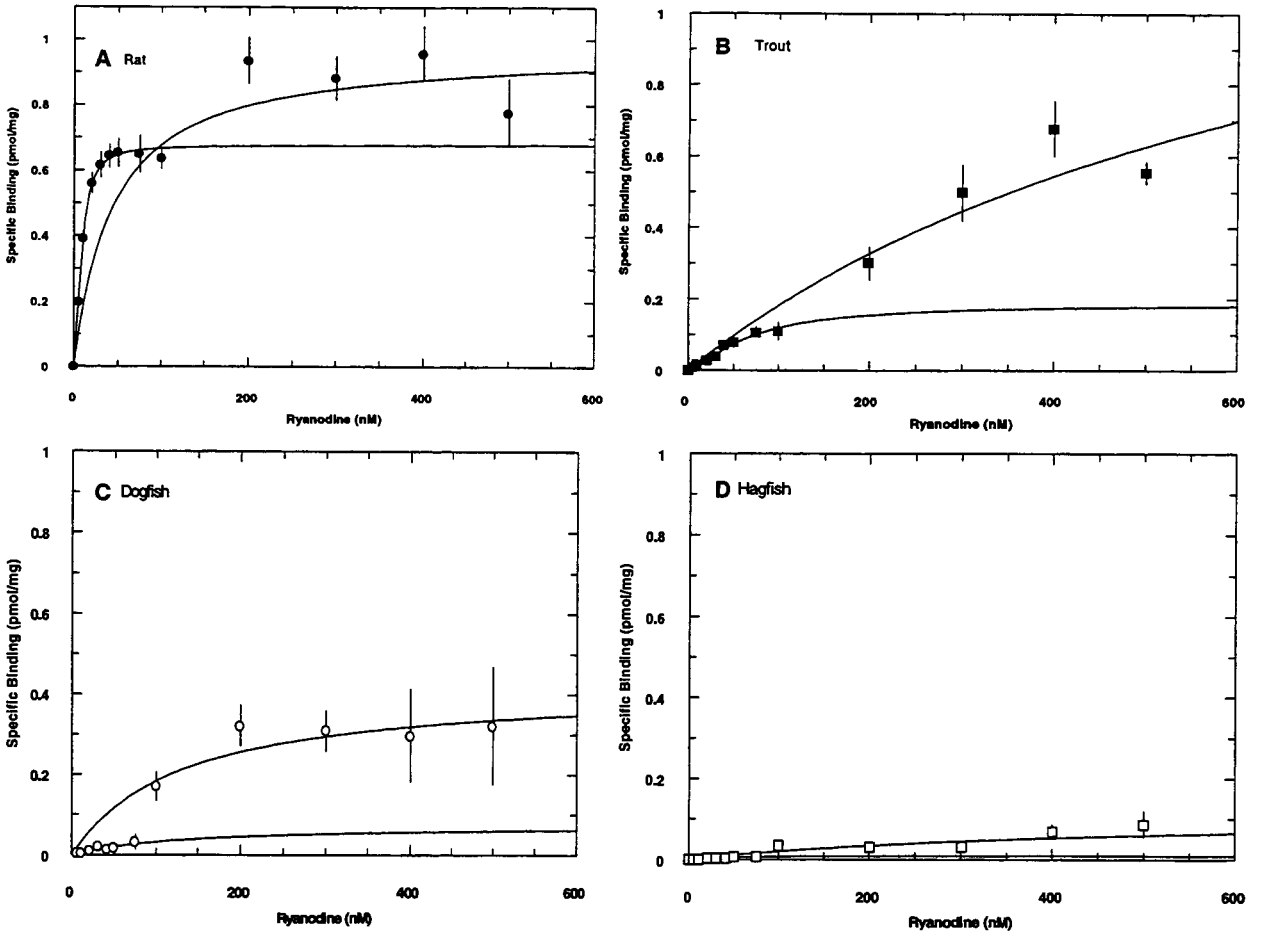

Figure 5. Specific [^{3}H]ryanodine binding in ventricular homogenates from the four species as a function of total ryanodine concentration (0-500 nM). The two curves represent best fits for the high- (0-75 nM) and low- (100-500 nM) affinity sites. Values for the high affinity site were fitted using the two-site Adair equation while those for the low affinity site were fitted using the one-site ligand binding equation, both from GRAFIT (Erithacus Software Ltd, UK). Panel A: rat (filled circles, n=10 individual ventricles); panel B: trout (filled squares, n=6 individual ventricles); panel C: dogfish (open circles, n=6 individual ventricles) and panel D: hagfish (n=6 assays with 2-6 hearts pooled per assay). Values are means ± S.E.M.

CHAPTER 6

CONCLUSIONS

CONCLUSIONS

EXERCISE ADAPTATIONS

The first paper (Chapter 2) assessed the effects of treadmill-training under five slightly different workrates on DHPR and RyR densities in ventricular homogenates using the same female rat model. In general, there was no change in either DHPR or RyR density over the range of workrates which have previously and subsequently been shown to enhance cardiac contractile function. However, an adaptation in receptor density is not the only mechanism by which ion transport can be altered. Channels may undergo differential isoform expression, altered modulation by numerous substances including associated/regulatory subunits and second messengers. Another finding was an apparent intensity threshold of ~30 m/min, 8% grade which did stimulate greater expression of these receptors. Under the training regimen, T2M, DHPR density remained unaltered while RyR density increased by 24%. The RyR density changes are somewhat suspect because the increase was reflected by an apparent reduction in the mean control value, the reasons for which are unknown. At the highest workrate, T1H resulted in a ~50% increase in DHPR. Unfortunately RyR densities were not assessed in this study. The less than physiological conditions of *in vitro* ligand binding assays precludes the determination of absolute receptor number, nor is information available with respect to receptor function or regulation. With the assumption that DHPR and RyR binding sites reflect the density of functional Ca^{2+} channels, the lack of any change in DHPR and RyR over workrates known to enhance contractile performance does not support the hypothesis that endurance training of sufficient intensity increases the expression of both

SL Ca^{2+} channels and SR Ca^{2+} release channels. The increases in DHPR and possibly RyR expression at the higher workrates may simply be a hypertrophic response in order to maintain myocardial contractility.

The second paper (Chapter 3) assessed the contractile properties and Ca^{2+} transients in sedentary-control and treadmill-trained rats. Cardiomyocytes from animals trained at the apparent threshold workrate (30 m/min, 8% grade) demonstrated enhanced contractile activation (maximal degree of shortening and rates of shortening/relengthening) in the presence of a reduced cytosolic Ca^{2+} transient. The maximum amount of SR releaseable Ca^{2+} was not increased by training, as assessed by rapid cooling contractures. Collectively, these data do not support the hypothesis that peak $[Ca^{2+}]_i$ is increased with each beat due to an adaptation in SR Ca^{2+} release. The lack of any significant change in DHPR and RyR expression observed at this workrate (T2M) and the reduced peak Ca^{2+} transient strongly suggest the Ca^{2+} sensitivity of the contractile element is enhanced with training. The underlying mechanisms are currently unknown. The major limitation in this study is a possible variation in the K_D of indo-1 for Ca^{2+} due to protein binding which was not assessed.

The third paper (Chapter 4) addressed whether or not CaM levels were enhanced as the result of endurance training. Calmidazolium inhibition of DHP binding (at 0.41 nM PN) was significantly greater in purified SL from the T animals. Electrophoresis and densitiometric analysis revealed a training-induced 70% increase in the amount of a SL-protein band of ~16 kDa, the same molecular weight as CaM. When CaM was quantified using an ELISA technique, there were no significant differences in the amount of CaM in

any fraction taken during the SL purification procedure. Collectively, the data are inconclusive and therefore do not support the hypothesis that CaM is increased as a consequence of training. Limitations of this study include the relative lack of sensitivity of SDS-PAGE and densitomentry, small sample size and possible antibody cross-reactivity in the CaM ELISA.

Further experiments should include an *in vivo* determination indo-1 K_D in both trained and control myocytes. This will reveal whether or not the reduced R_{peak} is due to an actual reduction in $[Ca^{2+}]_i$ or not. Additional experiments are also needed to examine the role of the contractile element in exercise-mediated adaptations, perhaps focusing on length-dependent changes in Ca^{2+} sensitivity, pH regulation and other cytosolic factors that may impact Ca^{2+} sensitivity.

LOWER VERTEBRATES

The fourth paper (Chapter 5) assessed the relative densities of DHPR and RyRs in ventricular homogenates of several phylogenetically distinct species namely, the rat, trout, dogfish, and hagfish. In contrast with results from purified SL, DHPR densities in ventricular homogenates from trout were slightly lower than the rat and not higher as originally believed. DHPR densities (receptors per unit cell volume) in the dogfish were comparable to the rat, and in the hagfish preparation barely above the level of detection. The reason for the low hagfish density remains unknown but may reflect different Ca^{2+} channel regulation, a low Ca^{2+} requirement or possibly Ca^{2+} influx via another mechanism such as Na^{+}/Ca^{2+} exchange. RyR densities in the same homogenates were

dramatically reduced in lower vertebrates compared to mammals. RyR density correlated with both the relative amount and complexity of SR among the lower vertebrate species as determined by electron microscopy. These results support our hypotheses. While the DHPR densities in trout and dogfish were within the range for mammals, the substantially lower RyR densities of all three lower vertebrates suggests that either SL Ca^{2+} influx is increased through channel modulation, or there is a reduced requirement for total Ca^{2+} increase because of differences in intracellular buffering, or there is a reduced contractile requirement for Ca^{2+} because of increased myofilament Ca^{2+} sensitivity. The latter has been demonstrated in both trout and amphibian hearts. A major limitation with these *in vitro* experiments is that receptor density does not give any indication of channel function or regulation. Therefore, further experimentation is needed focusing on quantitative measurements of SL Ca^{2+} influx in addition to quantitative analysis of cytosolic Ca^{2+} buffering. Characterization of TnC-Ca^{2+} binding would also help to determine the Ca^{2+} requirements and Ca^{2+} sensitivity of the myofilaments, although the greater Ca^{2+} sensitivity for a given physiological temperature in fish does not appear to be due to any differences in either TnC or TnC-Ca^{2+} binding (1). By clarifying the role of SR Ca^{2+} release in the more active teleost species, a greater understanding of E-C coupling may be achieved. Finally, the temperature dependence of these processes would further add to current knowledge of E-C coupling in these species and may help to explain changes in E-C coupling mechanisms accompanying temperature compensation.

REFERENCES

1. Moyes, C.D., T.J. Borgford, L. Leblanc, and G.F. Tibbits. Cloning and expression of salmon cardiac troponin C: titration of low affinity calcium binding sites using a tryptophan mutant. *Biochem.* (in press).